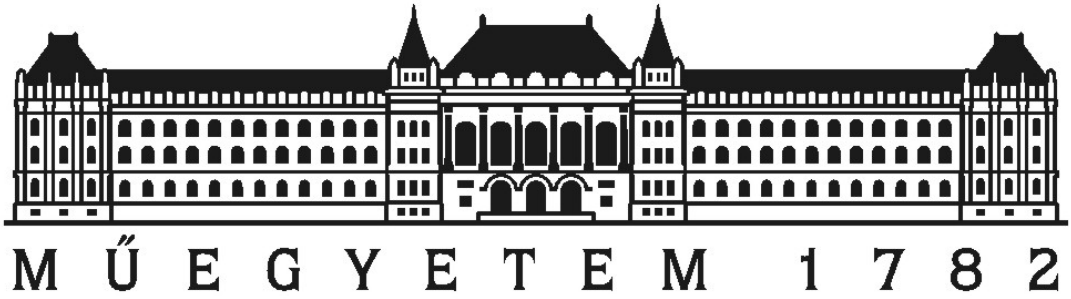

VARIATION OF LOAD BEARING CAPACITY OF THIN STEEL PLATE AS A FUNCTION OF POROSITY

GHULAM KIBRIYA

BSc Student

Supervisor: Dr. Imre Bojtár

A thesis submitted

for the Student's Scientific Conference

Budapest, November 2021

Abstract

The purpose of the study was to determine **variation in load bearing capacity** of a thin steel plate under axial load in its transition from a **solid** model (without voids) to a **porous** model (infinite voids). The load bearing capacity of solid model was calculated using analytical method, also in the case of porous model, an analytical approximation (Gurson's model) was used to determine the load bearing capacity. Gurson model allows for a good approximation for spherical voids in a *3D stress state* and as an approximation we shall use for the case of ellipsoidal voids.

The transition from solid to porous model was done by determining the load bearing capacity of increasing number of voids placed at random positions. The voids were either circular or elliptical. In case of elliptical voids, two different axes ratios of $b : a = 1 : 5$ and $b : a = 1 : 10$ were used.

The study uses a plane stress version for the analysis of the thin steel plate for porosities of 1.5%, 6%, 24% and 40% for different number of voids each with five variations each to increase the sample size.

A plane strain variation was also analyzed for porosity of 24% to make a comparison. To better understand the behavior of plate with voids, large strains were also analyzed for porosities of 6% and 24%.

Acknowledgements

Throughout the research and writing of this manuscript, I have gotten a lot of encouragement, support, assistance along with furtherance of my interests in the research in the field of mechanics.

I would first like to thank my supervisor, Professor Emeritus Imre Bojtár, for his guidance and direction through each stage of the research process. He, inspite of his retirement, supervised me throughout the research project along with giving me the necessary theoretical knowledge in the subject. His concise lecture notes in the subject of material models, nonlinear mechanics and then finally fracture mechanics helped me give a basic understanding of the subject. His advice on *"making the building stone by stone"*, that is taking one step at a time was invaluable for the duration of the whole project and will remain invaluable. His expertise in defining the methodology, research questions and the theoretical approximations to be considered was invaluable. His insightful feedbacks and honed skills of critical thinking have helped me made significant improvements in my ability to ask critical questions.

I would also like to thank my parents for always being there for me and counselling me. Finally, I would like to thank my friends for their support and happy distractions they provided to help me ease my mind.

Contents

List of Figures

Nomenclature

$\bar{\sigma}$	$1D$ yield strength
$\dot{f}$	Void growth
ε_{kl}	Strain tensor
ν	Poisson's ratio
ρ	Radius of curvature of hole or notch
σ_1, σ_2, σ_3	Normal stresses in principal directions
σ_e	von Mises equivalent stress
σ_m	Average normal stress
σ_x, σ_y, σ_z	Normal stresses in x, y, z direction
σ_∞	Stress at infinity
$\sigma_{\theta\theta}$	Hoop stress
σ_{ij}	Stress tensor
σ_{max}	Maximum stress due to stress concentrator
σ_{nom}	Nominal stress
σ_{rr}	Radial stress
$\tau_{r\theta}$	Shear stress in cylindrical coordinates
τ_{xy}, τ_{yz}, τ_{zx}	Shear stresses in x, y, z plane
a	Length of major axis of ellipse
b	Length of minor axis of ellipse
E	Elastic modulus
E_t	Tangent modulus
f	Porosity
F_{ij}	Elastic response function
H_k	Material parameter system
J_2	Second invariant of deviatoric stress tensor
k	Material parameter equal to $\bar{\sigma}/\sqrt{3}$
n	Number of holes
q_1, q_2, q_3	Experimental constants for porous materials
r	Radius of circular hole

Introduction

An opening or a hole in structural member causes a sudden increase in stress at the point of opening which will result in decrease in load bearing capacity. In this study, the change in load bearing capacity is analyzed with its shift from solid or intact model to Gurson model. Finite element analysis of a thin steel plate is used for this purpose. The shift between intact and porous model is done by increasing number of voids. It is to be noted that porous model is applied on either a 3D model. Also, the number of spherical pores approach towards infinity in porous model. So, a more reliable approach towards analyzing the shift would be to have minimum number of voids upto 10^5. But that isn't the case for this study as large number of voids come with some drawbacks listed below.

- Randomly placing large number of voids in geometry also has problem often resulting in infinite loop. Even for $n = 1000$ for circular voids and $n = 500$ for elliptical voids, zones were needed to be used to overcome the infinite loop.
- Increasing the number of voids increases difficulty in discretization of domain. Smaller edges of pores can't be ignored which results in an exponential increase in time required to discretize.
- Using large number of voids increases the computation time and also result in convergence problems specially in case of elliptical voids.

Even though having maximum number of voids would result in a more smooth shift from intact to porous model, it is not feasible in our current situation. So, for the purpose of this study maximum number of voids in case of circles are 1000 while in case of ellipsis are 500.

As we mentioned, the main objective of this study is to analyze the shift from solid to porous model shown in Figure 1 and deduce a mathematical form which is followed by this shift. The stress state of the model also varies in the transition from solid to porous model. Solid model has a 3D stress state. The numerical models created in the study have a 2D stress state i.e. *plane stress*. Porous model also has theoretically a 3D stress state.

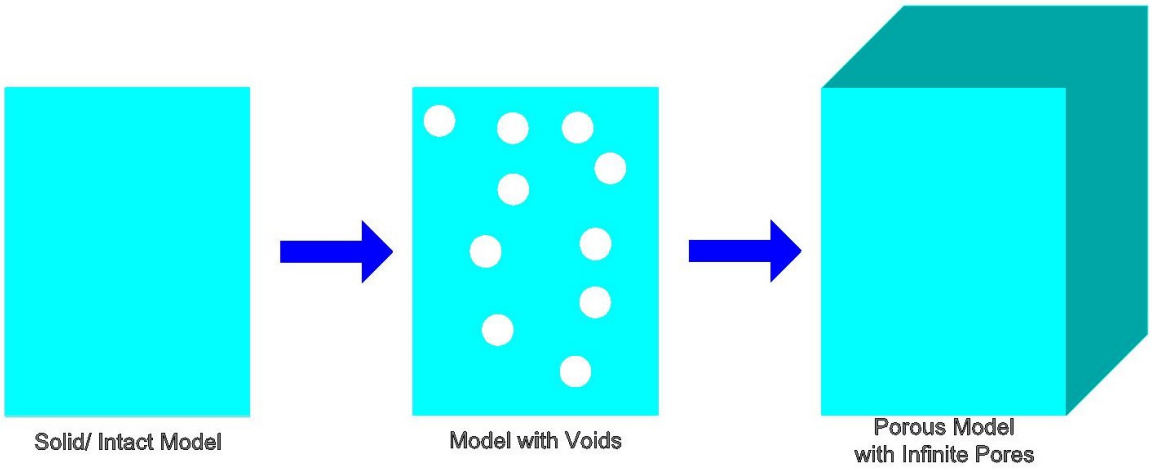

Figure 1: Transition from Intact to Porous Model

Outline of Chapters

An overview of chapters is given below.

1. **Material Models** gives a brief understanding of the behavior of applied mechanical material models. The characteristics, examples and brief mathematical introduction of elastic, elasto-plastic and porous material models are explained.

2. **Stress Concentration** explains stress concentration around the holes and how it differs from stress singularity. The effects of shape of voids on stress concentration are explained. An explanation into how stress concentration occurs in different materials.

3. **Numerical Solution** gives an introduction to Finite Element Method. Difference between plane stress and plane strain is also briefly explained.

4. **Finite Element Model** gives an overview of the applied numerical model. It introduces the geometries applied for each of porosities. Domain discretization for different geometries and applied boundary conditions are briefly described. The method for calculating load bearing capacity is given.

5. **Numerical Simulation Results** presents the calculated load bearing capacities for each of different porosities. The comparison between different hole shapes is also presented along with the comparison between different formulations (*plane stress - plane strain* and *small strain - large strain*).

1 Material Models

1.1 Introduction

The kinematic and equilibrium equations are not sufficient to solve a boundary or initial value problem in continuum mechanics. For a complete set of equations, a constitutive equation has to be formulated which characterizes the material response of a body under consideration. The constitutive theory describes either the “microscopic" or the “macroscopic" behavior of a material in response to the external effects [1].

Scale of observation is an important question in continuum mechanics. In continuum mechanics we assume that the space is filled with continuous set of material points connecting to each other’s infinitely close sense. In reality, the real material is not continuous with most of materials having some sort of discontinuity either due to manufacturing or other defects. Similarly, mechanical variables don’t represent a specific point in the continuity but an average value. For this reason, we can define a smallest element in a material whose state characterizes the whole material. The smallest representation element has different ranges for different materials. But as the size of the representative smallest element decreases, the applicability of continuum mechanics principles also ends. As we’ll now have to take into account the microscopic behaviors. An important question is how we can correlate two different scale models. Figure 2 shows the different scales of material models with their respective disciplines different disciplines [2].

The materials like steel and concrete commonly used for engineering purposes, a macroscopic model is sufficient. Steel plate is analyzed in current study, so only the macroscopic models will be discussed further.

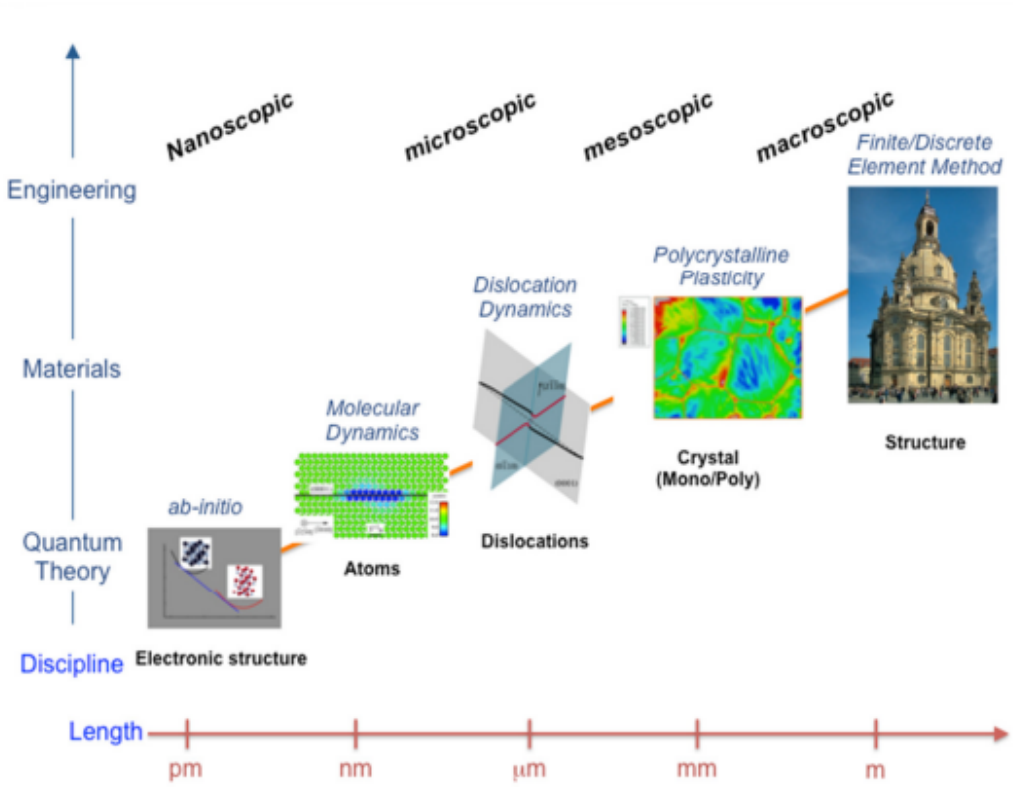

Figure 2: Different Scales of Material Models

Material model gives us constitutive equations that relate the stresses to strains in case of mechanics. Since real materials can exhibit very complex behavior, approximations have to be applied within the derivation process of constitutive equations. These, however, have to cover all effects observed in experimental investigations. The basic principles from mechanics have to be obeyed to obtain theoretically sound constitutive equations [1]. These constitutive equations are what make a material model. These equations are not simple approximations but the governing principles of how a material would behave theoretically, when subjected to certain external effects.

1.2 Elastic Material Model

The first attempt at scientific description of solid mechanics was done by Galileo. He treated bodies as to be inextensible. At that time, there were no experimental or physical hypothesis that could give the relation between deformations and forces that are producing deformations. The first one to give a law of proportionality was Robert Hooke in 1676 as *"extension is proportional to force [3]."* In the majority of engineering applications of structural and geological materials such as metals, concrete, soils, rocks, and rubber under short-term loading, time independence of the stress-strain relation can be assumed. So, time doesn't appear as an explicit variable in the constitutive equations. We also note that the materials are assumed to be under *isothermal conditions*.

The behavior of many engineering materials can be described using elastic material models. A material body is deformed when subjected to applied forces. If upon the release of the applied forces the body recovers its original shape and size, then the material body is called elastic. The linear elastic model is used to describe the behavior of metal materials at stress levels below the yield limit. Nonlinear elastic model can be used to describe the behavior of soft materials like rubber, biological tissues etc. Therefore, elastic constitutive relations are the basis for the theory of elasticity, which has found many applications in different engineering problems. It should be noted that the elastic constitutive models are also needed in the theory of plasticity as well. Elastic-plastic models are used quite a lot for metals in cases when stress is beyond *yield limit*.

For elastic material, the current state of stress depends only on the current state of deformation; that is, the stress is a function of strain [4]. This mathematical representation is given by,

$$\sigma_{ij} = F_{ij}(\varepsilon_{kl}), \tag{1.1}$$

where the function F_{ij} is the elastic response function. Thus, the elastic behavior described by Equation (1.1) is both reversible and path independent since strains are uniquely determined from the current state of stress. Also, there is no dependence on the path followed to reach the current state of stress or strain. But the fact is that there is no material which can be described as an ideal elastic material. All materials undergo some permanent deformations, sometimes even for low loads. Also, no material behaves similarly when loaded with different speeds. If these differences are small enough to be neglected safely, then that material can be modeled as an ideally elastic material. Elastic material model can be used for almost any material if the stresses are inconsiderable.

1.3 Elasto-Plastic Material Model

There are materials which behave in an elastic manner upto a specific threshold limit, beyond that permanent deformations are produced. These permanent deformations are one of the most

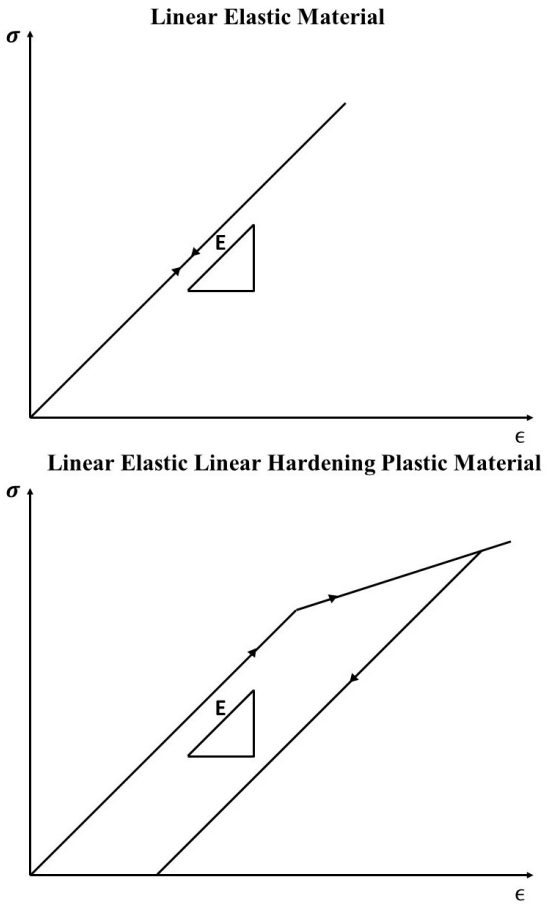

Figure 3: Linear elastic and linear elastic-linear hardening plastic material

important characteristics of plastic materials and must be taken into account. The material behaves plastic only over a definite stress state. The mathematical relations that describe the limit of elastic behavior and beginning of plastic behavior are called yield conditions. The geometrical representation of these mathematical relationships is called as yield surface. The yield condition is a function of *stress state* and *material parameter system* H_k. For ideal plastic materials (*no hardening*), H_k is stress limit of material. But in case of hardening, H_k is function of loading system and stress state. Now, the general form of yield condition for isotropic materials is given as

$$F(\sigma_{ij}, H_k) = 0. \tag{1.2}$$

There are different yield conditions each with their significance such as Huber-Mises-Hencky yield condition, Tresca model, Rankine model and Mohr-Coulomb model etc.

For the course of this study, Huber-Mises-Hencky yield condition will be explained. It is one of the most important yield condition for metals.

According to HMH yield condition, material becomes plastic if the second invariant of the deviatoric stress tensor becomes equal to $H_1 = k^2$.

$$F = J_2 - k^2 = 0, \tag{1.3}$$

where J_2 is second invariant of deviatoric stress tensor. After substituting value of J_2 in terms of elements of total stress tensor, we get

$$F = \frac{1}{6}\left((\sigma_x - \sigma_y)^2 + (\sigma_y - \sigma_z)^2 + (\sigma_z - \sigma_x)^2\right) + \tau_{xy}^2 + \tau_{yz}^2 + \tau_{zx}^2 - k^2 = 0. \tag{1.4}$$

The yield condition can also be written in terms of principal normal stresses as

$$F = \frac{1}{6}\left((\sigma_1 - \sigma_2)^2 + (\sigma_2 - \sigma_3)^2 + (\sigma_3 - \sigma_1)^2\right) - k^2 = 0. \tag{1.5}$$

The value of k can be determined by using a tensile strength test. As in case of tensile test, there is only one principal stress acting in longitudinal direction. Therefore, σ_2 and σ_3 become equal to zero. The parameter k can be given as,

$$k^2 = \frac{1}{3}\sigma_1^2, \tag{1.6}$$

$$k = \frac{\sigma_1}{\sqrt{3}} = \frac{\bar{\sigma}}{\sqrt{3}}. \tag{1.7}$$

Here, $\bar{\sigma}$, is one dimensional yield strength.

1.4 Material Models Used

Two different materials were used for the purpose of this study. It should be noted that the materials chosen for the purpose of this simulation were arbitrary. They don't reflect the actual engineering data used for numerical simulation of steel. These materials will be hereinafter referred to as **Material 1** and **Material 2**.

Material 1 will be used with Elastic Modulus $E = 200\ GPa$ and Poisson's ratio $\nu = 0.3$. Yield strength is $\bar{\sigma} = 250\ MPa$. Since this material has no hardening, therefore tangent modulus $E_t = 0\ GPa$.

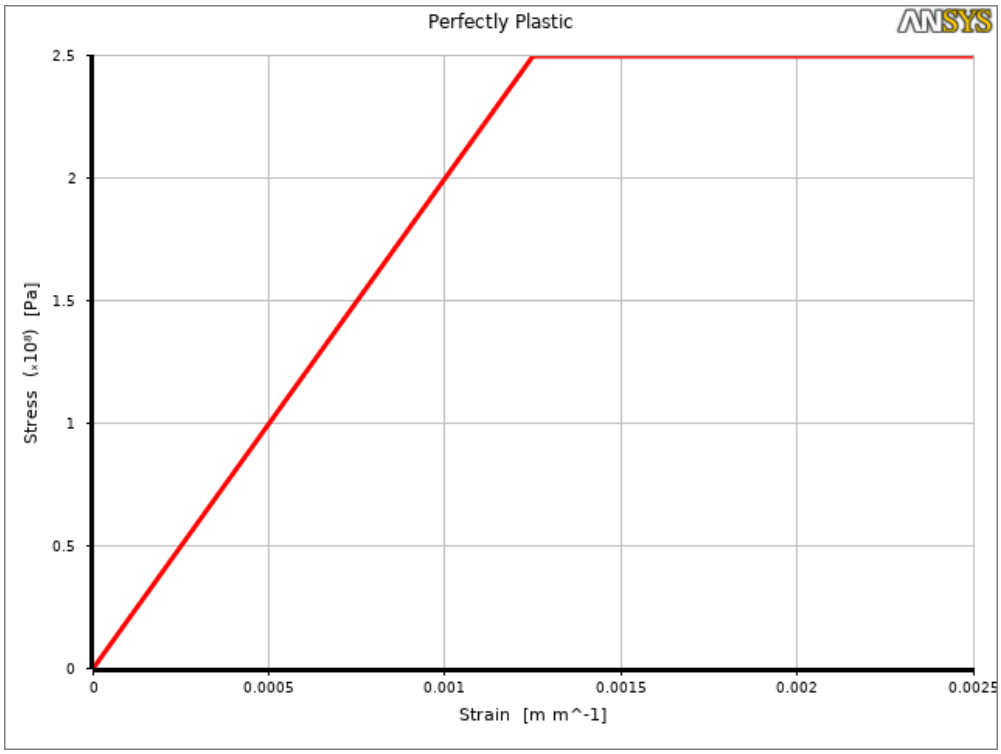

Figure 4: Stress Strain diagram of *Material 1*

Material 2 will be used with Elastic Modulus $E = 200\ GPa$ and Poisson's ratio $\nu = 0.3$. Yield strength is $\bar{\sigma} = 250\ MPa$. Since this material has linear hardening, tangent modulus $E_t = 60\ GPa$ is used for the purpose of this study.

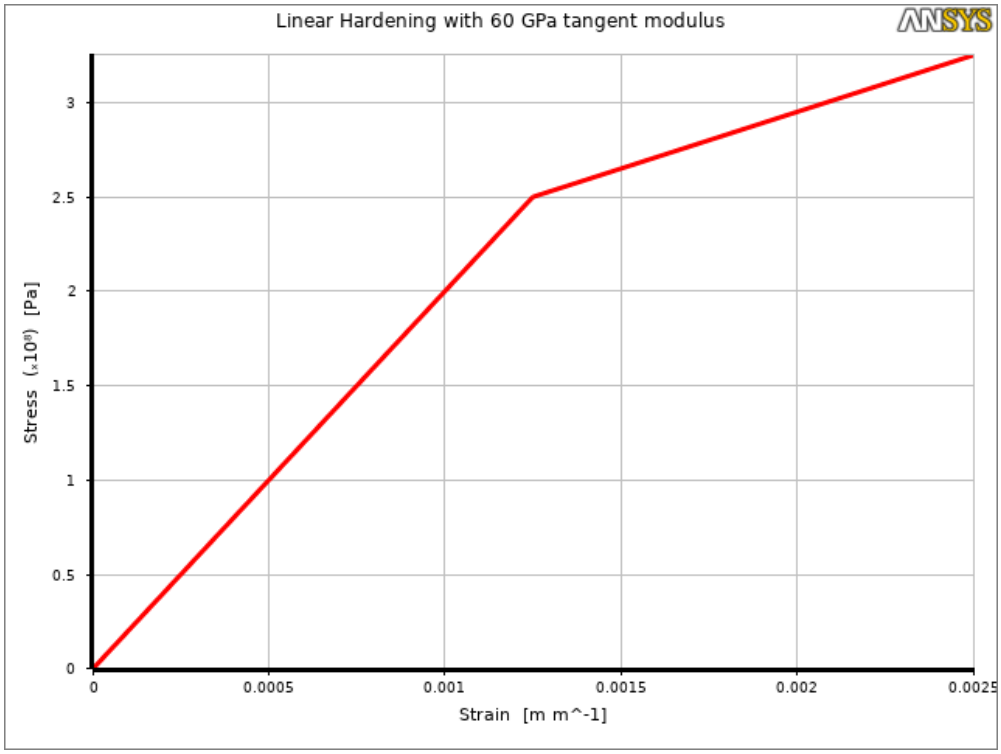

Figure 5: Stress Strain diagram of *Material 2*

1.5 Gurson's Model

The Gurson model [5] is used to represent plasticity and damage in ductile porous metals. We note that the model was then modified by Tvergaard, Chu and Needleman, and Tvergaard and Needleman. Gurson-Tvergaard-Needleman(GTN) model analyzes the plastic flow in porous materials assuming that the material behaves as a continuum. Voids appear in the model indirectly because of their effects on global flow behavior. The effect of the voids is averaged through the material which is assumed to be homogeneous and continuous. The main difference between classic plasticity of metals and GTN is that the yield surface is independent of hydrostatic stresses in classic metal plasticity while it is not in the case of GTN model [6]. The GTN model gives a yield criteria as

$$F(\sigma_e, \sigma_m, \bar{\sigma}, f) = \left(\frac{\sigma_e}{\sigma_m}\right)^2 + 2q_1 f \cosh\left(\frac{3}{2}\frac{q_2\sigma_m}{\bar{\sigma}}\right) - (1 + q_3 f^2) = 0. \tag{1.8}$$

Here, σ_e is the von Mises stress, σ_m is average normal stress, $\bar{\sigma}$ is the 1D yield stress, f is the porosity and q_1, q_2, q_3 are experimental constants. For metals, their values are $q_1 = 1.5$, $q_2 = 1$ and $q_3 = q_1^2$. For $f = 0$, we get von Mises yield criterion.

When plasticity and damage occur, ductile metal goes through a process of nucleation, void growth and coalescence. A void is formed around an inclusion when sufficient stress is applied to break the interfacial bonds between the particle and the matrix. When the voids are formed, hydrostatic stresses and plastic strain cause the void to grow. According to Chu and Needleman

[7], void nucleation can be given as

$$\dot{f} = (1-f)\dot{\varepsilon}^{p}_{kk} + \Lambda\dot{\varepsilon}^{p}_{eq}. \tag{1.9}$$

where the first part indicates the growth rate of existing voids while the second term indicates the nucleation of voids because of plastic strain.

Gurson's method models the process by incorporating these microscopic material behaviors into macroscopic plasticity behaviors based on changes in the porosity and pressure. An increase in porosity shows an increase in material damage, which results in a decreased load bearing capacity of material. Figure 6 shows nucleation (formation of voids), dilatation(growth of voids) and coalescence (establishing connections).

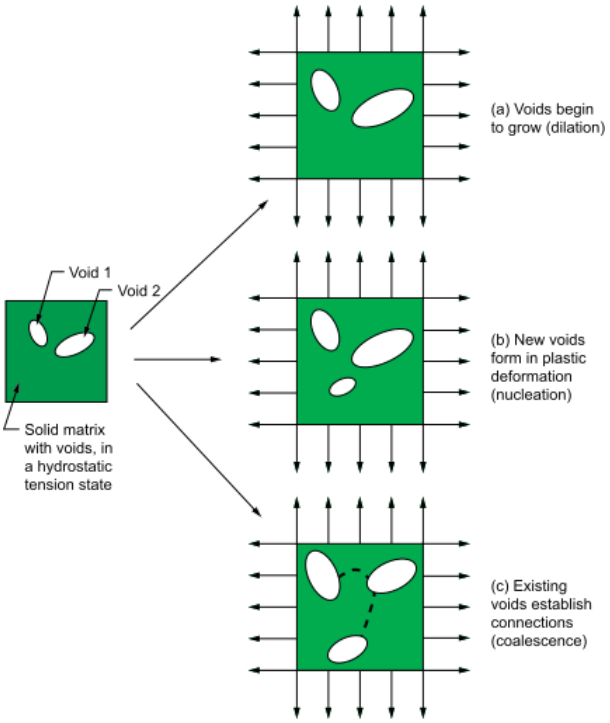

Figure 6: Growth, Nucleation, and Coalesence of Voids in Microscopic Scale [8]

In above figure, the shape of the voids shown are for illustration purpose only. The voids that are included in GTN model are theoretically spherical voids with a uniform distribution. Also, the stress state is a 3D stress state not a 2D stress state.

2 Stress Concentration

Since, the study involves analysis of steel plates with circular and elliptical voids with different porosities, it becomes imperative to have an understanding of stress concentration and how the material model affects stress concentration around voids. Stress concentration can be defined as accumulation of stress in a body due to sudden change in its geometry.

2.1 Elastic Solution of Circular Holes

The analysis of stress concentration began in 1898 by Kirsch [9], when he calculated a linear elastic solution for stresses around a circular hole in an infinite plate under uniaxial loading.

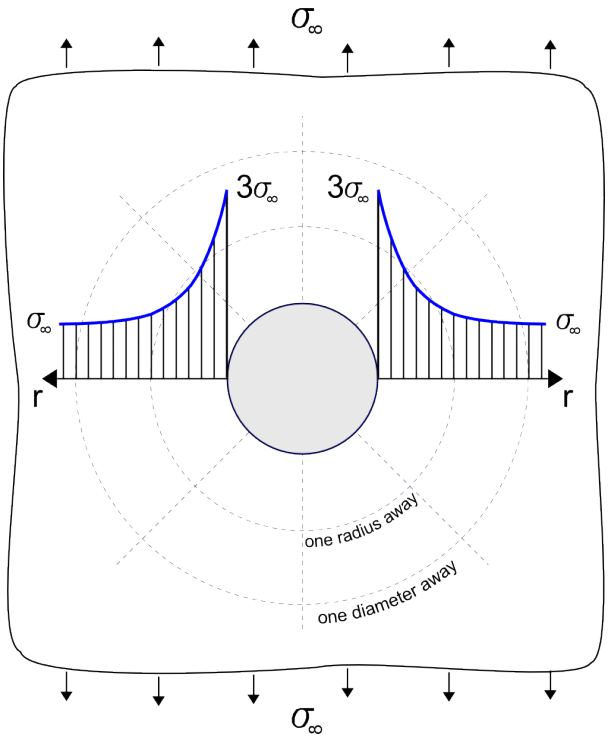

Figure 7: Hoop Stress around an Infinite Plate for $\theta = \pm 90$

The solution gives us a factor of 3 for uniaxial loading in an infinite plate with a circular hole. Kirsch's equations for stresses around a circular hole are as follows

$$\sigma_{rr} = \frac{\sigma_\infty}{2}\left(1 - \left(\frac{a}{r}\right)^2\right) + \frac{\sigma_\infty}{2}\left(1 - 4\left(\frac{a}{r}\right)^2 + 3\left(\frac{a}{r}\right)^4\right)\cos 2\theta, \tag{2.1}$$

$$\sigma_{\theta\theta} = \frac{\sigma_\infty}{2}\left(1 + \left(\frac{a}{r}\right)^2\right) - \frac{\sigma_\infty}{2}\left(1 + 3\left(\frac{a}{r}\right)^4\right)\cos 2\theta, \tag{2.2}$$

$$\tau_{r\theta} = -\frac{\sigma_\infty}{2}\left(1 + 2\left(\frac{a}{r}\right)^2 - 3\left(\frac{a}{r}\right)^4\right)\sin 2\theta. \tag{2.3}$$

At an infinite distance from the hole, the a/r terms become zero. The radial stress, σ_{rr}, equals σ_∞ at $\theta = 0°$ and 180°. The hoop stress, $\sigma_{\theta\theta}$, equals σ_∞ at $\theta = \pm 90°$. Shear stress, $\tau_{r\theta}$ is coordinate transformation of σ_∞.

While at the surface of hole, radial stress, σ_{rr}, and shear stress, $\tau_{r\theta}$, become zero. The remaining stress is $\sigma_{\theta\theta}$ which equals $-\sigma_\infty$ at $\theta = 0°$. The stress concentration occurs at $\theta = \pm 90°$ where $\sigma_{\theta\theta}$ equals $3\sigma_\infty$. It should also be noted that for an *infinite plate*, the maximum stress is independent of radius of hole. The increase in stress at boundary of hole with a factor of 3 gives us the *stress concentration* factor, denoted by K_t. Stress concentration is defined as the ratio of maximum stress due to a hole or a fillet (*not a crack*) to the remote stress. It is important not to misinterpret the stress concentration factor, K_t, with the stress intensity factor which occurs in crack analysis.

For the case of an infinite plate with a circular hole $K_t = 3$. Figure 7 shows the distribution of hoop stress at $theta = \pm 90°$. The stress concentration factor for plates with finite width can be calculated by using nominal stress, σ_{nom}, which is average stress at hole due to reduction in cross section. Now, the stress concentration factor becomes $\sigma_{max}/\sigma_{nom}$ instead of $\sigma_{max}/\sigma_\infty$. In a finite plate, the ratio of diameter of hole to the width affects the stress concentration factor.

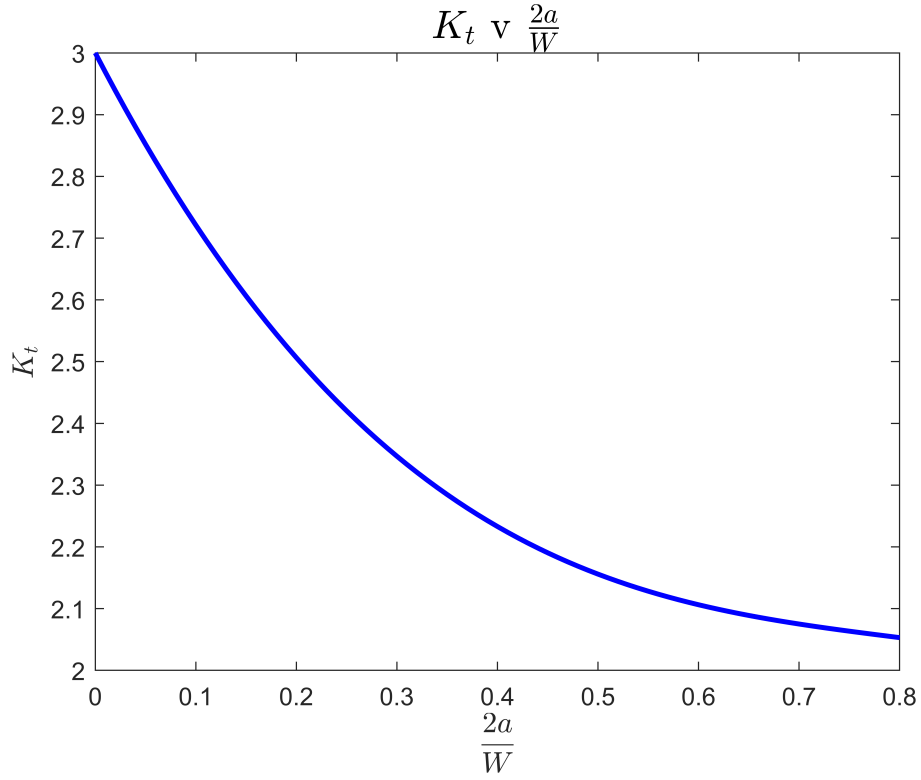

Figure 8: Stress Concentration Factor vs Diameter to Width Ratio

The stress concentration factor [9] for a finite plate is given as

$$K_t = 3 - 3.14\left(\frac{2a}{W}\right) + 3.667\left(\frac{2a}{W}\right)^2 - 1.527\left(\frac{2a}{W}\right)^3. \tag{2.4}$$

Figure 8 shows K_t equals 3 at $(2a)/W = 0$. Then, the value starts to decrease with increasing ratio and limits to 2 for maximum ratio possible. Since, the Kirsch's solution was linear elastic, therefore, maximum stress had no limit as a linear elastic material doesn't have a yield point and its stress continues to increase theoretically. But, in reality the materials do have a yield point and stress in a material can't increase beyond this point.

2.2 Elastic Solution of Elliptical Holes

Kirsch's [9] solution was the first to quantify increase in stress due to holes or voids but it was only applicable to circular holes. A more generalized solution was done by Muskhelishvili, Kolosov and Inglis for linear elastic material for elliptical holes. Inglis's [10] solution provided the stress field for the ellipsis, which can be applied to an infinite number of cases having different ratios of major to minor axis. It should however be noted that Inglis's solution, like Kirsch's, was linear elastic for an infinite plate. The maximum stress at the tip of ellipse is given as

$$\sigma_{max} = \sigma_\infty\left(1 + 2\frac{b}{a}\right). \tag{2.5}$$

Here a is the length of major principal axis while b is the length of minor principal axis as shown in Figure 9.

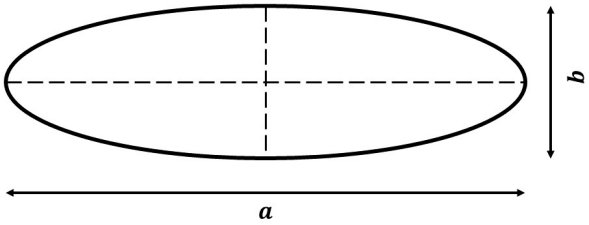

Figure 9: Major and minor principal axis

It can be seen from above equation that Inglis's solution equals to the Kirsch's solution for circular hole ($a = b$) and gives the same result of $\sigma_{max} = \sigma_\infty$. The radius of curvature of the tip of ellipse is given as

$$\rho = \frac{b^2}{a}. \tag{2.6}$$

Substituting above equation in Equation (2.5), we get

$$\sigma_{max} = \sigma_\infty \left(1 + 2\sqrt{\frac{a}{\rho}}\right). \tag{2.7}$$

Equation (2.7) shows that the maximum stress due to an elliptical hole depends on a, the distance of tip to center of ellipse, and radius of curvature, ρ, of the tip. Equation (2.7) is quite important because it shows that as ρ decreases, maximum stress increases.

When the ρ reaches zero, the stress becomes infinite. For $\rho = 0$, theoretically $\sigma_{max} = \infty$. An ellipse with $\rho = 0$ is infinitely sharp crack. This result caused concern when it was first discovered because no material is capable of withstanding infinite stress. A material that contains a sharp crack theoretically should fail upon the application of an infinitesimal load. But an infinitely sharp crack in reality is not possible because the materials are made of atoms. Metals upon plastic deformation would cause the sharp crack to become blunt. In the absence of any plastic deformation, smallest possible radius for crack tip is of the order of atomic radius [11]. To predict the increase in stress near the tip of sharp cracks or notchs, *stress intensity factor* is used which can be applied to linear elastic materials.

Introducing sharp cracks results in infinite stress (stress singularities) according to Equation (2.7) but stresses can't increase beyond the yield limit. The solution done by Inglis uses Hooke's law and has therefore no limiting value.

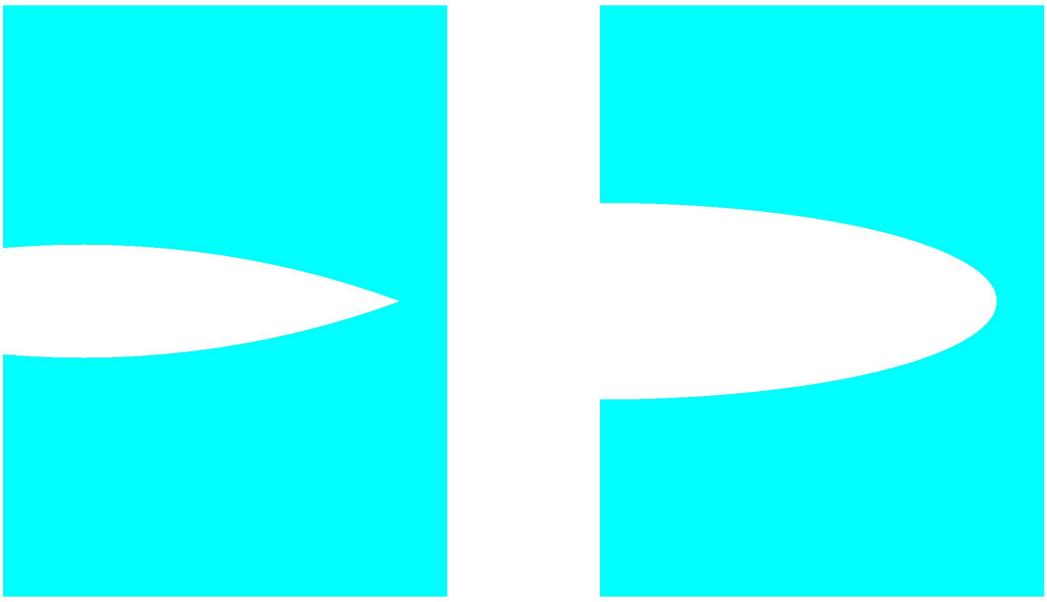

(a) Sharp Crack (b) Elliptical Void

Figure 10: Crack and an elliptical void

2.3 Elasto-Plastic Case

In case of plastic materials, whenever stress reaches the *yield limit* around a stress concentrator, a plastic zone starts to form around it. The formation of plastic zone decreases the stress concentration due to redistribution of forces into neighboring areas. Even though the stress concentration factors decrease, the strain starts to increase in the plastic zone. If the force continues to increase, the plastic zone starts to grow and if the failure criteria is reached material fails. In this case, the stress concentration factor will have a finite value. It is to be noted that the extreme cases, that is sharp cracks and infinite stress will not be the scope of this study due to time constraints.

The J integral is widely used as a fracture characterizing parameter for nonlinear materials. By idealizing elastic–plastic deformation as nonlinear elastic, G.P.Cherepanov in 1967 and James R. Rice in 1968 provided the basis for extending fracture mechanics methodology beyond the limits of *Linear Elastic Fracture Mechanics*. The loading behavior for both, nonlinear elastic and elastic-plastic, materials is identical in their work. But the material responses differ on the unloading path. The elastic–plastic material follows a linear unloading path with the slope equal to Young's modulus, while the nonlinear elastic material unloads along the same path as it was loaded. There is a unique relationship between stress and strain in an elastic material, but a given strain in an elastic–plastic material can correspond to more than one stress value if the material is unloaded or cyclically loaded. Consequently, it is much easier to analyze a nonlinear elastic material than a material that exhibits irreversible plasticity. As long as the stresses in both materials increase, the mechanical response of the two materials is identical.

When the problem is generalized to three dimensions, it does not necessarily follow that the

loading behavior of the nonlinear elastic and elastic–plastic materials is identical, but there are many instances where this is a good assumption. Thus an analysis that assumes nonlinear elastic behavior may be valid for an elastic–plastic material, provided no unloading occurs. Cherepanov and Rice independently applied deformation plasticity to the analysis of a crack in a nonlinear material. He showed that the nonlinear energy release rate, J, could be written as a path-independent line integral as

$$J = \int_{\Gamma} \left(wdy - T_i \frac{\partial u_i}{\partial x} ds \right). \tag{2.8}$$

Here, w is strain energy density, T_i are components of traction vector at the contour line, u_i are the displacement vector components and ds is a length increment along the contour Γ [12].

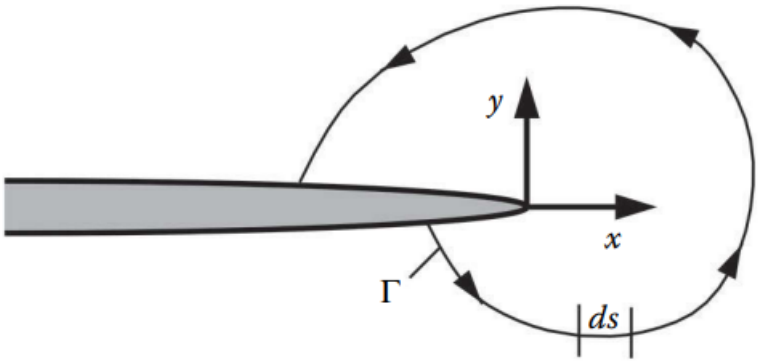

Figure 11: Arbitrary contour Γ around a crack

3 Numerical Solution

The finite element method is a numerical method for solving problems of engineering and mathematical physics. For physical systems involving complicated geometries, loadings, and material properties, it is generally not possible to obtain analytical mathematical solutions to simulate the response of the physical system. Analytical solutions are those given by a mathematical expression that yields the values of the desired unknown quantities at any location in a body (here total structure or physical system of interest) and are thus valid for an infinite number of locations in the body. These analytical solutions generally require the solution of ordinary or partial differential equations. Because of the complicated geometries, loadings, and material properties, the solution to these differential equations is usually not obtainable. Hence, we need to rely on numerical methods, such as the finite element method, finite difference method and finite volume method, that can approximate the solution to these equations. Here, we'll only use the finite element method

3.1 Finite Element Method

In finite element solutions (according either to any orthogonality or stationarity condition) finally we have to solve an equation system:

$$\mathbf{K}\underset{\sim}{u} = \underset{\sim}{f}. \tag{3.1}$$

Here, $\mathbf{K}$ is coefficient (e.g. stiffness) matrix of the analysed problem, while $\underset{\sim}{u}$ contains unknown nodal values. $\underset{\sim}{f}$ represent the boundary conditions, such as pressure, displacements, or temperature, that will be applied on nodes.

It should be noted that we can encounter also nonlinearities too, while solving FEM. In our current case, material is nonlinear, therefore stiffness matrix is nonlinear too. There are different methods to solve these nonlinear equations, one of the most important is the Newton-Raphson method. The details of this method will not be discussed here.

3.2 Plane Stress

Plane stress is used to model the thin steel plate. As the plane stress is generally applied, when the thickness of member is considerably smaller and the load acts in plane of member. Therefore, we use plane stress for analysis of thin steel plate. Plane stress can be defined as a stress state in which normal stress and shear stresses directed perpendicular to the plane of plate are assumed to be zero. If the plate is in $x-y$ *plane*, then the normal stress σ_z and shear stresses τ_{xz} and τ_{yz} are assumed to be zero.

3.3 Plane Strain

Along with plane stress, plane strain is also used for modeling select porosities.Contrary to plane stress, plane strain is applied when the thickness of member is considerably large. Plane strain can be defined as a strain state in which normal strain and shear strains directed perpendicular to plane of member are assumed to be zero. If the plate is in $x-y$ *plane*, then the normal stress ε_z and shear stresses γ_{xz} and γ_{yz} are assumed to be zero.

4 Finite Element Model

The finite element model always starts with building an accurate geometry which represents the actual physical problem. The next task is to perform a domain discretization. This process can affect the results adversely, the details of which will be discussed further in the study. After performing discretization, we can apply the boundary conditions for domain. Next step is to solve the set of equations which also requires a good understanding of the processes involved to get the maximum efficiency along with accuracy. Final step is to perform the post-processing of the solution and get required results.

4.1 Geometry

The domain to be analyzed using numerical simulation consists of a rectangular plate with either circular or elliptical holes placed at the random positions in rectangular plate. Figure 12

shows the rectangular plate.The parameters of the rectangular plate are as follows.

$$\begin{aligned} \text{Width} &= 50\,\text{cm}, \\ \text{Height} &= 150\,\text{cm}, \\ \text{Thickness} &= 1\,\text{cm}. \end{aligned}$$

Figure 12: Rectangular Geometry

For geometries with circular holes, five random geometries were created for each of $n = [1, 2, 10, 100, 1000]$, if possible to fit the holes within rectangular plate. Table 2 and 3 shows the radii for each n corresponding to different porosity variations. Porosity is defined as ratio of area of holes to the total area of rectangular domain.

Porosity	n	r [mm]
1.5%	1	60
	2	42.3
	10	18.9
	100	6
	1000	1.89
6%	1	120
	2	84.6
	10	37.8
	100	12
	1000	3.78
24%	1	240
	2	170
	10	76
	100	23.9
	1000	7.57
40%	2	218.5
	10	97.7
	100	30.9
	1000	9.78

Table 1: Circular hole geometries

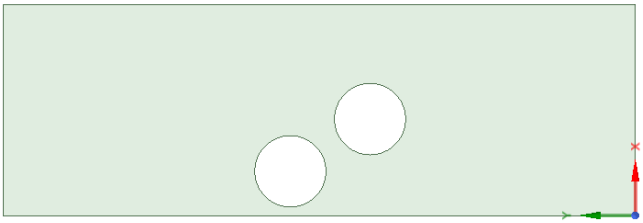

(a) 6% Porosity

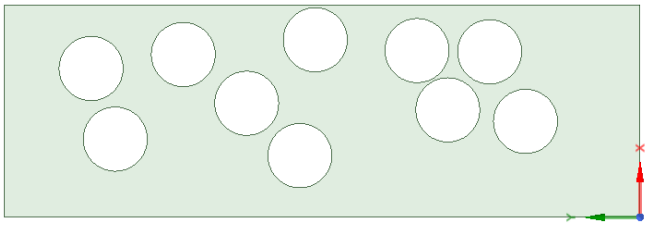

(b) 24% Porosity

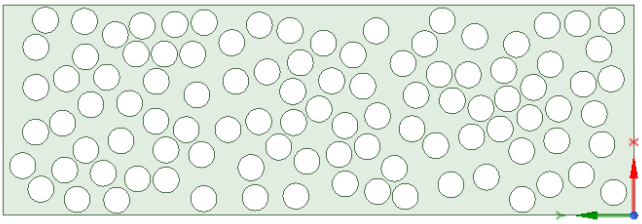

(c) 40% Porosity

Figure 13: Examples of circular hole geometries

For geometries with elliptical holes, five random geometries were created for each of $n = [1, 2, 10, 100, 500]$, if possible to fit the holes within rectangular plate. The number of holes for ellipsis were reduced because of the difficulties in discretizing and solving the problems with larger number of elliptical holes. Table 1 shows the radii for each n corresponding to different porosity variations.

Porosity	n	a [mm]
1.5%	1	134
	2	94.6
	10	42.3
	100	13.4
	500	5.98
6%	2	189.2
	10	84.6
	100	26.8
	500	1.20
24%	10	169
	100	53.5
	500	23.9
40%	10	218.5
	100	69.1
	500	30.9

Table 2: Elliptical hole geometries with axis ratio $b : a = 1 : 5$

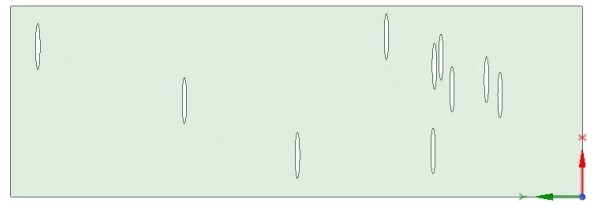

(a) 24% Porosity

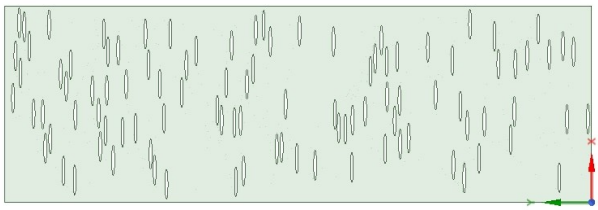

(b) 40% Porosity

Figure 14: Examples of elliptical hole geometries with $b : a = 1 : 5$

Porosity	n	a [mm]
1.5%	1	189
	2	133.8
	10	59.8
	100	18.9
	500	8.46
6%	10	119.7
	100	37.8
	500	16.9
24%	10	239.4
	100	75.7
	500	33.8
40%	100	97.7
	500	43.7

Table 3: Elliptical hole geometries with $b : a = 1 : 10$

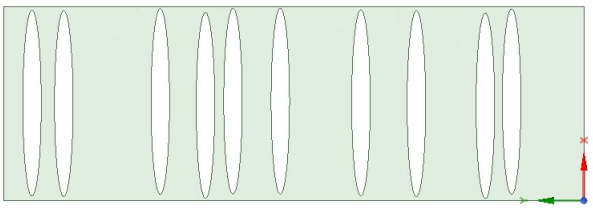

(a) 24% Porosity

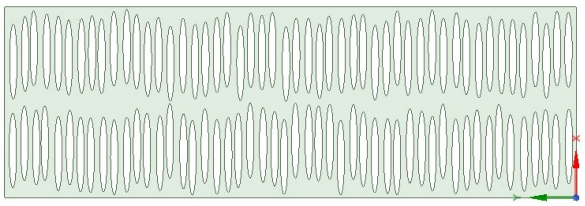

(b) 40% Porosity

Figure 15: Examples of elliptical hole geometries with $b : a = 1 : 10$

There is a constrain for the edge of circles or ellipse. The minimum distance between the edges of circular or elliptical holes to any rectangular edge is set to 5 mm.

Creation of Geometry

An important aspect of the geometry creation was to decide on which algorithm should be used for placing holes at random places in geometry. There are different solutions possible that can

be used to place random circular holes in a rectangle. Some algorithms simulate the particles to fall into the rectangle under gravity and then allow them to become stable. But for the purpose of this study, to place circles and ellipsis a a geometric algorithm was used in which a random point was selected in range of $(x,y) = ([5+r, 495-r], [5+r, 1495-r])$ shown in Figure 16.

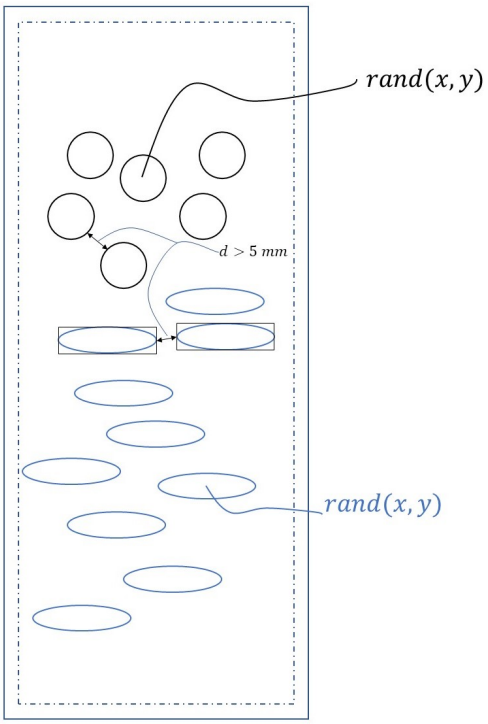

Figure 16: Constrained geometry for holes

Then, the circle was placed if the boundary of the circle didn't intersect with any other circle. A constraint was also introduced here to have the boundary of two circles to be at least 5 mm away from each other. This works well for lower porosity and less number of circles. But for higher porosity and more number of circles, the placement can't work under these conditions. For this reason, rectangular regions were created to divide the rectangular domain into smaller regions (as in Figure 17), so that the placement of holes could be done easily.

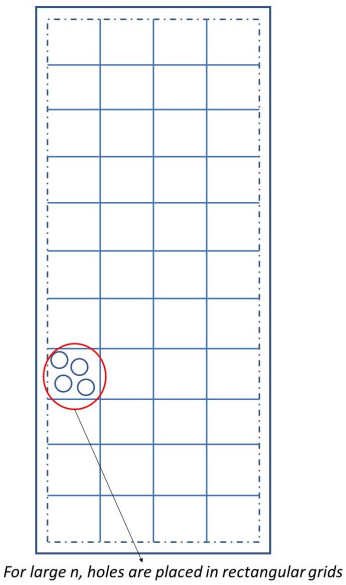

Figure 17: Rectangular grids for large number of holes

Geometric placement rule used for circles is quite simple as the distance between center of two circles should be greater than the diameter plus the boundary constraint that is applied. But in case of ellipsis, it is a bit complex. The complexity of it was avoided by using a rectangle around the elliptical boundary with width and height equal to major axis plus the boundary constraint and minor axis plus the boundary constraint respectively.

The script to generate the coordinates for center of circular and elliptical holes was written in *MATLAB*, while all the geometries were created in *Ansys SpaceClaim* using a Python script. See Appendix B for the codes attached.

4.2 Discretization

All the geometries were discretized using *Ansys* **PLANE183** element. Figure [18] shows the geometry of PLANE183 element. PLANE183 element is a quadratic 2-D element with either 8 nodes or 6 nodes. In this study, both the arrangements with 8 and 6 nodes were used. 8 node elements were used for $n \leq 100$ while 6 node elements were used for $n > 100$. It should be noted that if $KEYOPT(1)$ is not set to 1, then all the triangular elements will be degenerated rectangular elements with 8 nodes. PLANE183 has quadratic displacement behavior and is well suited to modeling irregular meshes. This element is defined by eight nodes or six nodes. It can be used as a plane element (plane stress, plane strain and generalized plane strain) or as an axisymmetric element (with or without torsion). In most cases, the element has two degrees of freedom at each node: translations in the nodal x and y directions. It should be noted that the element can be used for plasticity, hyperelasticity, creep, stress stiffening, large strain and large strain [13]. In this study, this element was used for both linear hardening plasticity and large strain cases.

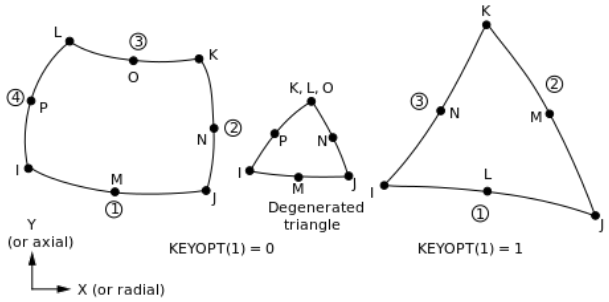

Figure 18: Geometry of *PLANE183* Element

Generating a correct mesh is quite important and a difficult task in solution of FEM problem. Having a coarse mesh could render all your results incorrect. The general trend is that accuracy of a solution increases with increasing the fineness of mesh, that is by having smaller and smaller elements. By decreasing element size could achieve more and more accurate results, but the first question to be asked here is how much error in the solution could be safely ignored. The reason for this question is that by increasing mesh fineness, the time and computational cost for solution increase a lot. Also, the space required to store all the results increases in similar proportion. So, we have to find a trade off between the mesh fineness and accurateness of solution.

To be able to find the point where we could get our desired accuracy at smallest possible number of nodes, a **mesh convergence study** needs to be done. The process of mesh convergence involves decreasing the element size and analyzing the impact of this process on the accuracy of the solution. In current study, mesh convergence study can't be performed for each single geometry. Therefore, we did the mesh convergence for a few geometries. These results gave us a good approximation of the parameters that we should use for mesh while keeping our solutions accurate.

Different methods were used for creation of mesh. In first method, an inflation layer with a maximum aspect ratio of 3 was used around all the hole boundaries. In the second method, a rectangular face was created around the boundary of hole with an offset and then a fine mesh was generated for that face. Both the methods, lead to similar results. The parameters used for mesh are as follows

$$\begin{aligned} \text{Global Element Size} &= 20\,\text{mm}, \\ \text{Number of Inflation Layers} &= 2-5, \\ \text{Thickness of Inflation Layer} &= 1-5\,\text{mm}. \end{aligned}$$

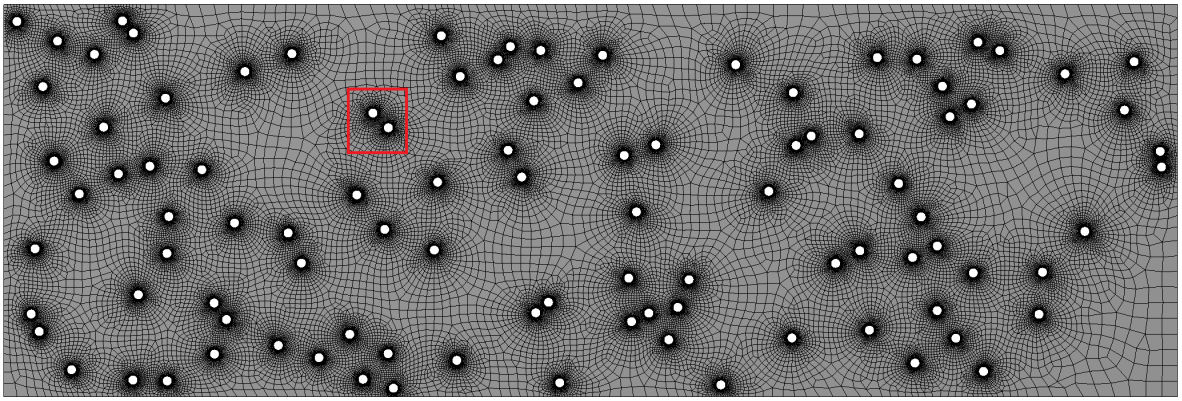

(a) Mesh of circular hole porosity variation

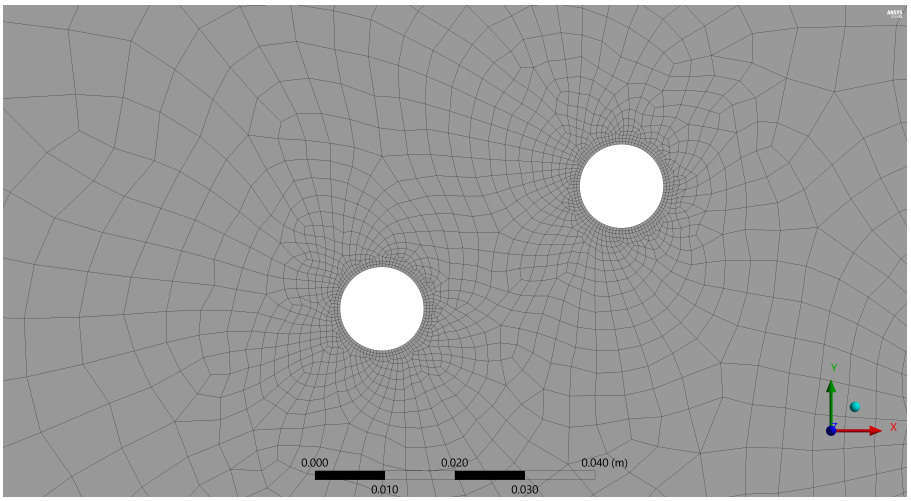

(b) Zoomed Red Rectangular Area

Figure 19: Mesh of plate with 100 circular holes

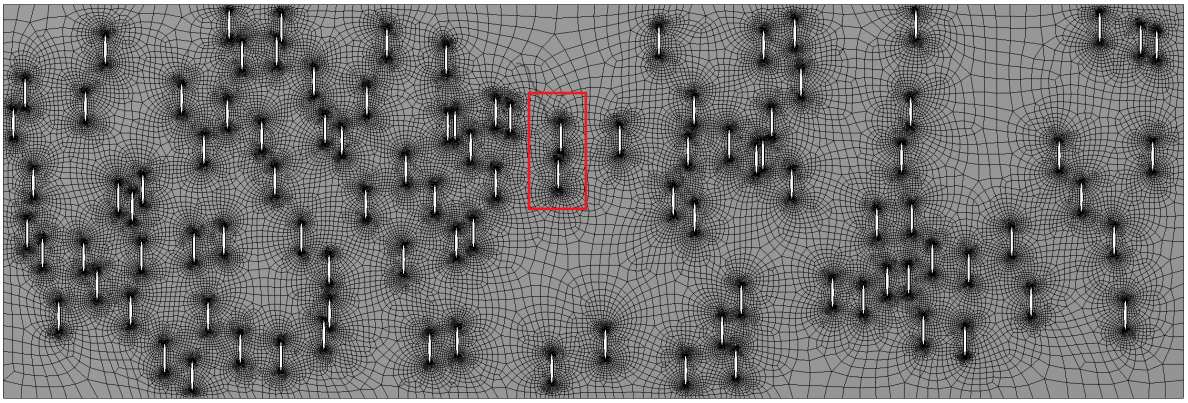

(a) Mesh of elliptical hole porosity variation

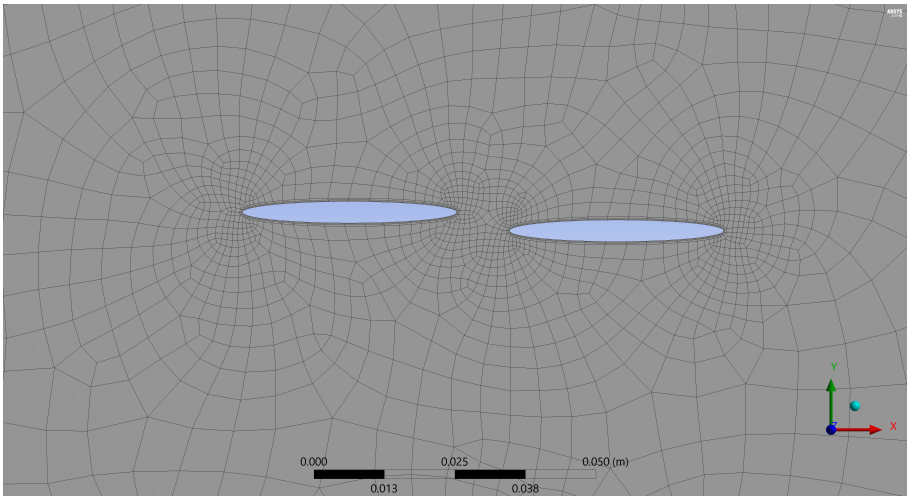

(b) Zoomed Red Rectangular Area

Figure 20: Mesh of plate with 100 elliptical holes

4.3 Boundary Conditions

Boundary conditions in FEM are actually the boundary conditions of *PDEs*. Models in FEM are mathematical representation of a physical phenomenon happening. So, the choice of boundary conditions also comes with approximations that best represent the actual physical conditions. Also, an important thing is that even when we apply a continuous boundary condition, FEM then applies those boundary conditions on discretized nodes.

In our case, all the boundary nodes are restricted in only x direction, except one node which is restricted in both, x and y, directions as shown in Figure 21. The benefit of using this boundary condition is that we'll not have any stress disturbances in the plate as shown in Figure 22.

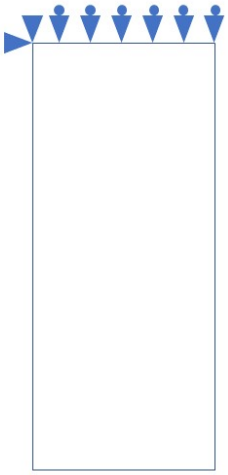

Figure 21: Boundary Conditions of Analyzed Problem

(a) Stress distribution around support for applied support condition

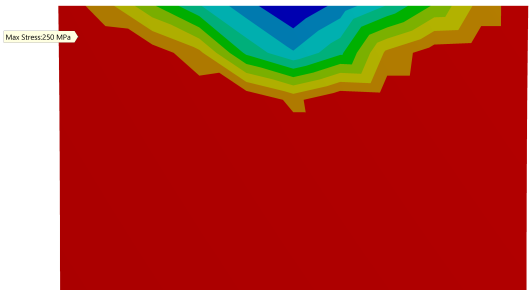

(b) Stress distribution around support for all nodes with hinge support

Figure 22: Stress distribution differences due to support disturbance

4.4 Load bearing capacity calculation

To calculate load bearing capacity, load is applied in small time-steps until the **maximum strain reaches the 2.5‰ limit for the small strain case**. The value for which the **strain limit is reached is defined as load bearing capacity of steel plate**. Load is applied as pressure normal to the lower edge of plate which is similar to uniaxial tension. For the large strain problem analyzed, prescribed displacement is applied in small steps. The load bearing capacity in this case is then extracted from the prescribed displacement value.

5 Numerical Simulation Results

After an explanation into the setting up of Finite Element Model for the current problem. After performing solutions for all the different variations. Stress and strain diagrams at the yield loading and ultimate loading were plotted for all the variations of the problems analyzed. $\sigma - \varepsilon$ diagrams and $F_l - \varepsilon$ diagrams were also plotted.

Different variations of the problem that were analyzed are as follows

- 1.5%, 6%, 24% and 40% porosity variations were analyzed for circular holes placed at

random positions.

- 1.5%, 6%, 24% and 40% porosity variations were analyzed for elliptical holes with $\mathbf{b/a = 1/5}$ placed at random positions.
- 1.5%, 6%, 24% and 40% porosity variations were analyzed for elliptical holes with $\mathbf{b/a = 1/10}$ placed at random positions.
- 24% porosity variation was analyzed for *plane strain* problem for circular holes placed at random positions.
- 6% and 24% porosity variation were analyzed for *large strain* problem for circular holes placed at random positions.

Since, the main aim of this study is to present a mathematical approximation of LB capacity transition from solid to porous material, therefore regression analysis was done to get a function dependent on n, so that LB capacity can be given as a function of n.

$$\text{LB Capacity} = f(n). \tag{5.1}$$

Regression analysis is the process of finding the relationship between a dependent variable, in this case n, and outcome which in this case is *LB capacity*. There are different types of regression analysis, so choice of type of regression is quite important. The most simple form of the regression is linear regression. A nonlinear function can also be approximated by linearizing the nonlinear function. In this case, the function chosen for regression is as follows

$$f = \frac{p_1 \cdot x + p_2}{x + q_1}. \tag{5.2}$$

Here, p_1, p_2 are the coefficients of linear term in numerator while q_1 is coefficient for denumerator.

5.1 Circular Holes

In case of circular holes, we had five different geometric variations for each n. These variations were then analyzed for both *Material 1* and *Material 2*. The LB capacity for all these cases is shown in Figures 23 and 24. The figures show us the transition from *solid* to *porous* model. From the figures, it can be seen that the solid model for **Material 1 has LB capacity of** 2500 kN/m while **Material 2 has LB capacity of** 3250 kN/m. After we start adding holes, the LB capacity first drastically decreases for smallest n, as we start increasing n then the LB capacity starts to increase.

In case of smallest number of holes, the stress concentration is maximum but when we start increasing the number of holes, the stress concentration decreases, which results in an increase in LB capacity.

An important deduction can be made here about the LB capacity that if we start increasing the number of holes in a body for a given porosity, then after a certain limit, the **LB capacity of body starts to become independent of position of the holes**. This can be seen in Table [4] as we start to increase the number of holes from $n = 1 \rightarrow 1000$, then the general trend is that the mean value of LB capacity starts to increase while the standard deviation starts decreasing.

By using the regression analysis for the LB capacity data, we get regression curves as shown in Figures [25,26]. The regression functions we get are given below.

For Material 1

$$f(n,1.5) = \frac{2450 \cdot n + 4.33 \cdot 10^6}{n + 4062.5}, \tag{5.3}$$

$$f(n,6) = \frac{2282.94 \cdot n + 3.5 \cdot 10^6}{n + 5090.74}, \tag{5.4}$$

$$f(n,24) = \frac{1604.68 \cdot n + 7.54 \cdot 10^5}{n + 3730.92}, \tag{5.5}$$

$$f(n,40) = \frac{1000.6 \cdot n + 1.26 \cdot 10^5}{n + 1447.27}. \tag{5.6}$$

Now, for Material 2

$$f(n,1.5) = \frac{3193.01 \cdot n + 8.64 \cdot 10^6}{n + 7896.42}, \tag{5.7}$$

$$f(n,6) = \frac{2971.3 \cdot n + 5.19 \cdot 10^6}{n + 6506.21}, \tag{5.8}$$

$$f(n,24) = \frac{2087.67 \cdot n + 1.06 \cdot 10^6}{n + 4394.14}, \tag{5.9}$$

$$f(n,40) = \frac{1301.36 \cdot n + 1.79 \cdot 10^5}{n + 1700.72}. \tag{5.10}$$

From the above equations, we can see that in regression analysis **coefficient p_1 converges to the value of approximated value of LB capacity** calculated from the Gurson's model.

Table 4: LB Capacity of geometry with circular holes

Porosity	n	LB capacity[kN/m]			
		Material 1		Material 2	
		Mean	SD	**Mean**	SD
1.5%	1	**704.00**	261.81	**806.40**	293.10
	2	**1041.25**	118.31	**1204.00**	136.34
	10	**917.50**	204.70	**1062.25**	234.43
	100	**948.20**	21.16	**1097.60**	38.53
	1000	**1212.60**	54.68	**1328.40**	53.22
6%	1	**462.50**	182.83	**533.90**	209.80
	2	**694.80**	212.80	**807.50**	236.90
	10	**733.00**	247.25	**861.25**	290.79
	100	**695.20**	44.95	**809.60**	47.46
	1000	**950.40**	25.32	**1088.00**	25.30
24%	1	**67.86**	6.19	**79.00**	10.55
	2	**270.60**	69.05	**315.00**	79.14
	10	**190.80**	54.60	**227.00**	65.73
	100	**322.40**	18.89	**383.00**	22.25
	1000	**487.00**	6.71	**570.00**	7.50
40%	2	**72.19**	20.39	**86.80**	23.48
	10	**91.60**	29.87	**108.90**	34.66
	100	**170.66**	19.13	**201.96**	22.38
	1000	**389.40**	86.13	**464.40**	102.49

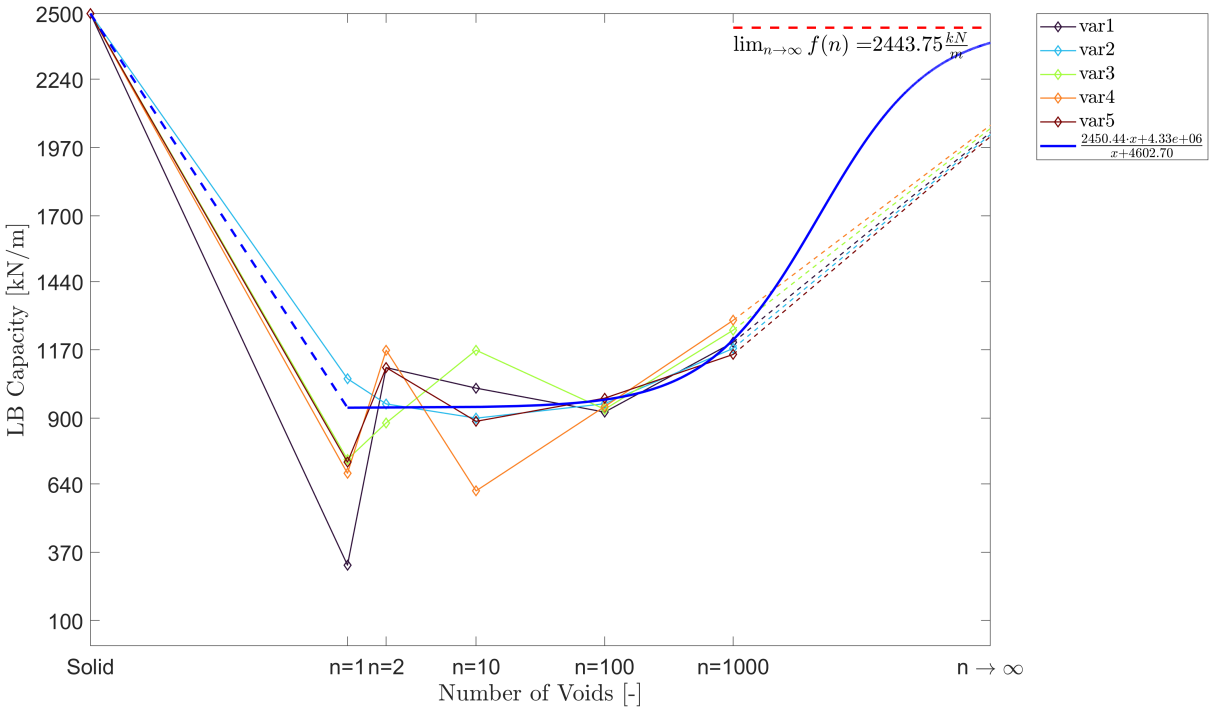

(a) 1.5% Porosity

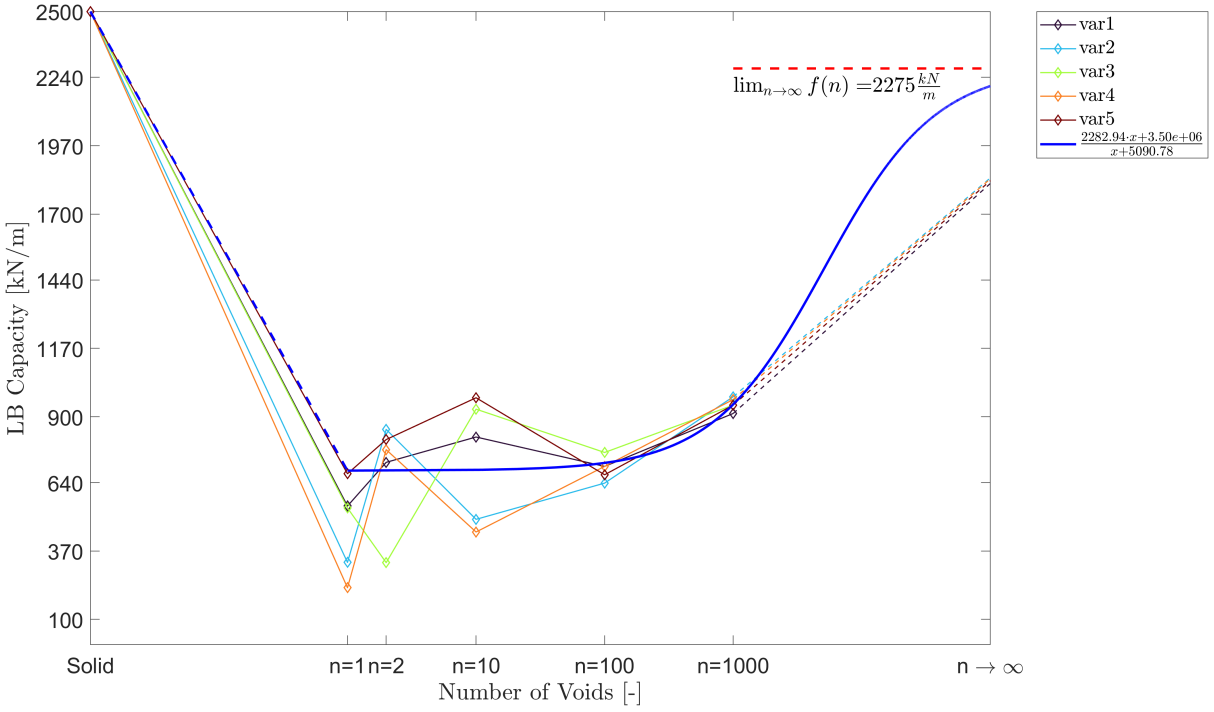

(b) 6% Porosity

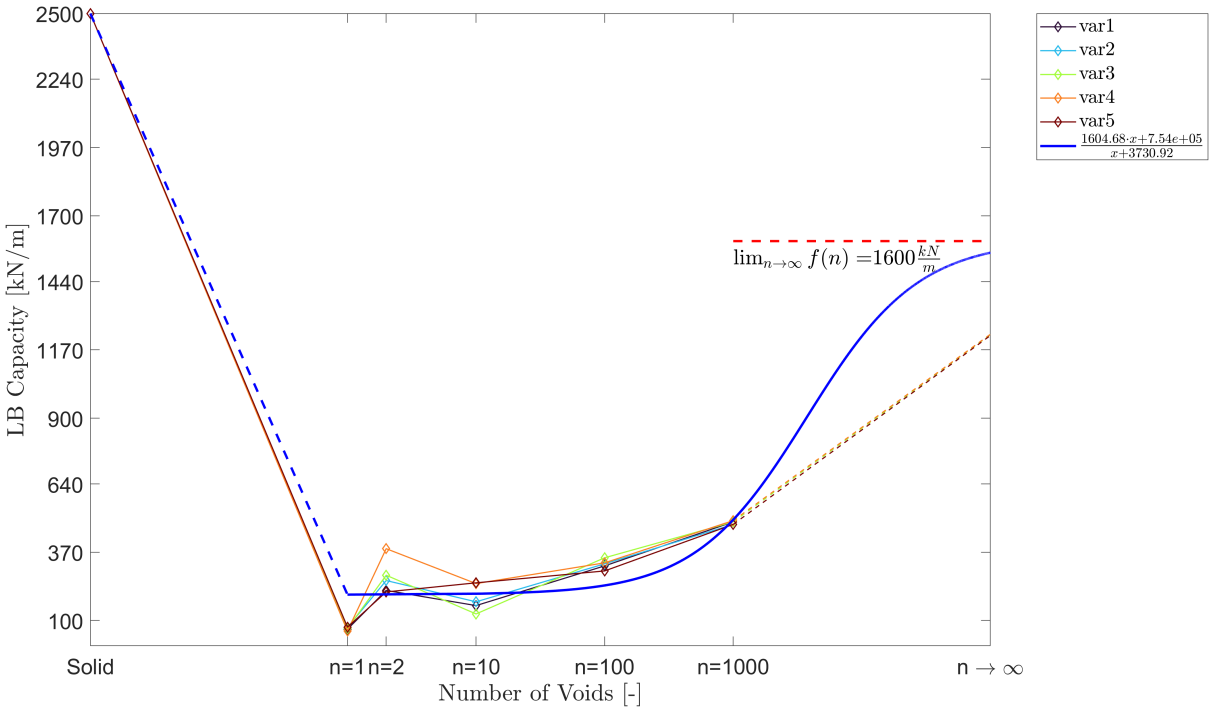

(c) 24% Porosity

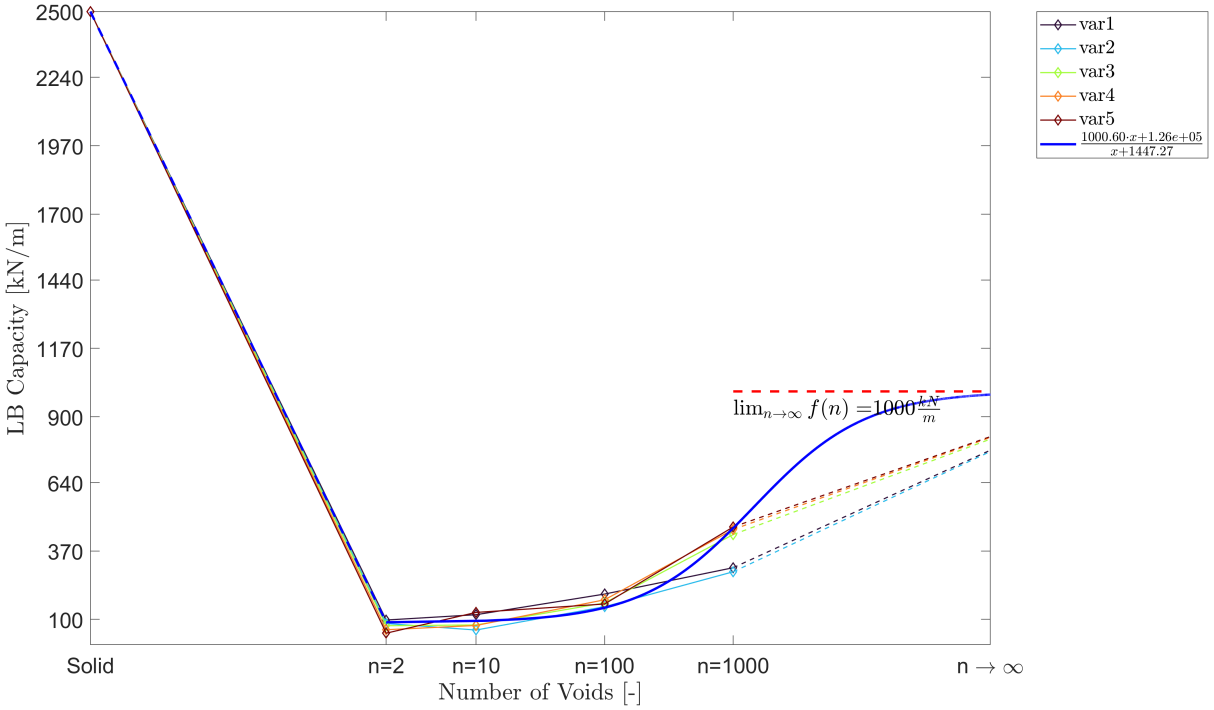

(d) 40% Porosity

Figure 23: LB capacity of *Material 1* for circular holes

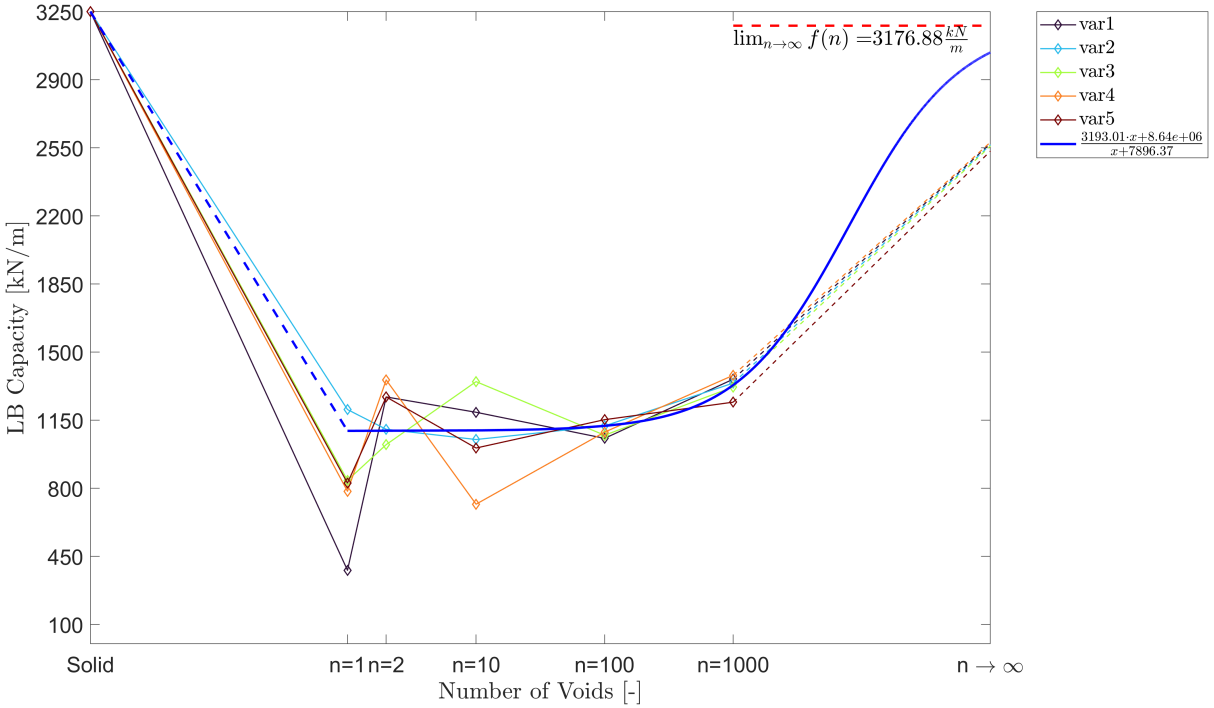

(a) 1.5% Porosity

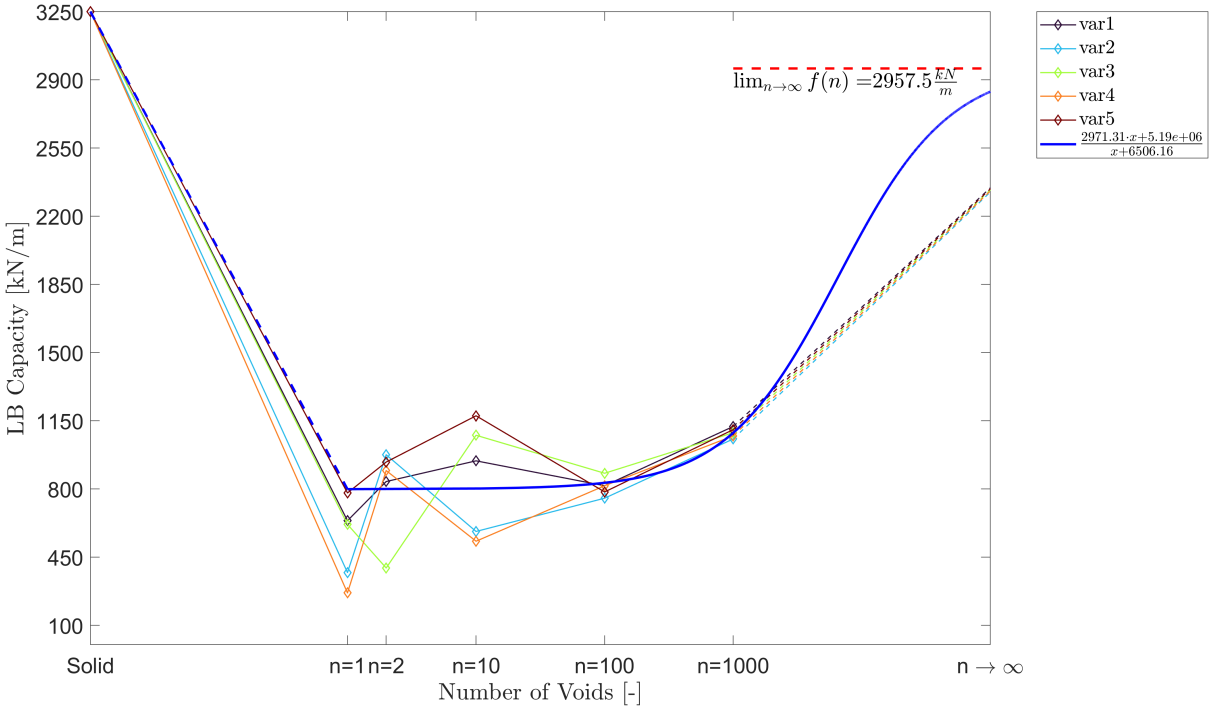

(b) 6% Porosity

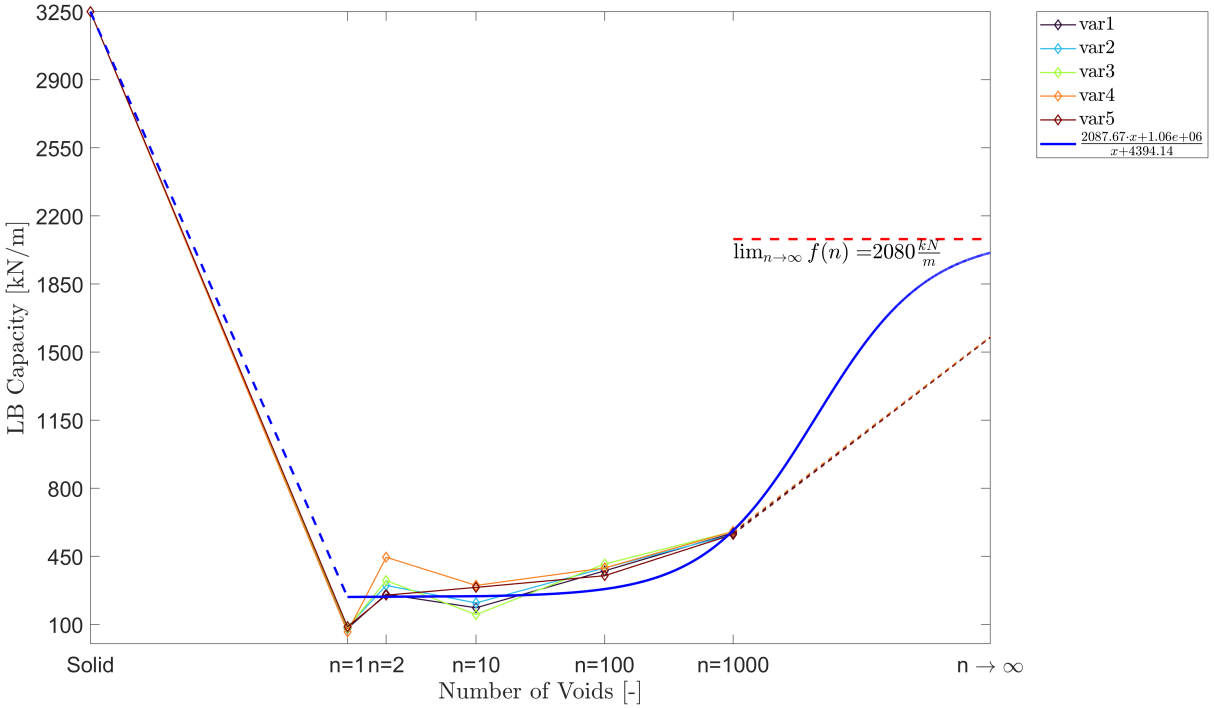

(c) 24% Porosity

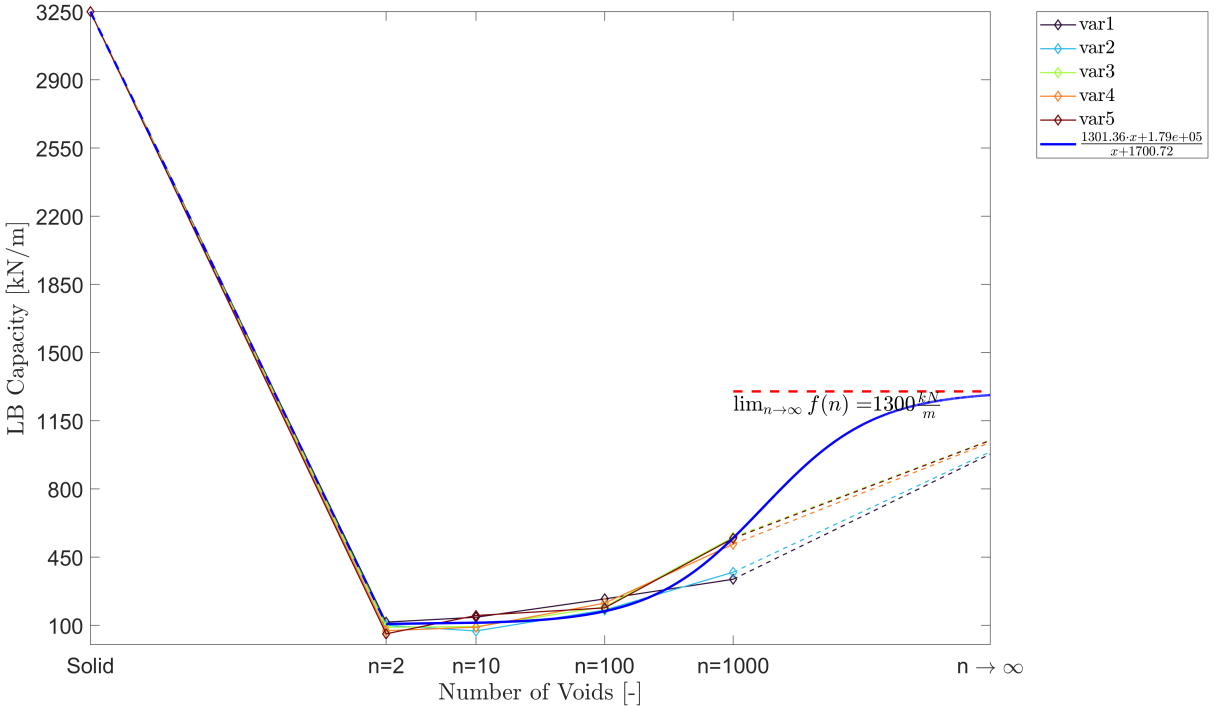

(d) 40% Porosity

Figure 24: LB capacity of *Material 2* for circular holes

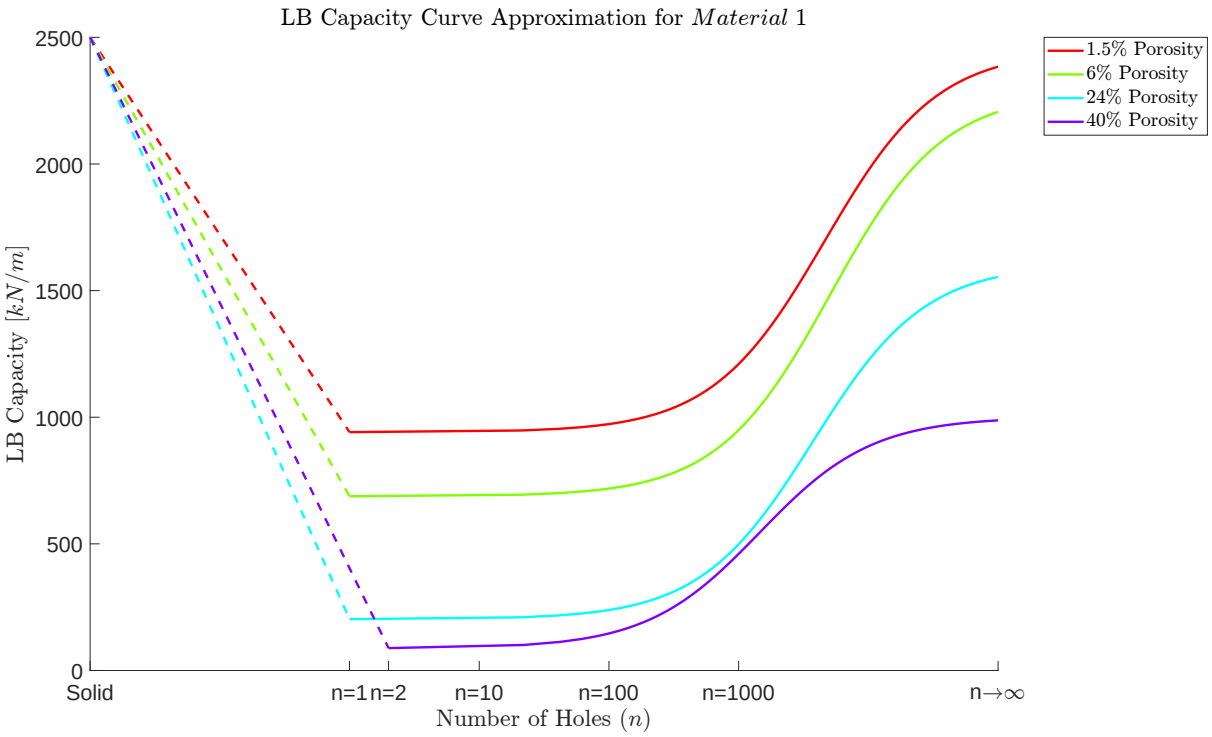

Figure 25: Regression curves for LB capacity of *Material 1* for circular holes

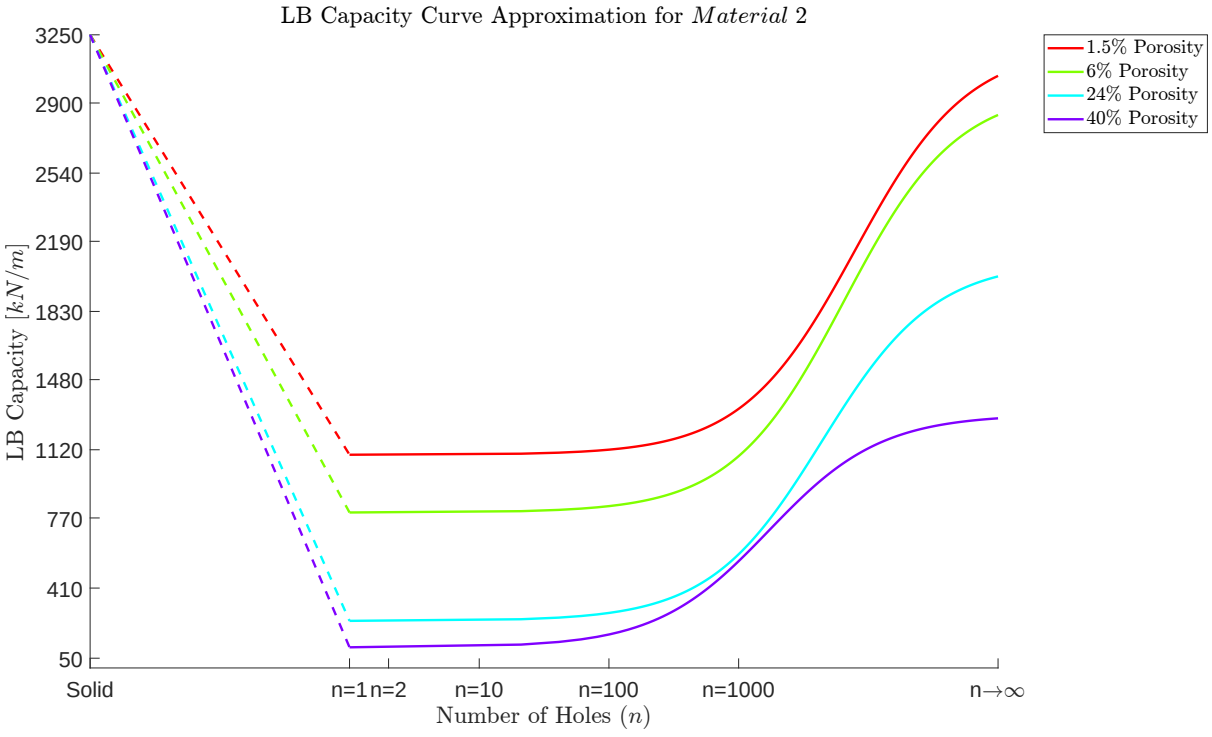

Figure 26: Regression curves for LB capacity of *Material 2* for circular holes

5.2 Elliptical Holes

In case of elliptical holes, **two different elliptical holes and five different geometric variations** for each n were created. These variations were then analyzed for both *Material 1* and

Material 2. The LB capacity for all these cases is shown in Figures [27,28,29,30]. The figures show us the transition from *solid* to *porous* model. It should be noted that the approximated value of LB capacity is actually calculated for a 3-D stress state with spherical holes placed in the continuum. But for the purpose of this study, the approximation is also considered for the elliptical holes as well. The geometries with smaller axis ratio will have higher LB capacity than the ones with larger axis ratio as can be seen in Tables [5,6]. The reason for this is that the radius of curvature of tip of ellipse with smaller axis ratio is higher, which results in a lower stress concentration factor.

Like circular holes, in case of smallest number of holes, the stress concentration is maximum but when we start increasing the number of holes, the stress concentration decreases, which results in an increase in LB capacity. Also the deduction about the independence of load bearing capacity from the position of holes for higher n is same.

By using the regression analysis for the LB capacity data, we get regression curves as shown in Figures [31,32]. The regression analysis was done only for $a/b = 1:5$. Regression functions are as follows.

For Material 1

$$f(n,1.5) = \frac{2471.89 \cdot n + 2.69 \cdot 10^6}{n + 12617.28}, \tag{5.11}$$

$$f(n,6) = \frac{2354.61 \cdot n + 4.83 \cdot 10^6}{n + 37113.59}, \tag{5.12}$$

$$f(n,24) = \frac{1600 \cdot n + 4.68 \cdot 10^5}{n + 23096.86}, \tag{5.13}$$

$$f(n,40) = \frac{1000 \cdot n + 3.49 \cdot 10^5}{n + 10338.12}. \tag{5.14}$$

Now, for Material 2

$$f(n,1.5) = \frac{3222.22 \cdot n + 3.79 \cdot 10^6}{n + 15470.14}, \tag{5.15}$$

$$f(n,6) = \frac{3040.91 \cdot n + 4.08 \cdot 10^6}{n + 29581.32}, \tag{5.16}$$

$$f(n,24) = \frac{2137.94 \cdot n + 7.3 \cdot 10^5}{n + 28209.07}, \tag{5.17}$$

$$f(n,40) = \frac{1315.47 \cdot n + 4.73 \cdot 10^5}{n + 12264.43}. \tag{5.18}$$

Table 5: LB Capacity of geometry with elliptical holes ($b/a = 1/5$)

Porosity	n	LB capacity[kN/m]			
		Material 1		Material 2	
		Mean	SD	Mean	SD
1.5%	1	**180.00**	79.65	**204.60**	91.32
	2	**261.60**	45.40	**299.20**	51.09
	10	**187.60**	61.94	**215.70**	71.42
	100	**228.10**	31.99	**266.70**	39.44
	500	**299.60**	3.99	**337.50**	8.42
6%	2	**133.10**	17.46	**150.40**	18.46
	10	**148.00**	46.00	**126.00**	26.31
	100	**129.50**	19.69	**150.50**	27.52
	500	**161.70**	16.30	**186.80**	15.79
24%	10	**16.60**	8.74	**19.68**	10.03
	100	**25.60**	2.97	**33.26**	1.52
	500	**54.06**	2.52	**63.00**	3.26
40%	10	**36.40**	10.91	**41.75**	11.85
	100	**40.48**	10.26	**46.00**	11.09
	500	**78.80**	6.61	**89.10**	8.39

Table 6: LB Capacity of geometry with elliptical holes ($b/a = 1/10$)

Porosity	n	LB capacity[kN/m]			
		Material 1		Material 2	
		Mean	SD	Mean	SD
1.5%	1	**71.90**	18.58	**83.40**	21.15
	2	**103.60**	29.75	**118.80**	33.58
	10	**110.80**	32.21	**123.60**	34.75
	100	**145.20**	30.09	**158.40**	31.71
	500	**192.00**	13.04	**226.50**	15.27
6%	10	**57.30**	14.29	**66.00**	16.92
	100	**58.66**	22.97	**65.00**	25.20
	500	**69.20**	7.01	**79.60**	6.84
24%	10	**16.42**	8.42	**18.90**	9.66
	100	**26.40**	1.95	**28.00**	1.41
	500	**20.34**	2.17	**23.00**	1.90
40%	100	**21.58**	8.80	**24.75**	10.09
	500	**52.60**	5.37	**61.00**	2.12

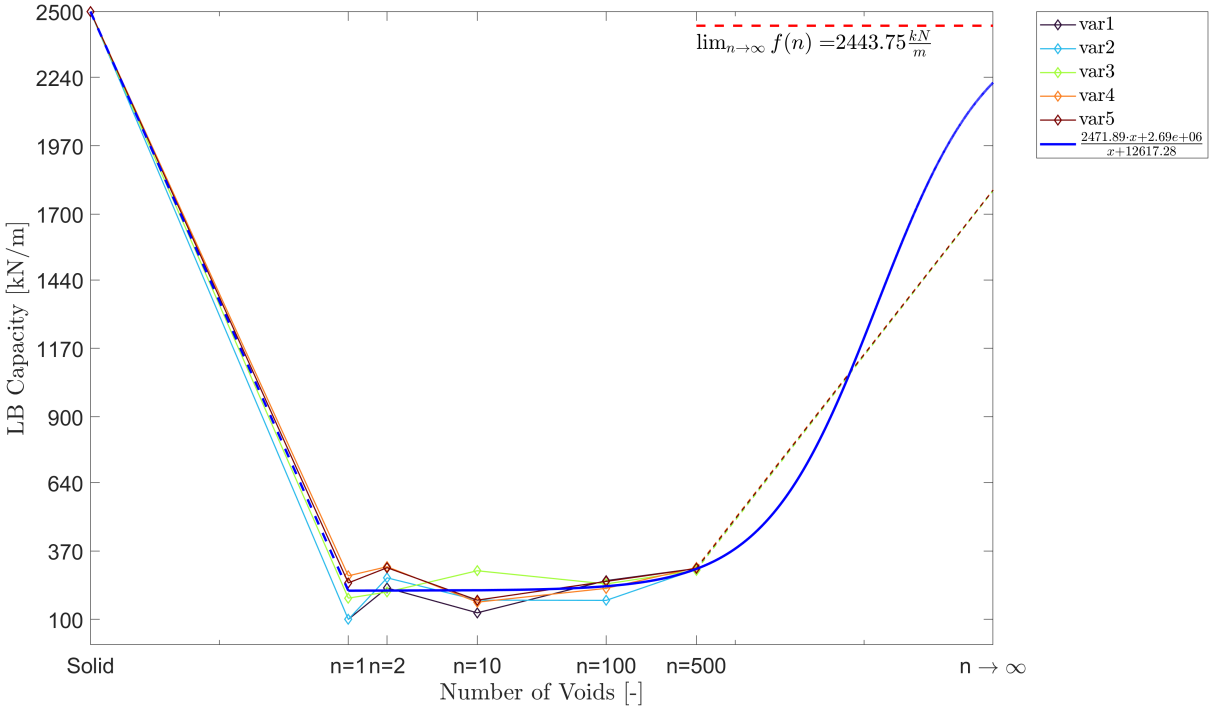

(a) 1.5% Porosity

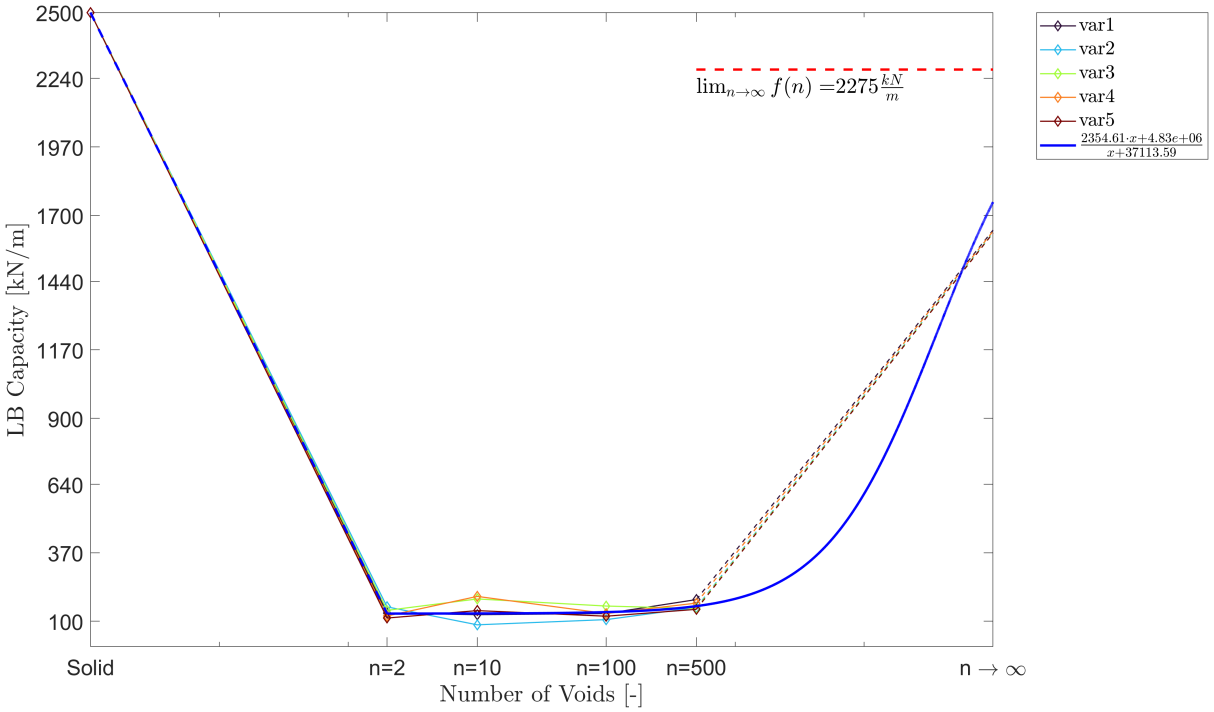

(b) 6% Porosity

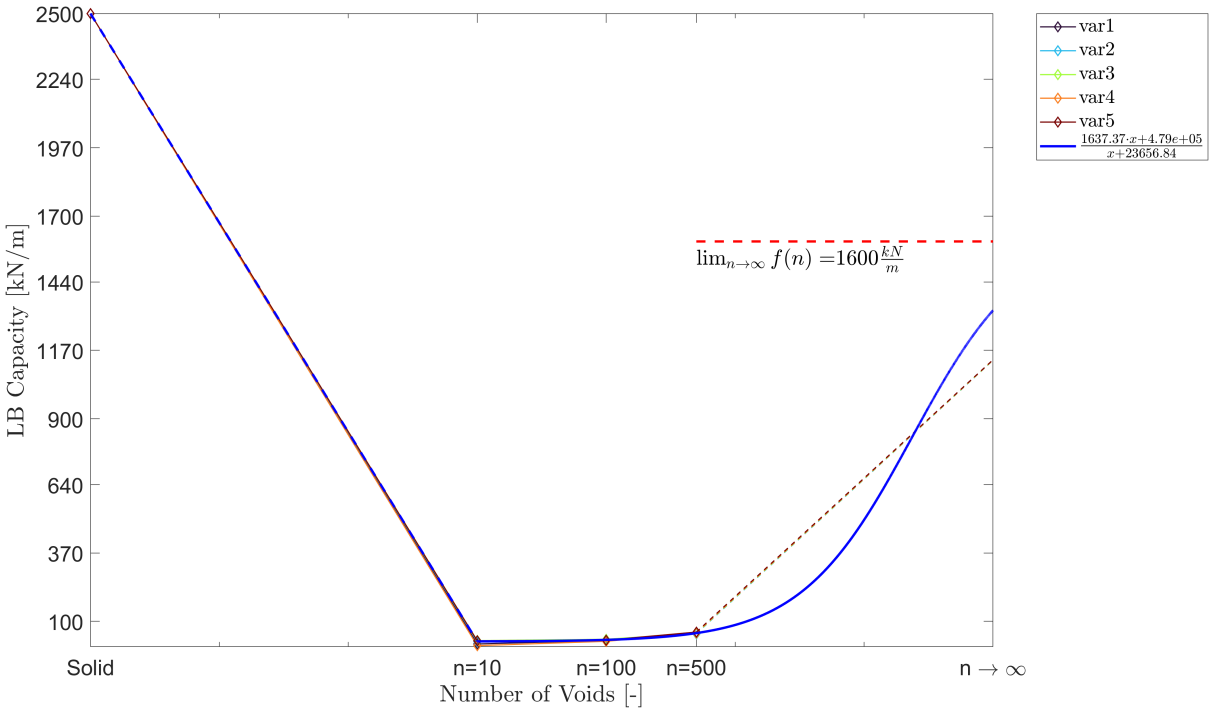

(c) 24% Porosity

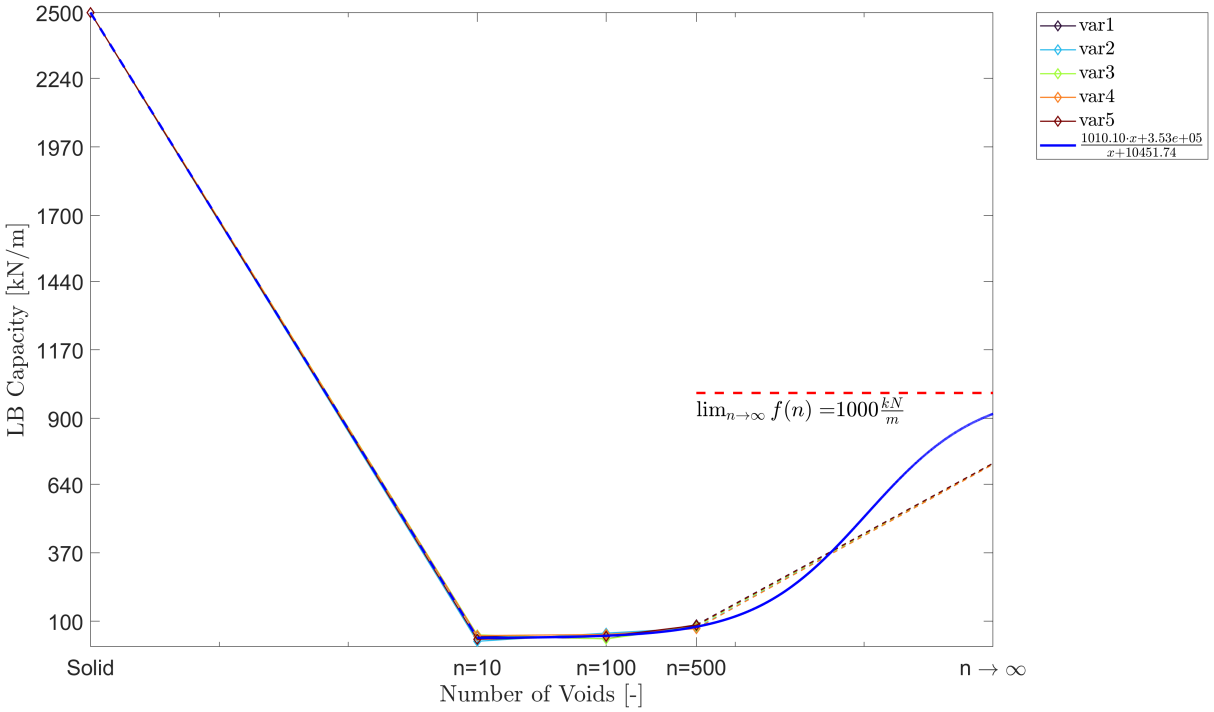

(d) 40% Porosity

Figure 27: LB capacity of *Material 1* for elliptical holes with $b/a = 1/5$

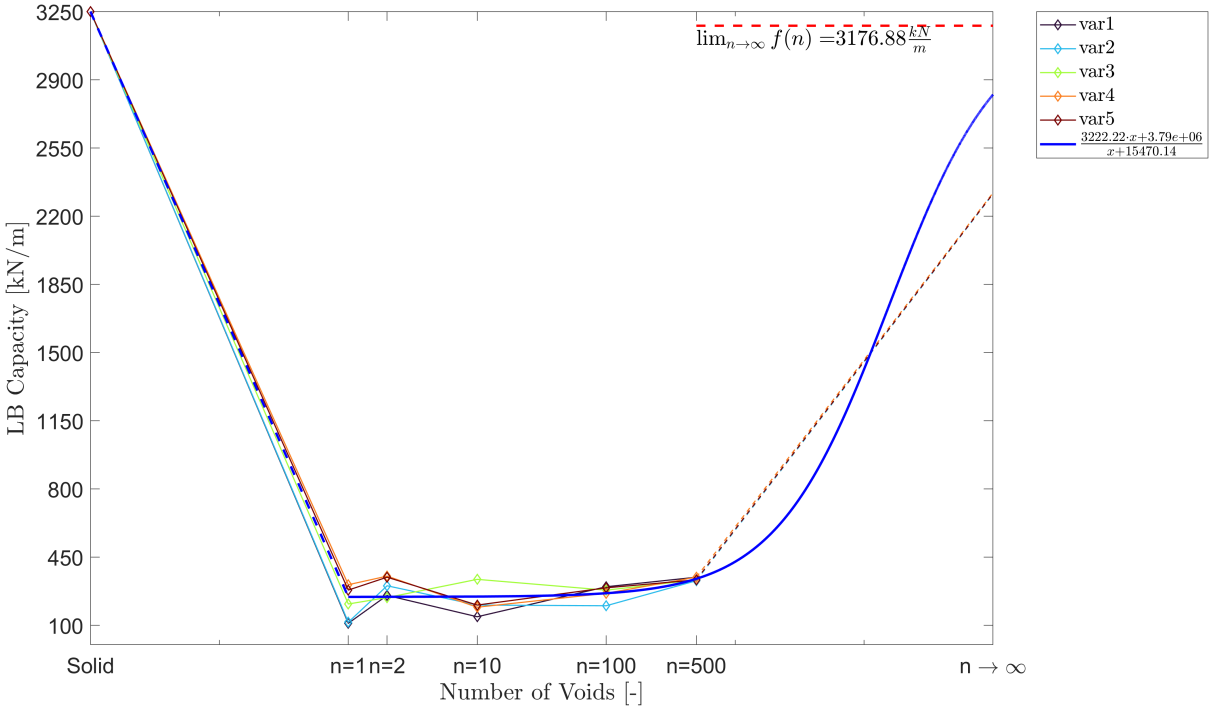

(a) 1.5% Porosity

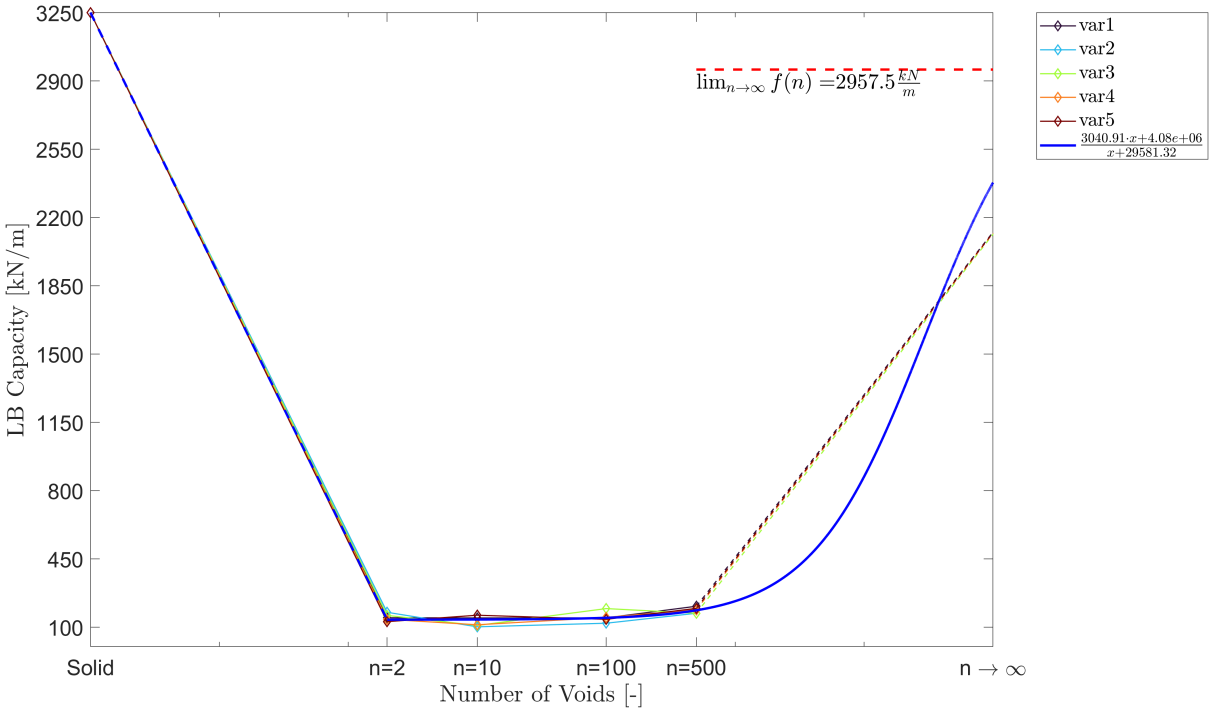

(b) 6% Porosity

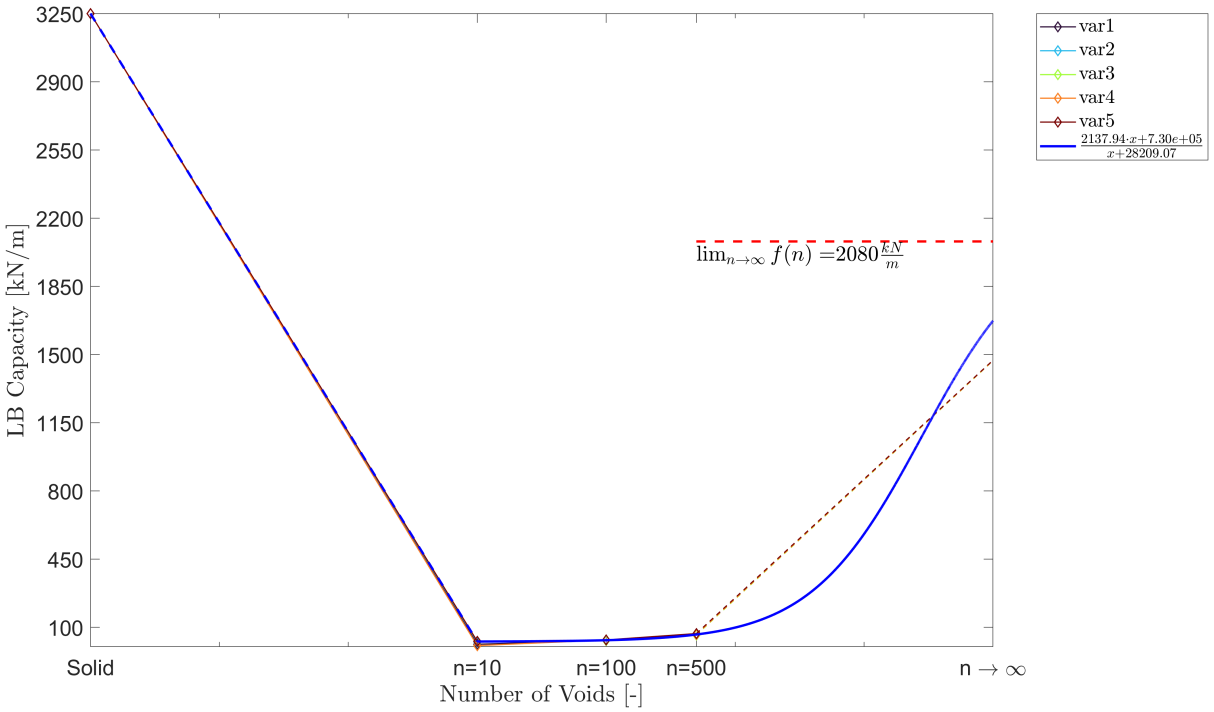

(c) 24% Porosity

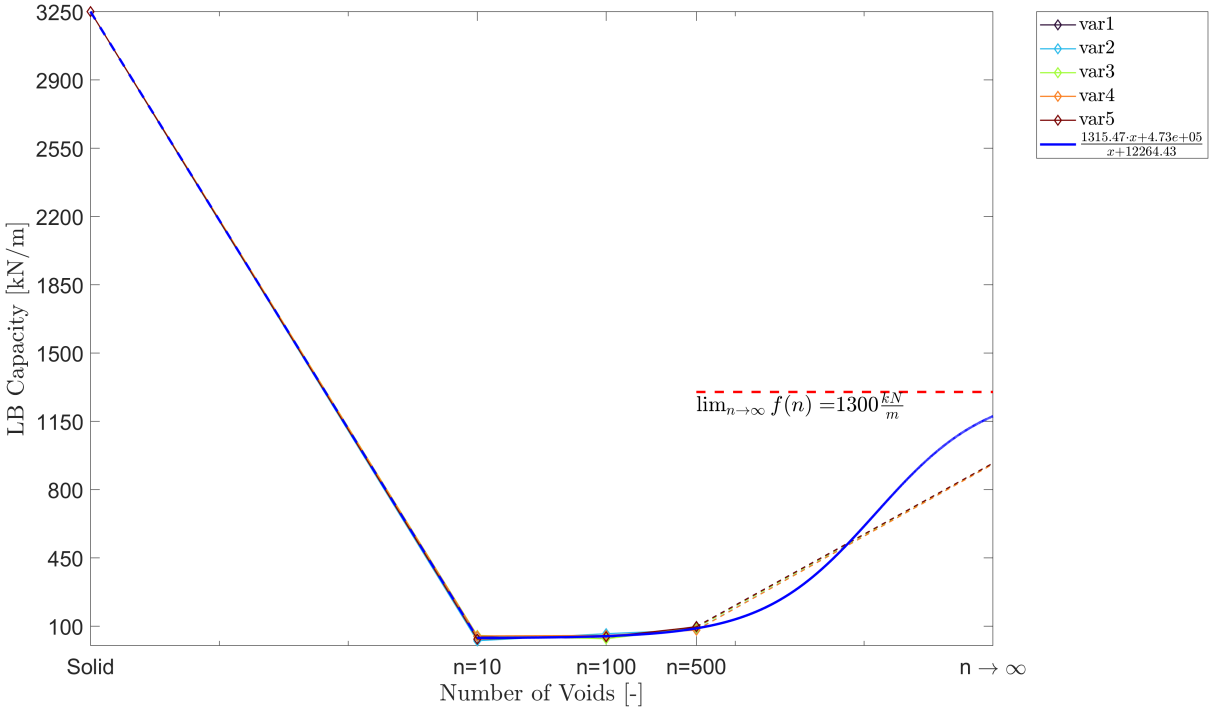

(d) 40% Porosity

Figure 28: LB capacity of *Material 2* for elliptical holes with $b/a = 1/5$

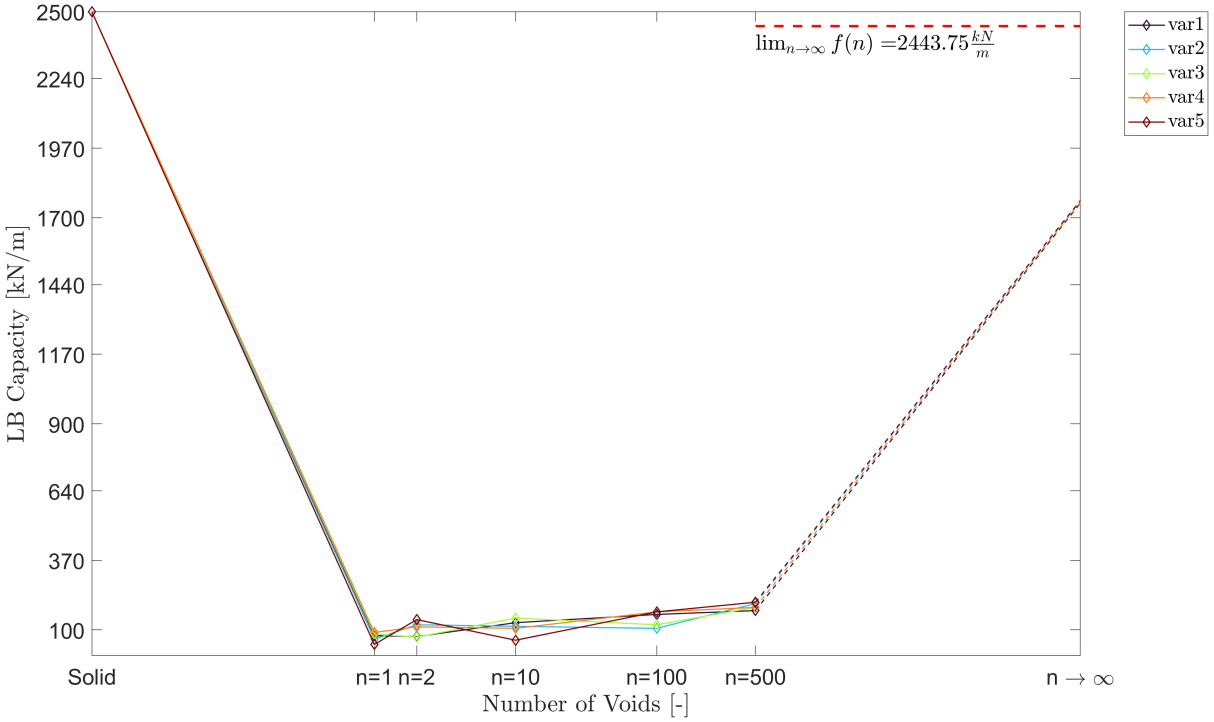

(a) 1.5% Porosity

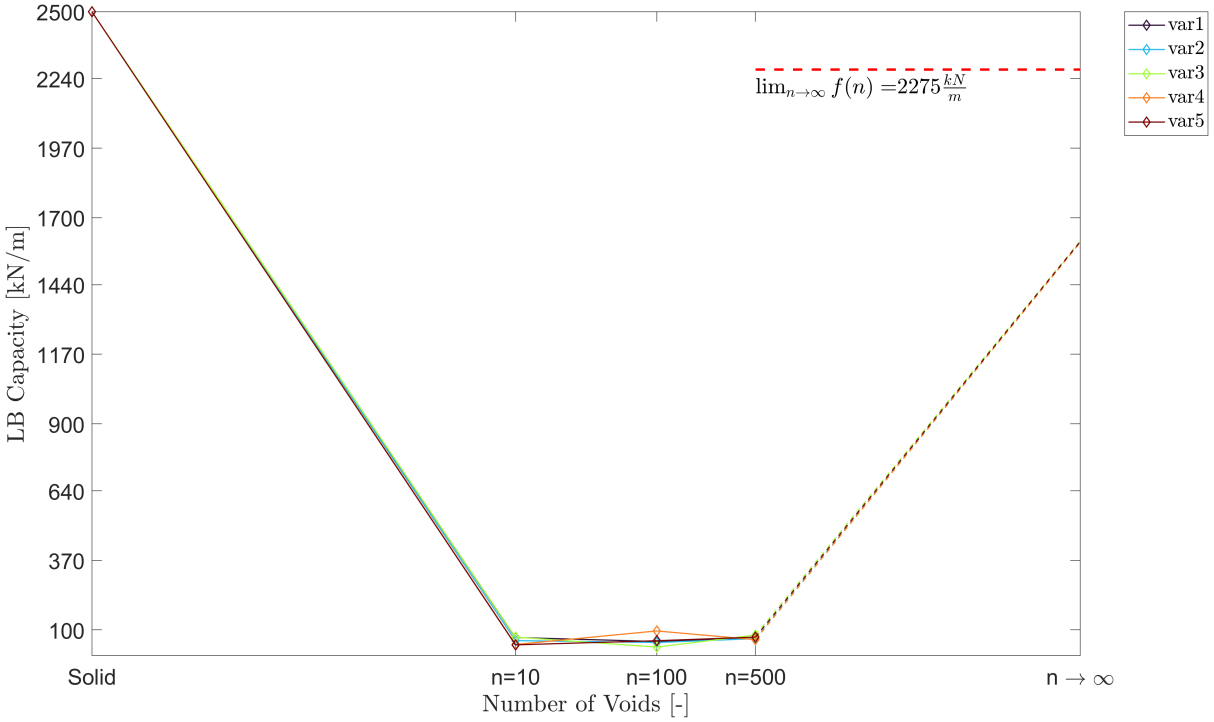

(b) 6% Porosity

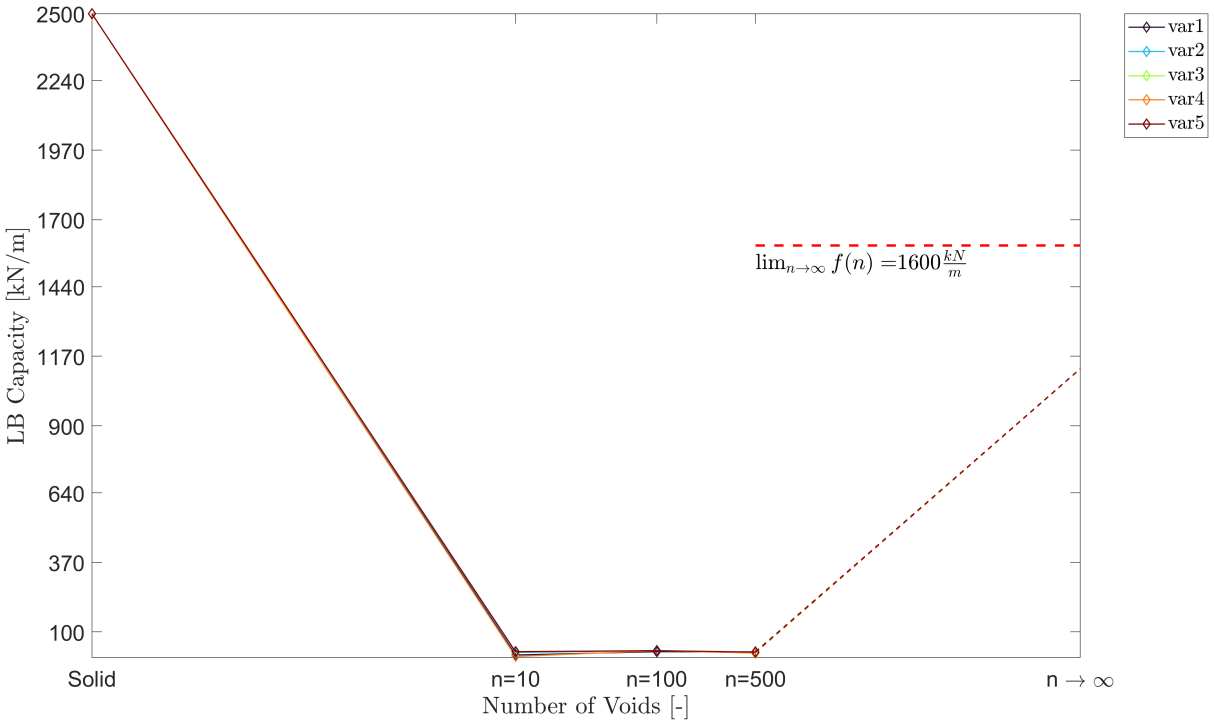

(c) 24% Porosity

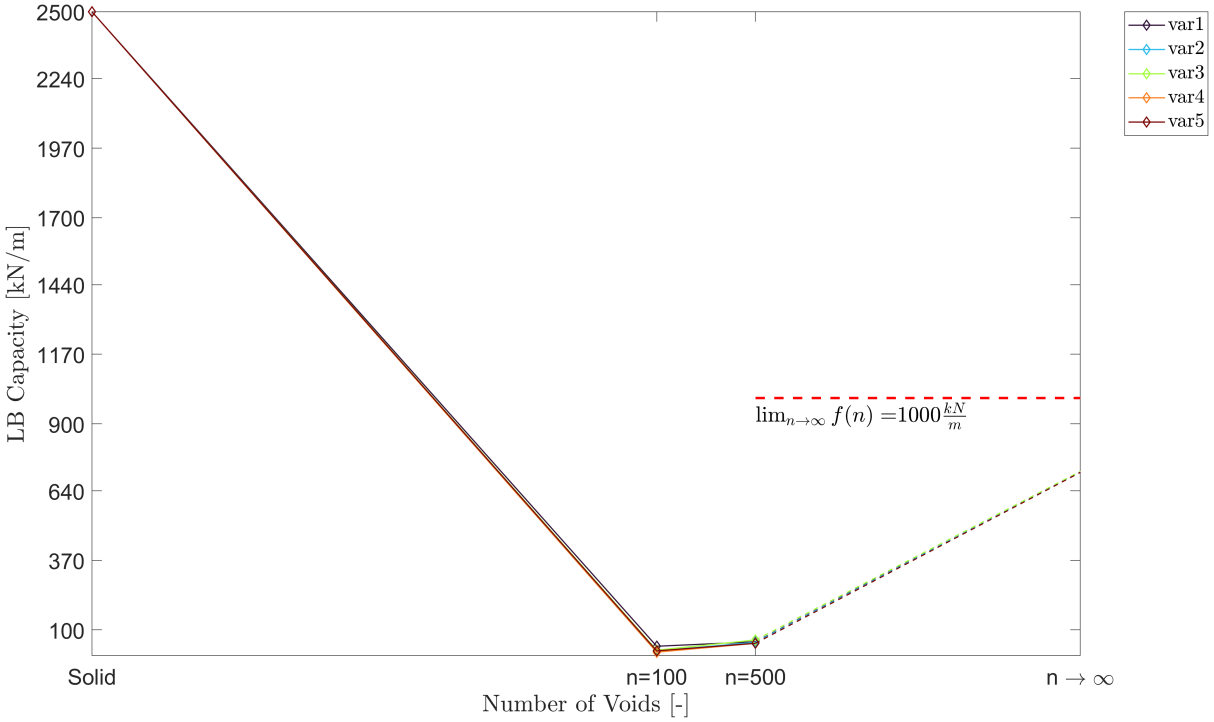

(d) 40% Porosity

Figure 29: LB capacity of *Material 1* for elliptical hole with $b/a = 1/10$

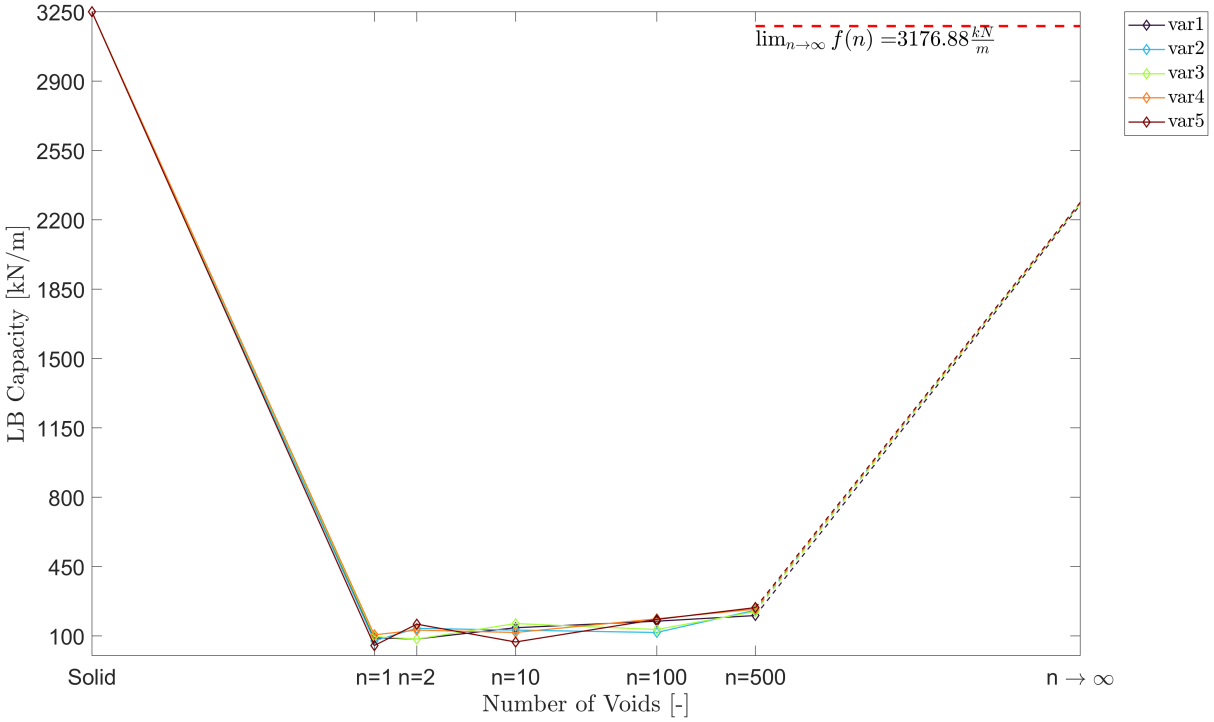

(a) 1.5% Porosity

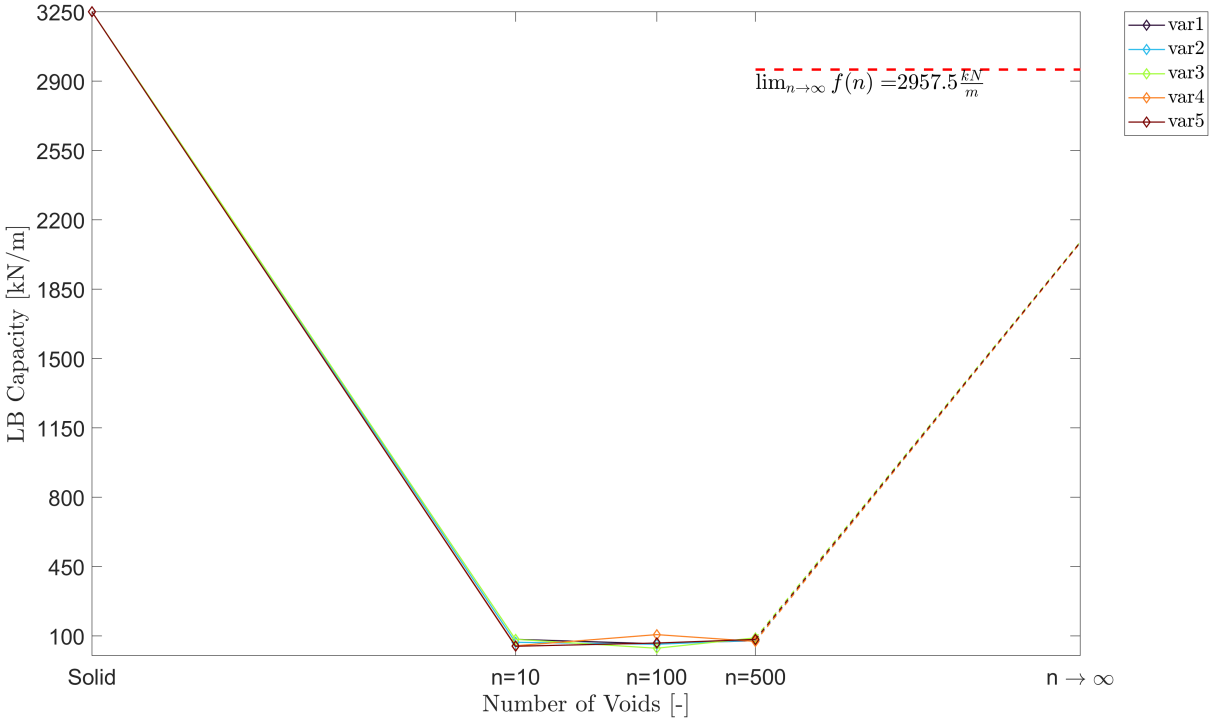

(b) 6% Porosity

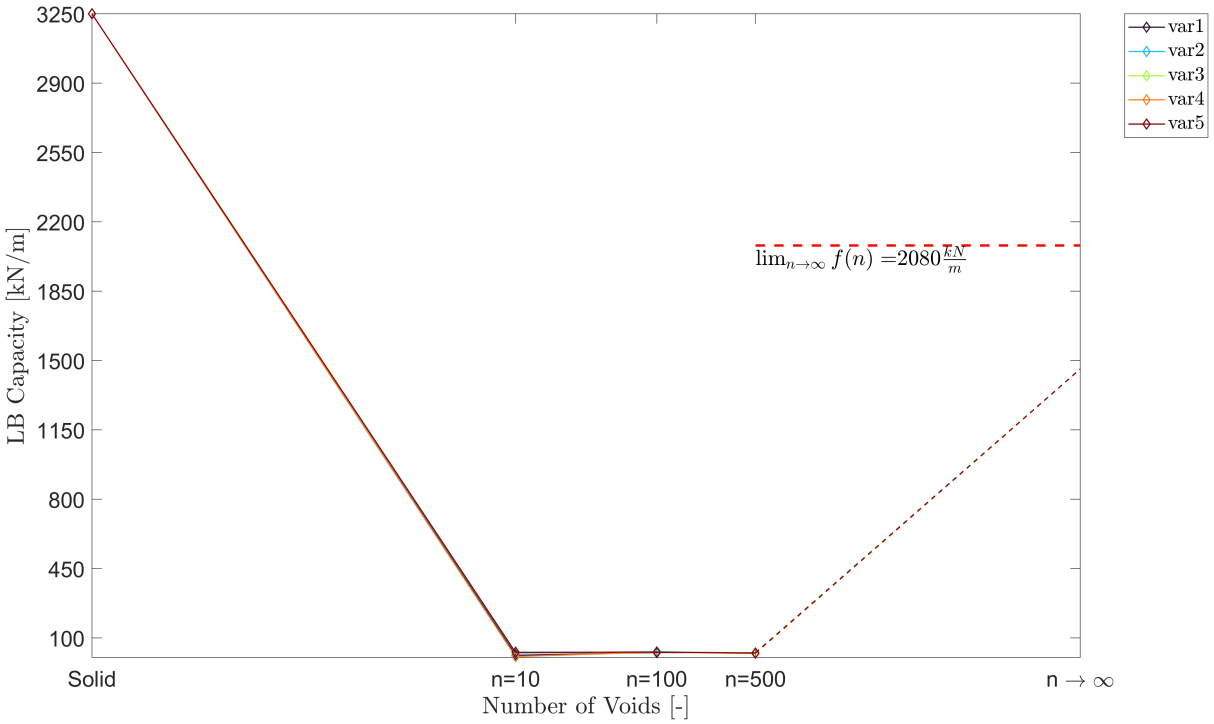

(c) 24% Porosity

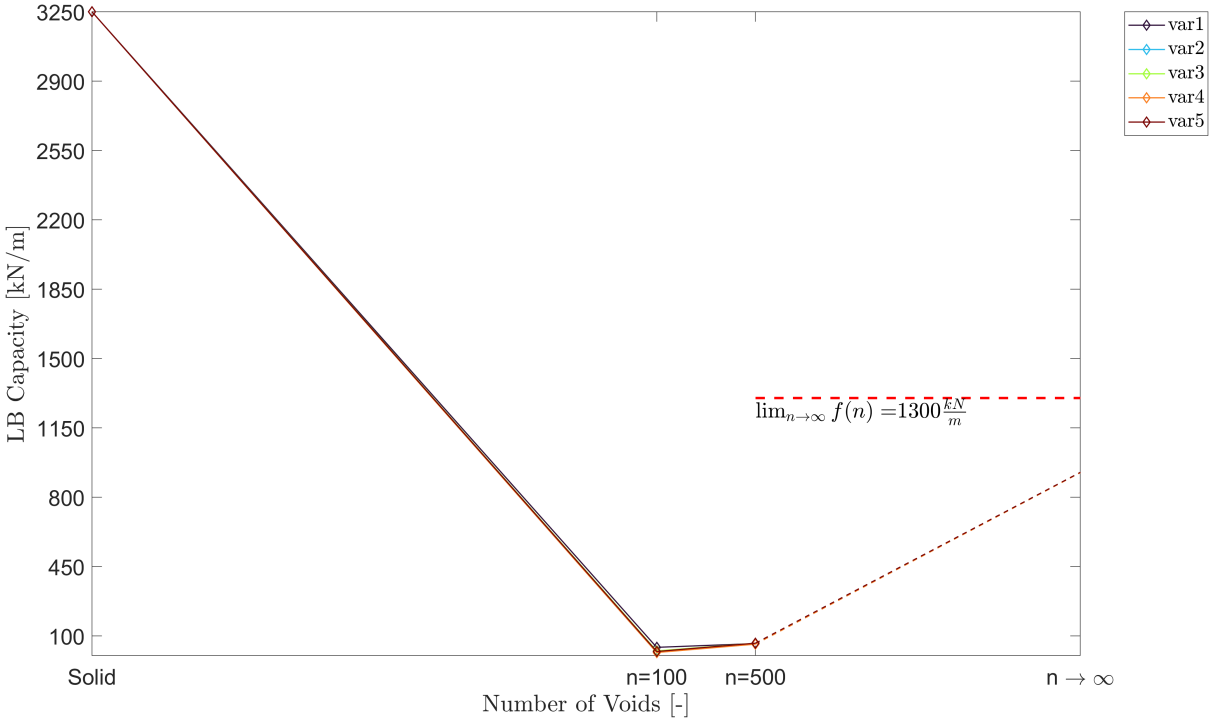

(d) 40% Porosity

Figure 30: LB capacity of *Material 2* for elliptical hole with $b/a = 1/10$

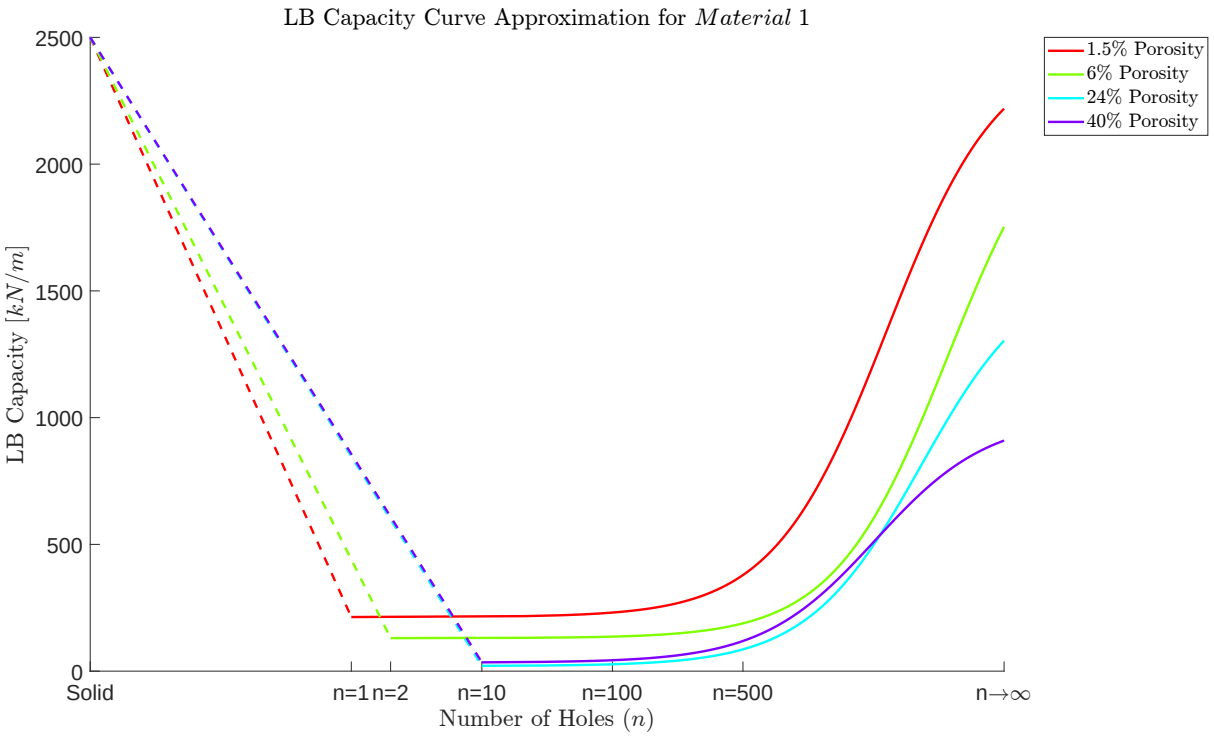

Figure 31: Regression curves for LB capacity of *Material 1* for elliptical holes

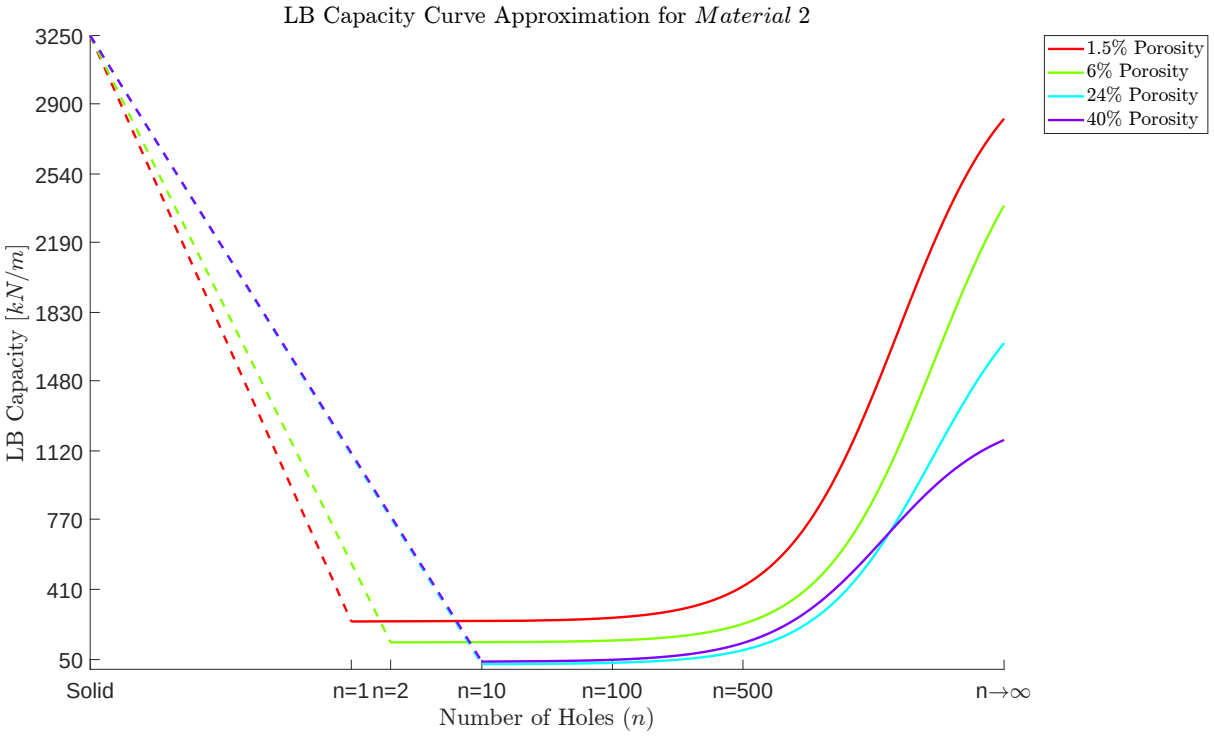

Figure 32: Regression curves for LB capacity of *Material 2* for elliptical holes

5.3 Comparison between Geometric Variations

The purpose of creating three different versions of holes was to see how the change in shape affects the LB capacity of material. Figures [33,34] show that the LB capacity of plates with

circular holes is greater than the plates with elliptical holes. We can also see that in case of elliptical holes with smaller minor to major axis ratio has more LB capacity than the ones with larger ratios. Another important thing that can be observed from Figures [33,34] is that the difference in LB capacity decreases between different geometric variations as the porosity increases.

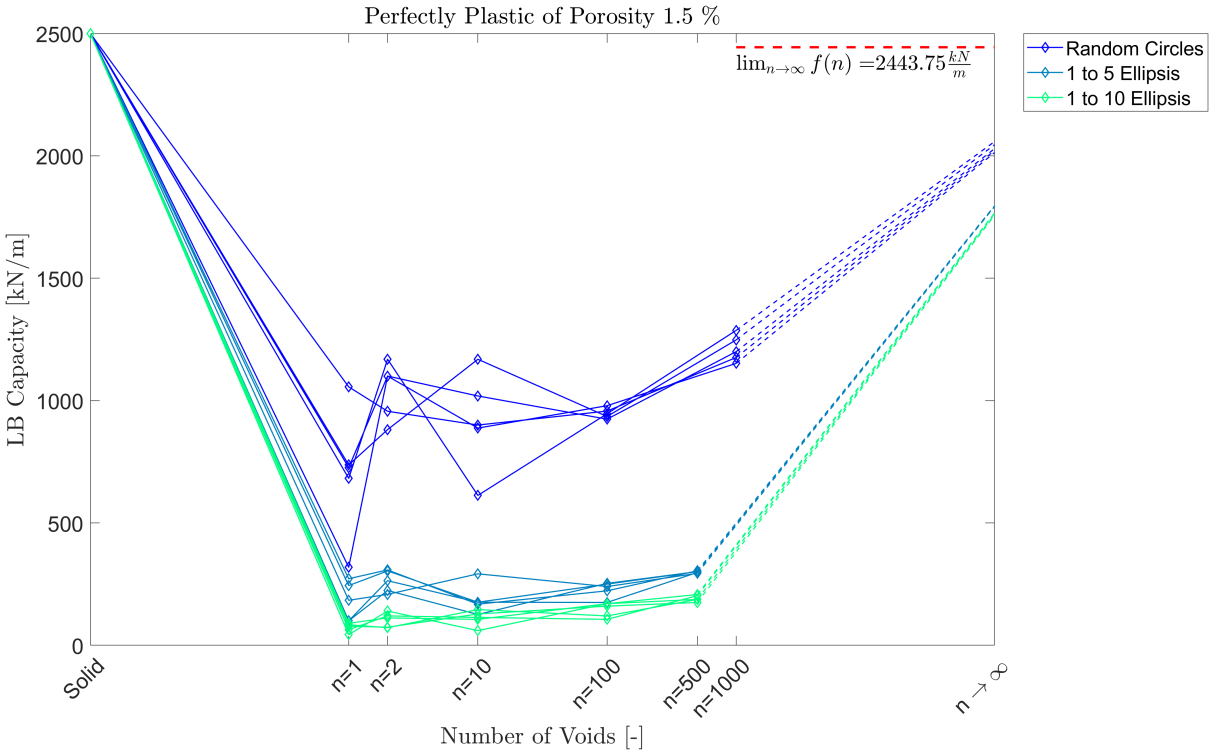

(a) 1.5% Porosity

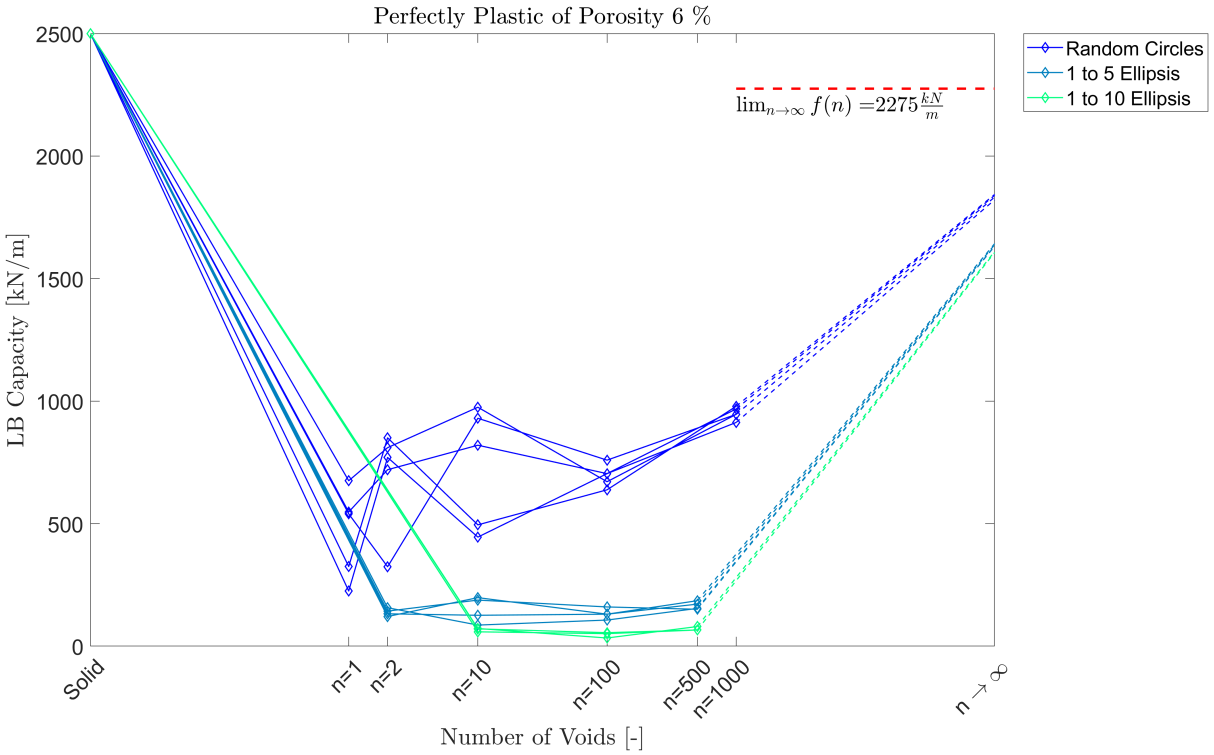

(b) 6% Porosity

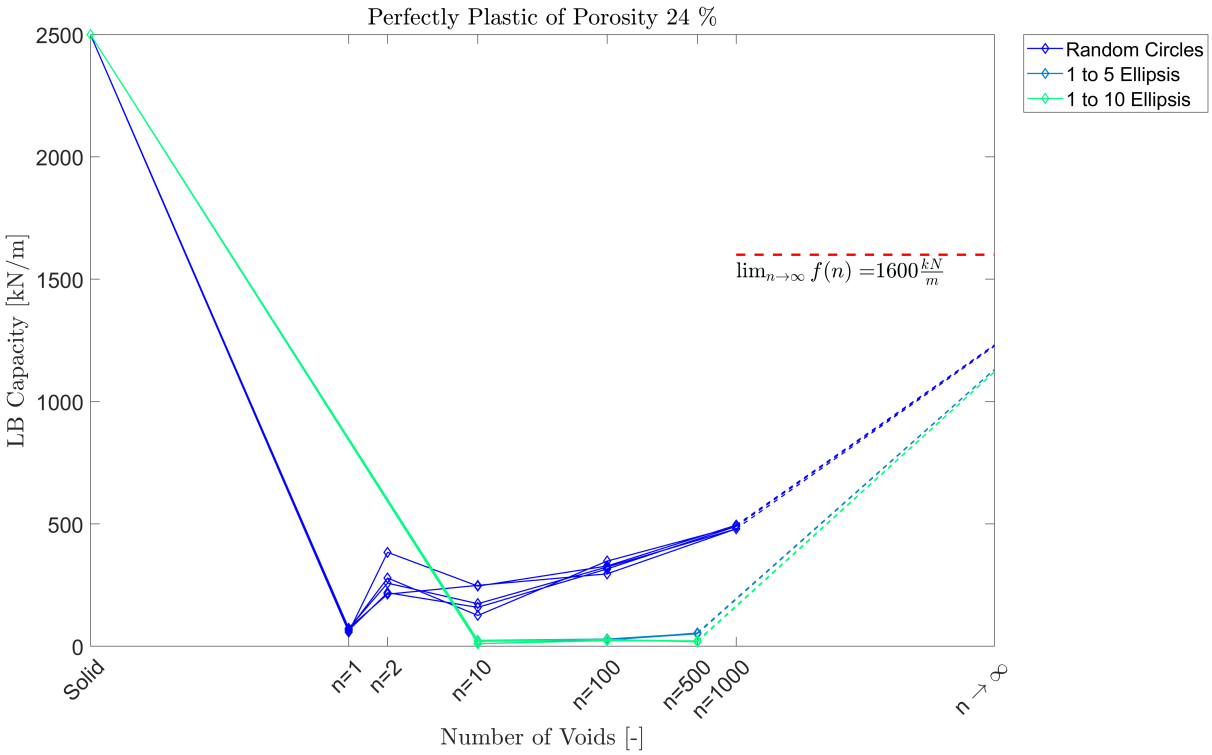

(c) 24% Porosity

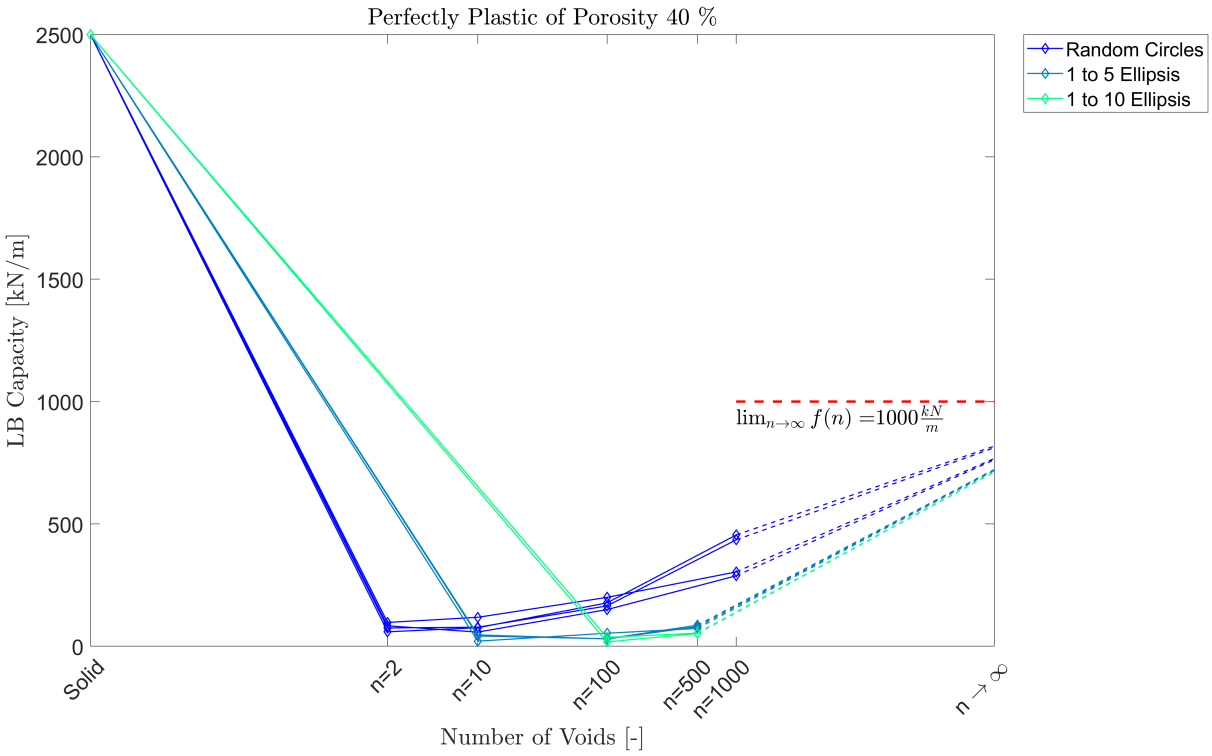

(d) 40% Porosity

Figure 33: Comparison of LB capacity of Geometric variations for *Material 1*

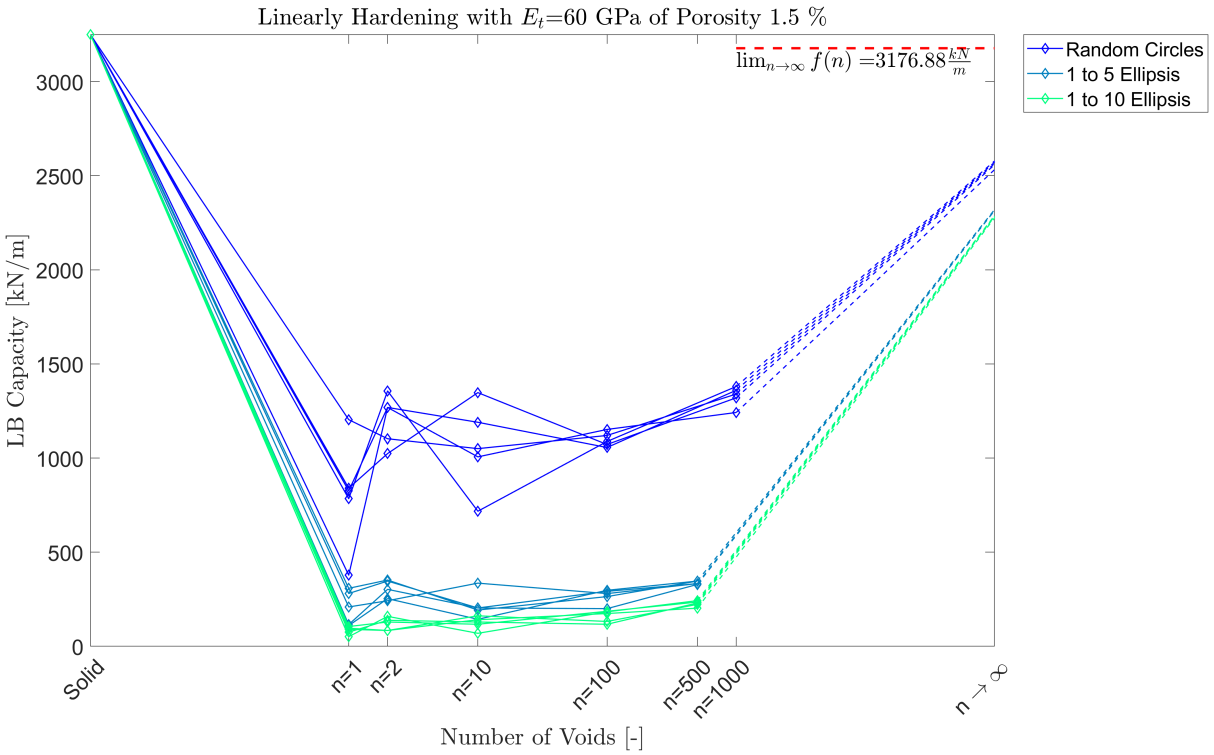

(a) 1.5% Porosity

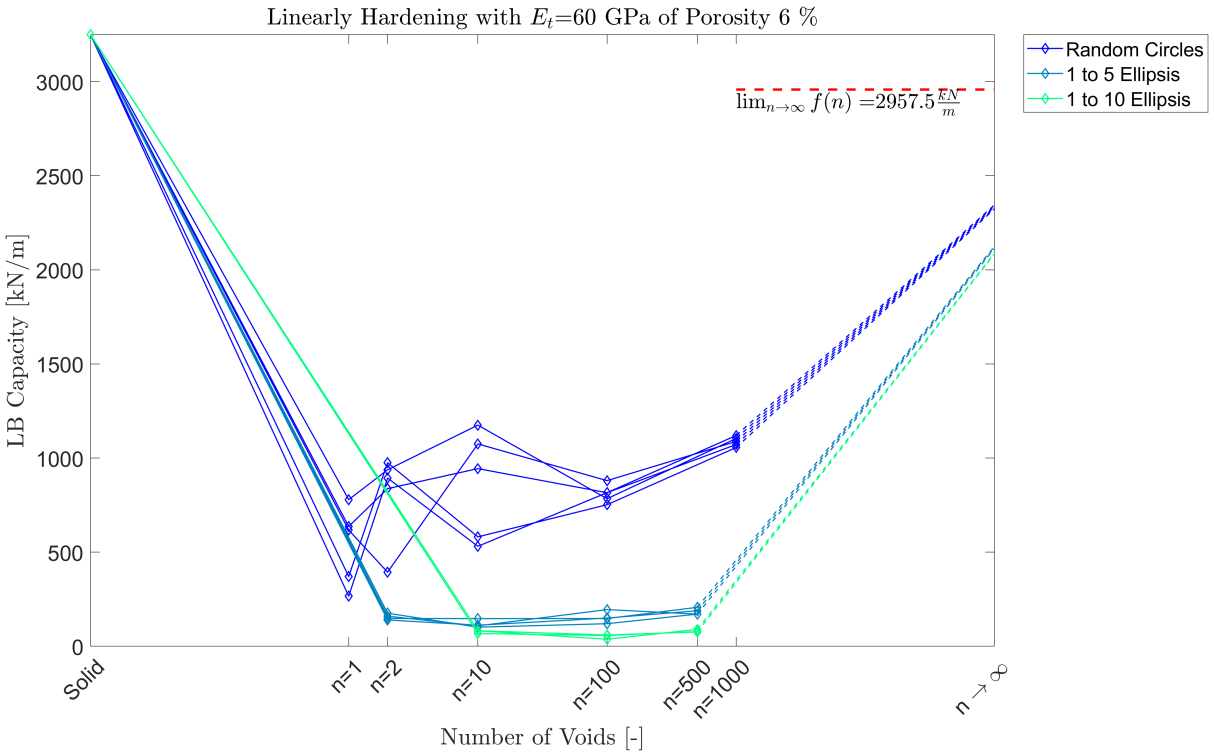

(b) 6% Porosity

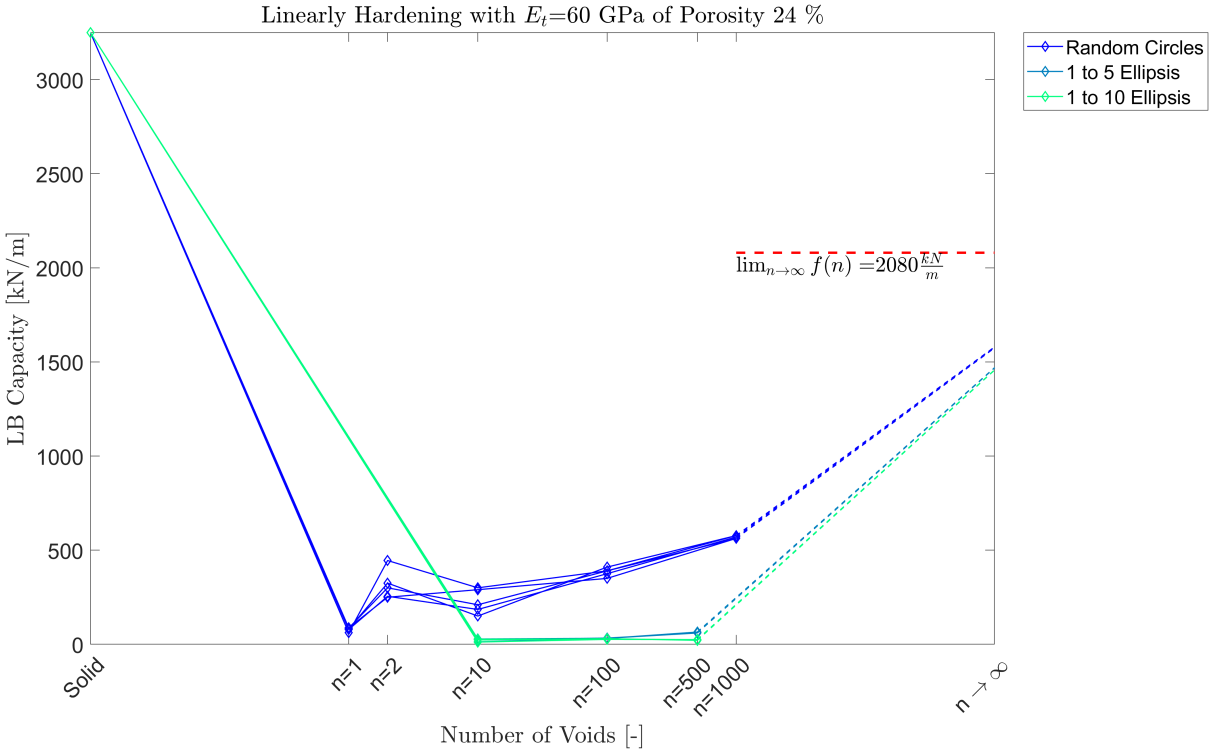

(c) 24% Porosity

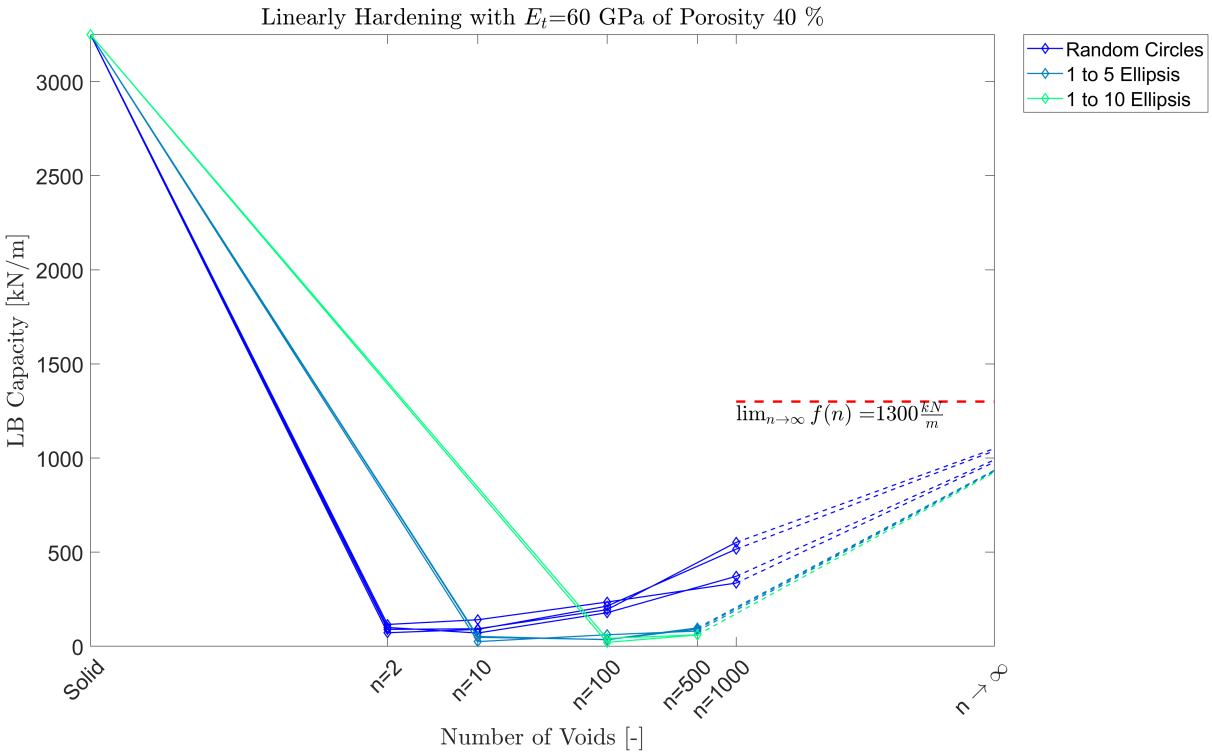

(d) 40% Porosity

Figure 34: Comparison between geometric variations for *Material 2*

5.4 Comparison between Plane Stress and Plane Strain

The actual problem was analyzed using plane stress formulation as it works well for thin elements with unit thickness. But to check whether using a different formulation would have an

effect on the values of LB capacity, plane strain formulation was also used to analyze the problem for a selected porosity for circular holes. Figures [35,36] show that by using plane strain formulation results in a small increase in the value of LB capacity under the same loading.

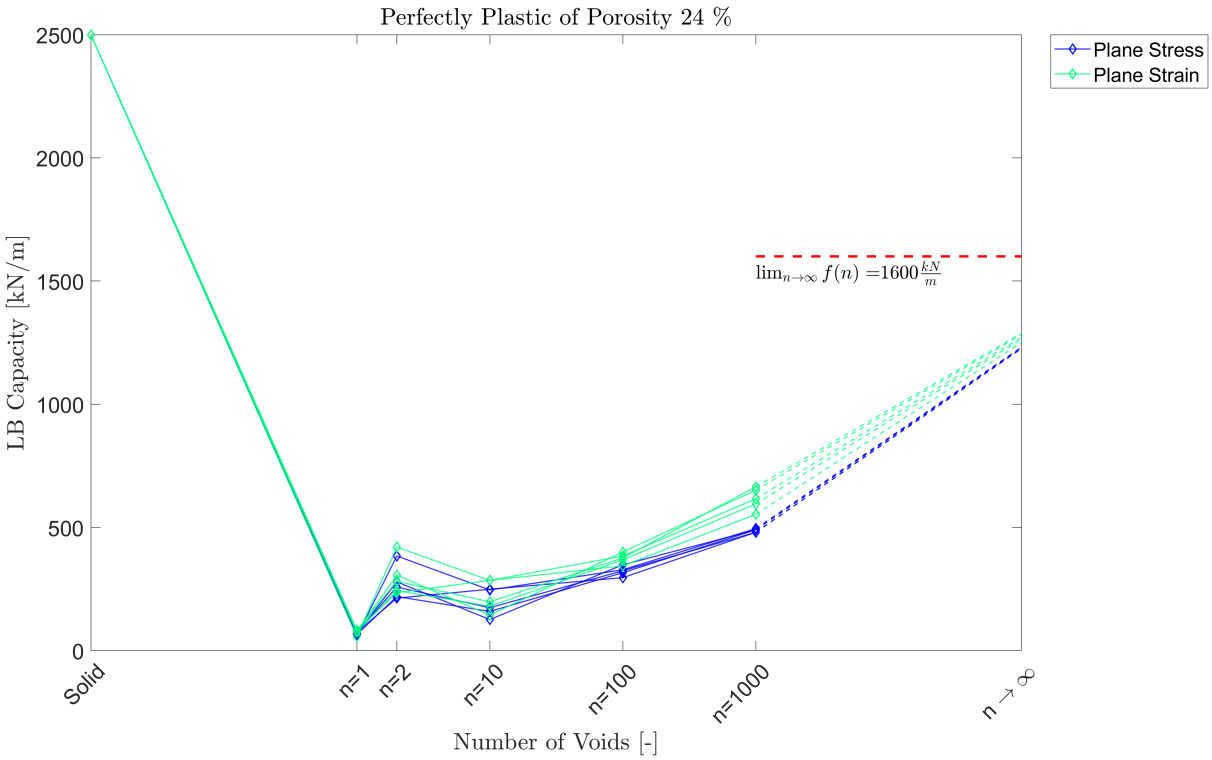

Figure 35: Comparison between *plane stress and plane strain* for *Material 1*

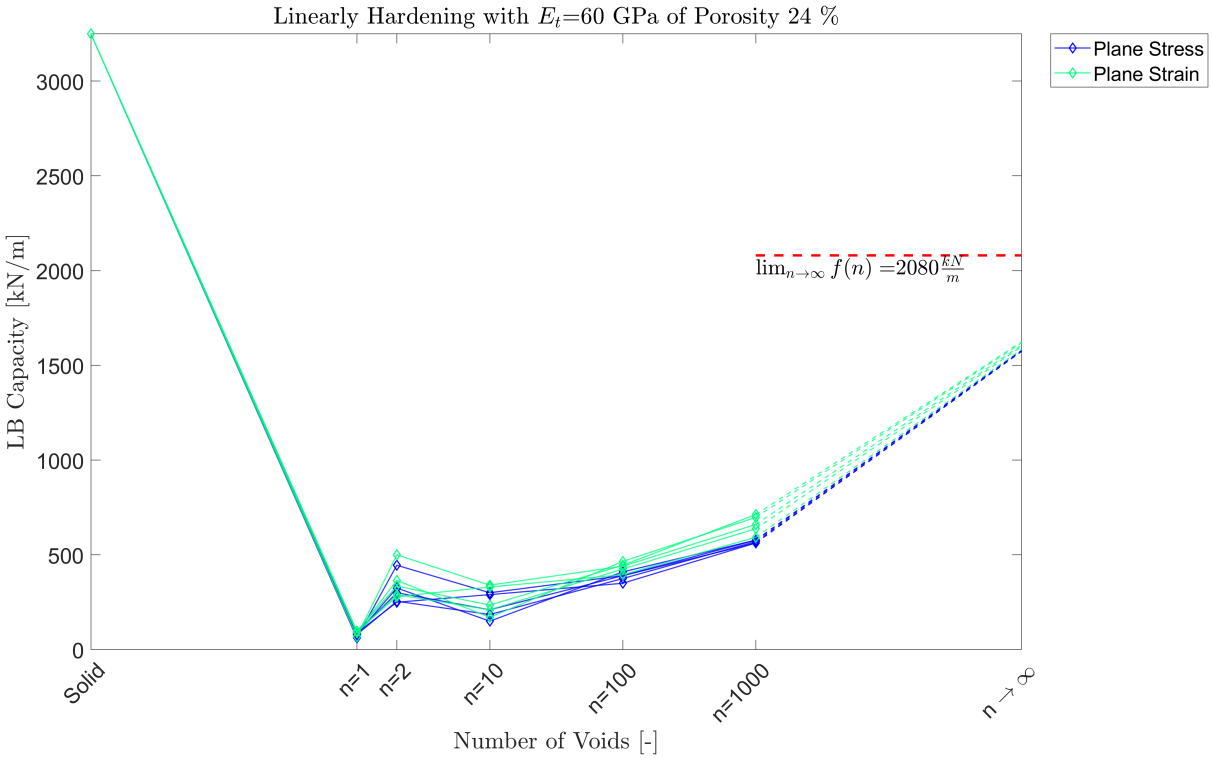

Figure 36: Comparison between *plane stress and plane strain* for *Material 2*

5.5 Comparison between Small Strain and Large Strain

The maximum of small strain conidtion was taken as **2.5‰** at any point of the structure for which the maximum value of LB capacity occurs. The maximum displacement of the structure for this case was approximately 0.4 mm. In order to compare the difference in LB capacity, large strain analysis was also done for selected porosities using Material 1 and Material 2.

In case of large strains, a prescribed displacement of 4 mm, approximately **10 times higher**, as was in previous case, was applied. It should be noted that for the Material 1, stress can't increase over 250 MPa. While, in case of Material 2, the stress can theoretically keep on increasing after reaching the yield point along with a relatively higher tangent modulus than usual materials.

Another interesting situation in the case of large strains is the analytical approximation of LB capacity for large strain. Approximations were done to calculate the LB capacity for strain limit of **2.5‰** but in case of large strains (25% to 35% at specific points), these approximations can't be ignored.

An approximation done for small strain case to ignore the softening of materials after reaching the initial yield stress. But in reality, the material undergoes softening under uniaxial tension because of the growth of voids and possible formation of new voids. This complex behavior is prominent in case of large strains. Therefore, a good approximation for LB capacity can't be made in case of large strains for both materials. Figure 37 shows the softening and hardening behavior of a linearly elastic perfectly plastic material with a porosity under uniaxial tension and compression respectively.

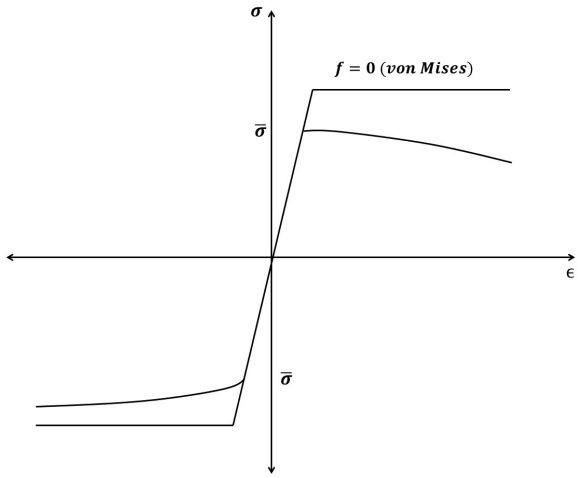

Figure 37: Softening and hardening of porous material under uniaxial tension and compression

Here, we will only focus on the comparison between the small strain and large strain for Material 1. The strain limit was not fixed in the current case. Strains ranged from 25% to 35% at some points of the structures. Figure 38 shows the maximum strain zone around the holes. The case of Material 1 is simpler than the case of Material 2 where the stress keeps on increasing with a tangent modulus quite higher than usual materials. The behavior of Material 2 for the large strain case can be an interesting question but will not be discussed here.

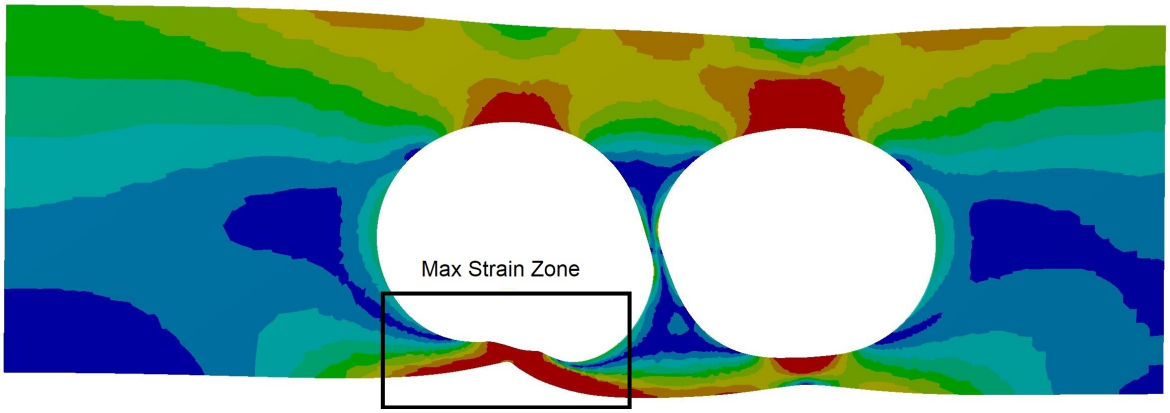

Figure 38: Maximum strain zone for large strain

It can be seen in Figures 39 and 40, the LB capacity of large strain case is higher than the small strain. It should be noted that $n = 1$ for 24% porosity is special case because it has the hole with maximum length perpendicular to uniaxial tension that's why both small and large strain situation has similar LB capacity values.

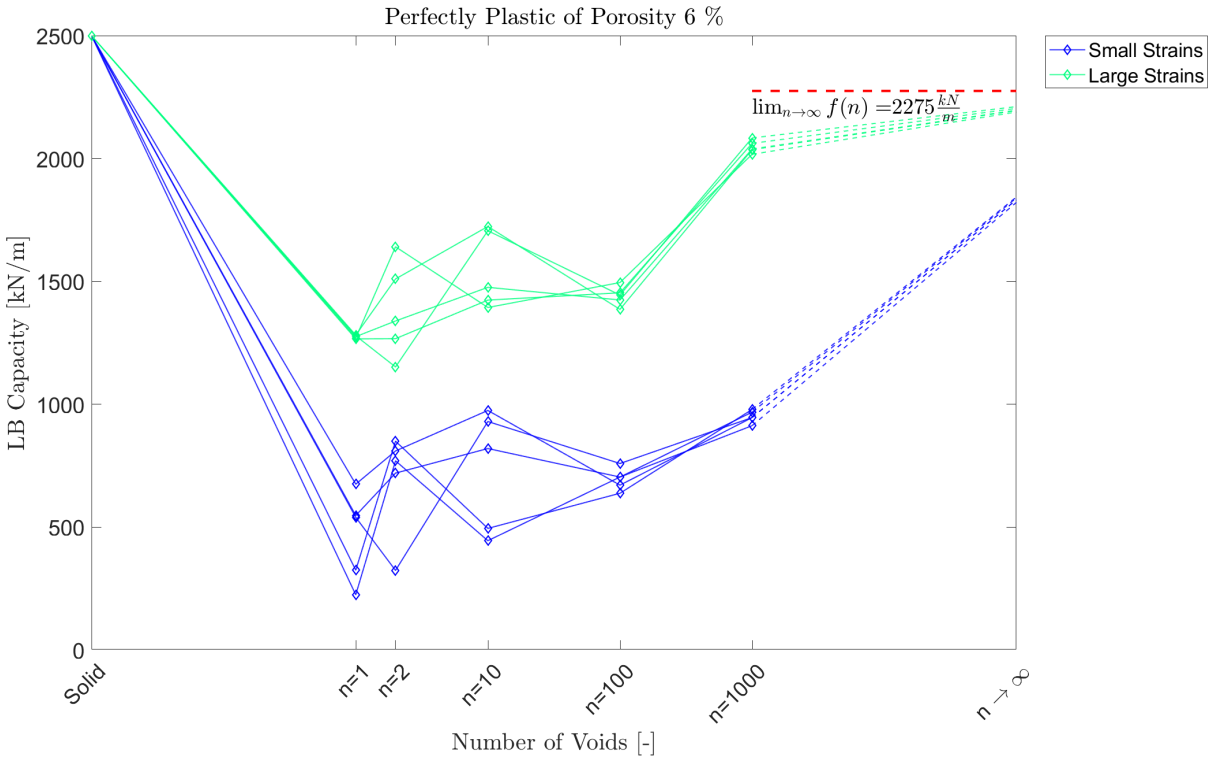

Figure 39: Comparison between *small and large strain* for *Material 1* for 6% porosity

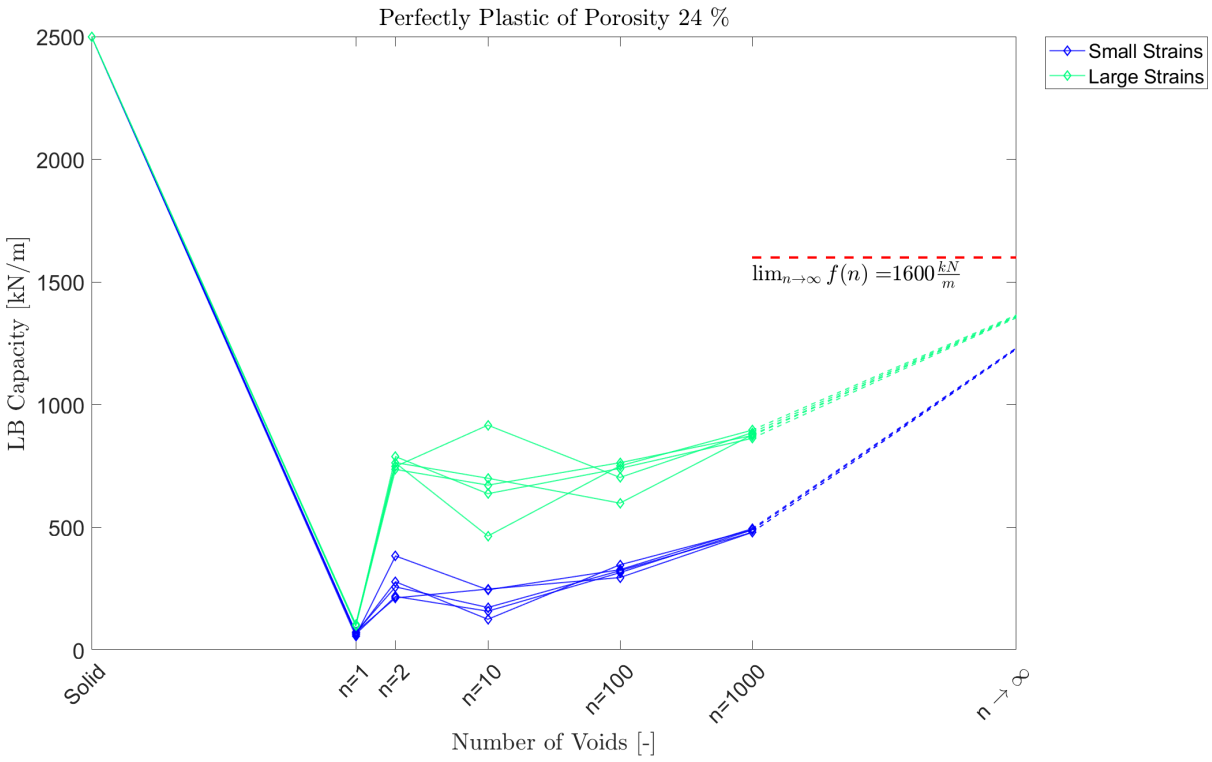

Figure 40: Comparison between *small and large strain* for *Material 1* for 24% porosity

Summary

The purpose of the study was to understand the effect of porosity on the LB capacity of a thin plate. The effect of the change in the number of holes with different shapes and positions for a porosity was analyzed. The conclusion that can be made here is that the LB capacity tends towards a value close to LB capacity approximated by the Gurson Model as we increase the number of n. A numerical drawback here is that we can't increase the number of holes to the same scale as of the Gurson Model, but it presents a good transition between the solid model with no voids to porous model. The Gurson's model is only applicable for spherical voids but here as an approximation we use it both for circular and elliptical holes. A study of the comparison between use of spherical voids (Gurson's mdoel) and ellipsoidal voids in a 3D stress state could be performed to have a better approximation models for different shapes of holes.

In current case, only tension analysis was done. This could be expanded to the use of study of bending and the interaction of bending and tension as well. Another interesting problem would be the analysis of large strain behavior of the plate.

References

[1] Peter Wriggers. “Nonlinear finite element methods”. In: 1st ed. Springer, 2008, pp. 19–81.

[2] Bojtár Imre. *Material Models: Lecture 4*. Faculty of Civil Engineering, Budapest University of Technology and Economics, July 2020.

[3] I.S. Sokolnikoff. “Mathematical Theory of Elasticity”. In: 1st ed. McGraw Hill, 1946.

[4] Atef F. Saleb Wai-Fah Chen. “Constitutive Equations for Engineering Materials”. In: 2nd ed. Vol. 1. Elsevier, 1994, pp. 142–155.

[5] A.L. Gurson. “Continuum theory of ductile by void nucleation and growth: Part 1—Yield criteria and flow rules for porous ductile media”. In: *Journal of Engineering Materials and Technology* 99 (1977), pp. 2–15.

[6] T.L. Anderson. “Fracture Mechanics: Fundamentals and Applications”. In: 4th ed. CRC Press, 2017, pp. 229–242.

[7] A. Needleman C.C. Chu. “Void nucleation effects in biaxially stretched sheets”. In: *Journal of Engineering Materials and Technology* 102 (1980), pp. 249–256.

[8] Ansys. *Ansys Theory Reference*. 2017. URL: `https://www.mm.bme.hu/~gyebro/files/ans_help_v182/ans_thry/thy_mat1.html`.

[9] Kirsch. “Die Theorie der Elastizität und die Bedürfnisse der Festigkeitslehre”. In: *Zeitschrift des Vereines deutscher Ingenieure* 42 (1898), pp. 797–807.

[10] C.E. Inglis. “Stresses in Plates Due to the Presence of Cracks and Sharp Corners”. In: *Transactions of the Institue of Naval Architects* 55 (1913), pp. 219–241.

[11] T.L. Anderson. “Fracture Mechanics: Fundamentals and Applications”. In: 4th ed. CRC Press, 2017, pp. 25–30.

[12] T.L. Anderson. “Fracture Mechanics: Fundamentals and Applications”. In: 4th ed. CRC Press, 2017, pp. 109–121.

[13] Ansys. *Ansys Elements Reference*. 2017.

Appendix A: Plastic Zone Propagation

The red zone in the figures below shows the plastic zones. It should be noted here that only red zones show the yielded structure. The colors transitioning from the blue to red show an increase from smallest value to maximum value possible.

A.1 6% Porosity

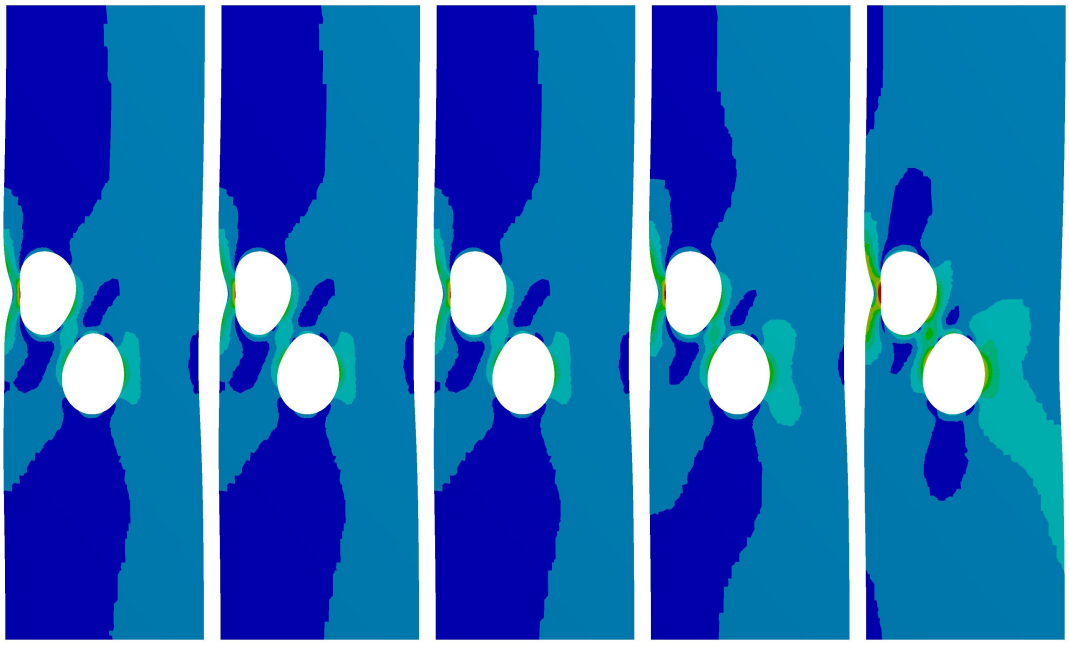

(a) Small Strain Case

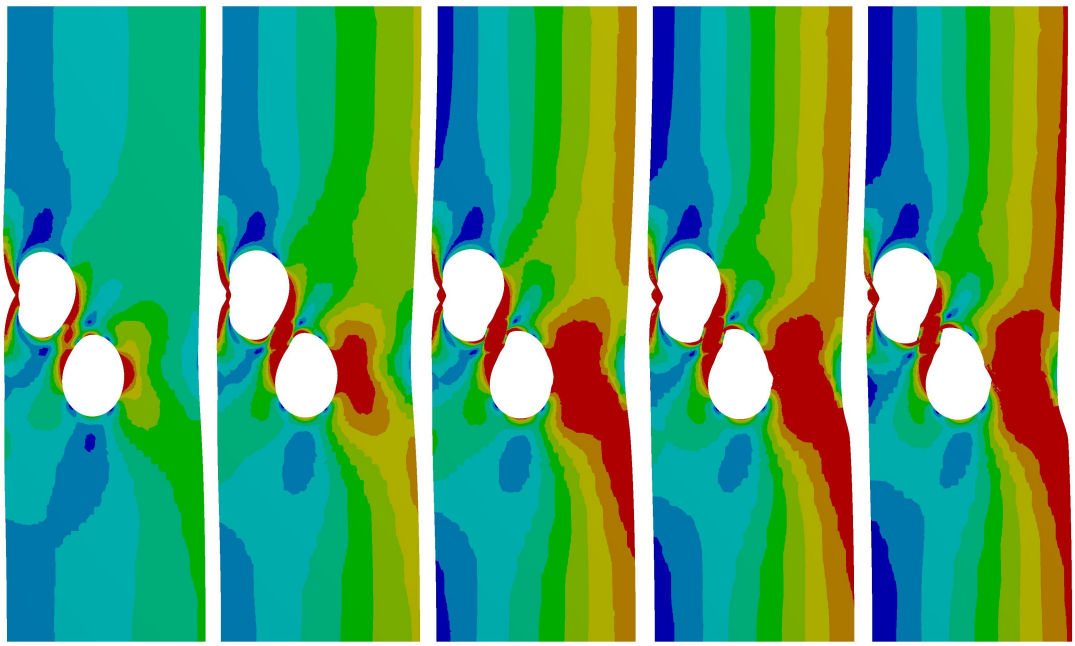

(b) Large Strain Case

Figure 41: Example of Plastic Zone Propagation for Material 1 with n=2 and f=6%

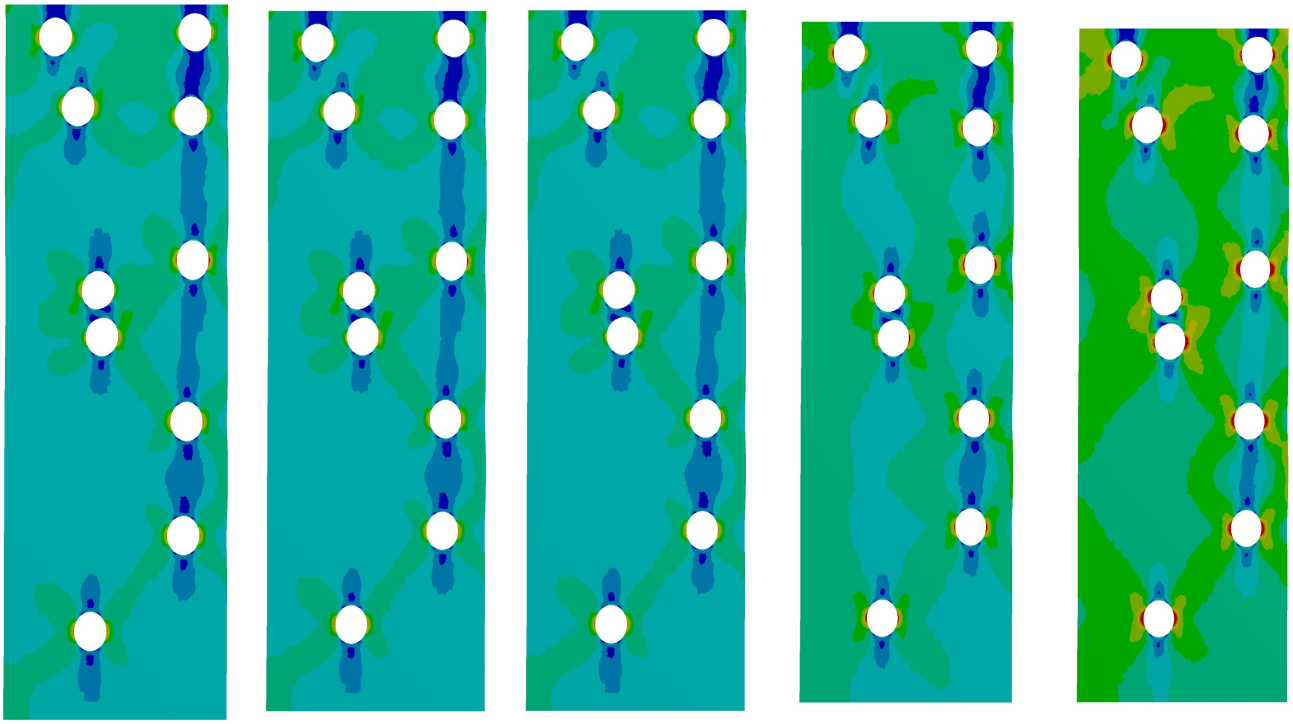

(a) Small Strain Case

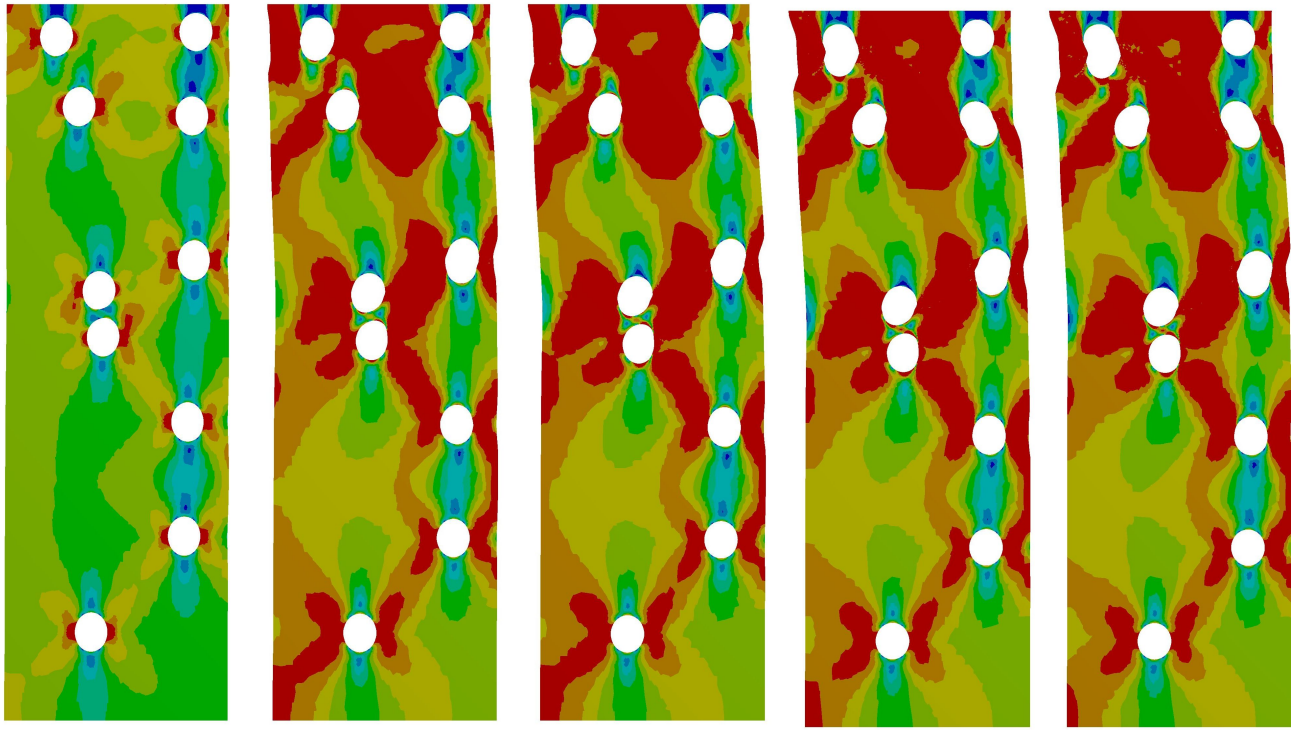

(b) Large Strain Case

Figure 42: Example of Plastic Zone Propagation for Material 1 with n=10 and f=6%

A.2 24% Porosity

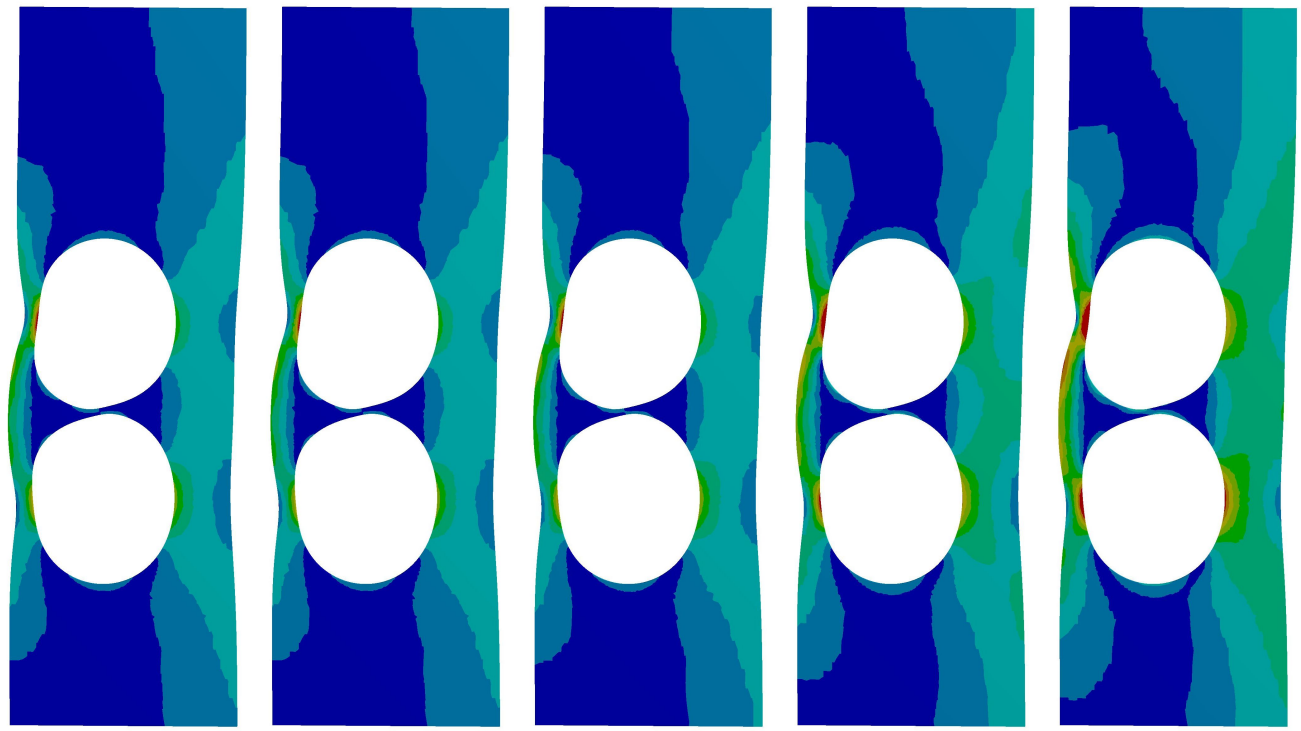

(a) Small Strain Case

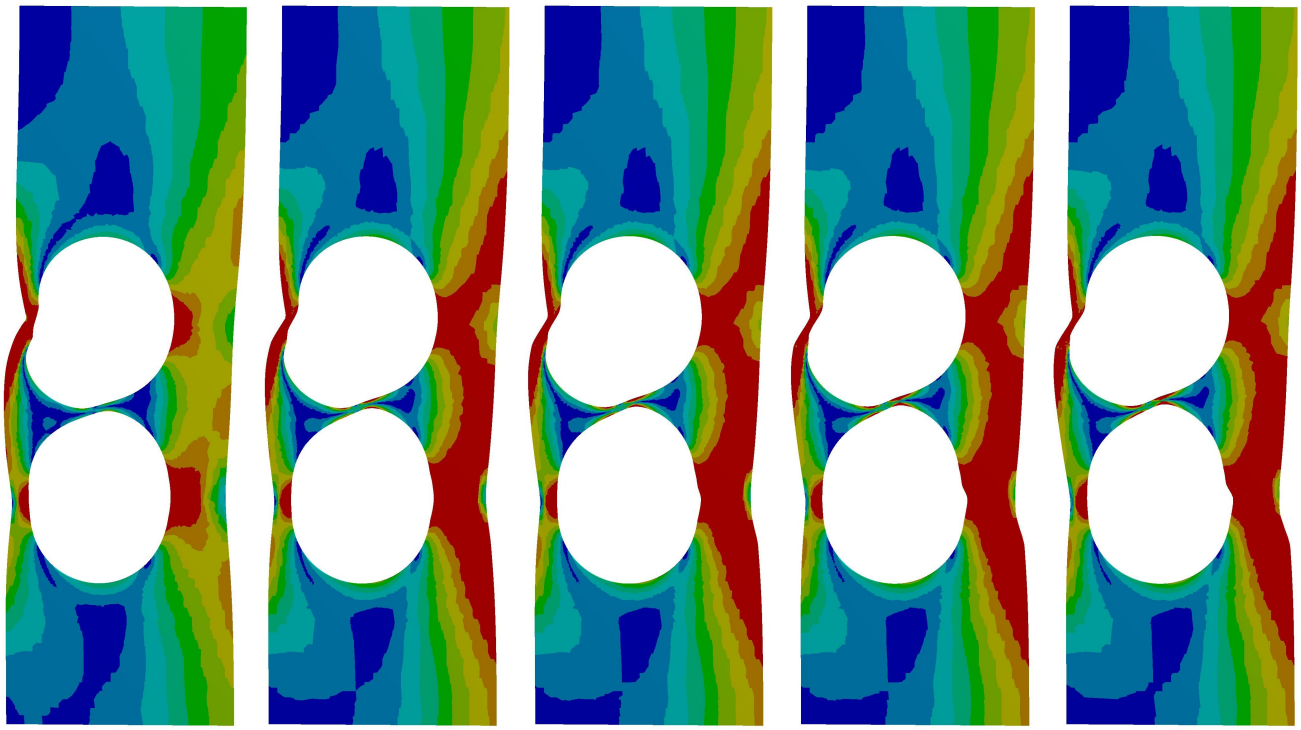

(b) Large Strain Case

Figure 43: Example of Plastic Zone Propagation for Material 1 with $n = 2$ and $f = 24\%$

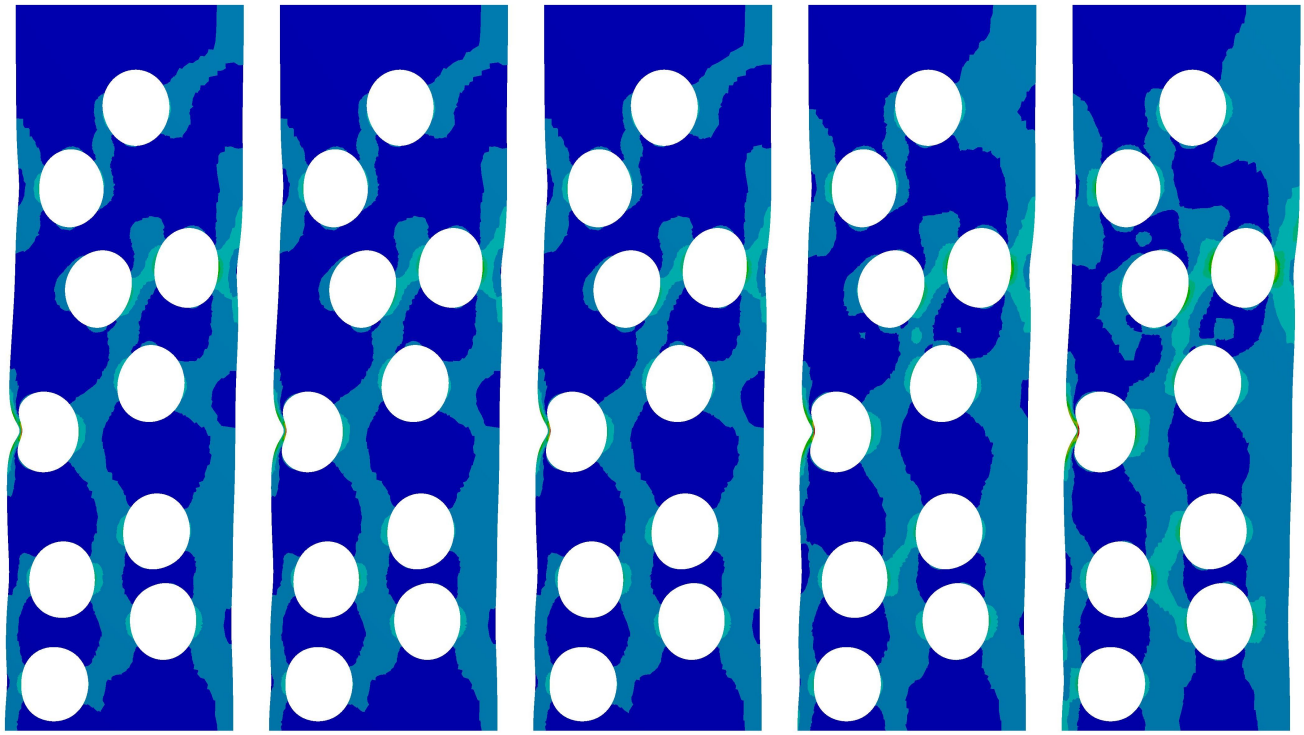

(a) Small Strain Case

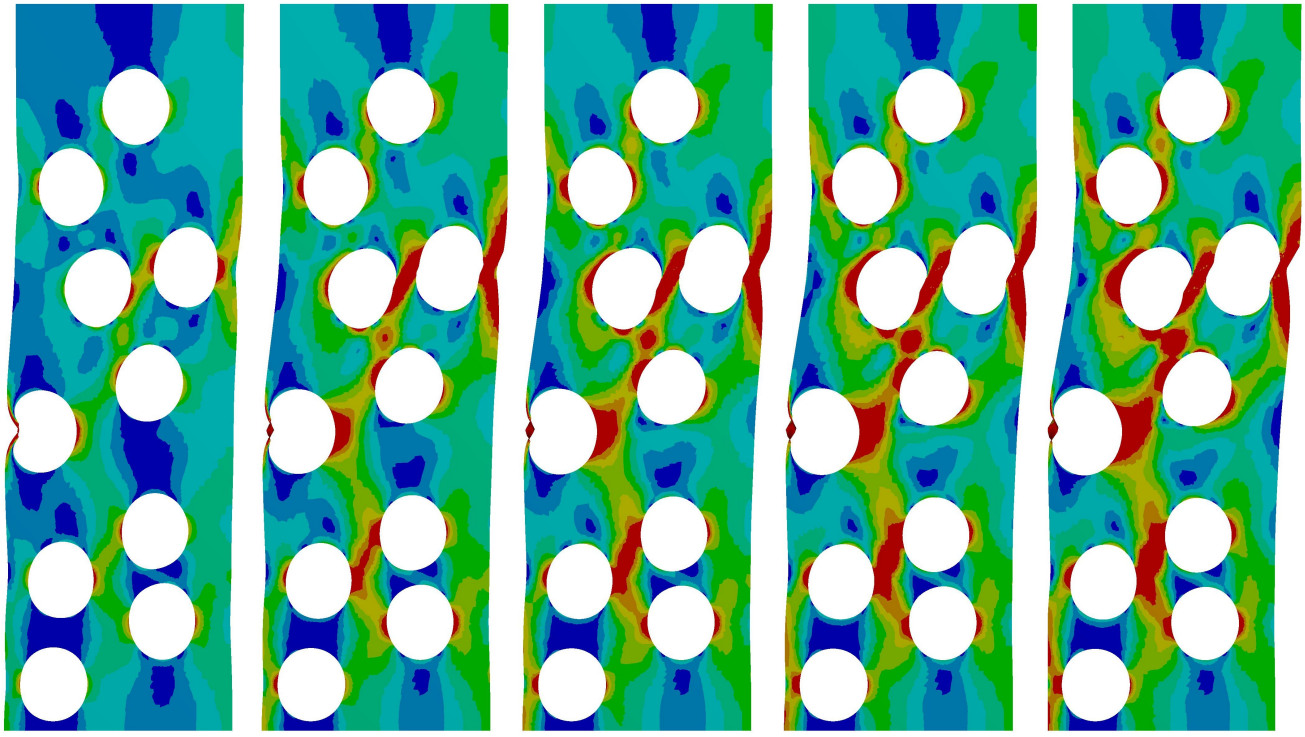

(b) Large Strain Case

Figure 44: Example of Plastic Zone Propagation for Material 1 with $n = 10$ and $f = 24\%$

Appendix B: Codes for Creation of Geometry

B.1 Circular Holes

```
function cs = geometry(porosity,number_circles)
radius = sqrt((porosity*1500*500)/(pi*number_circles));
l_limits = [5 5]+radius;
u_limits = [495 1495]-radius;
counter = 1;
c_coords = zeros(number_circles,2);
f = 0;
while counter<=number_circles
    coords = l_limits+rand(1,2).*(u_limits-l_limits);
    if counter==1
        c_coords(counter,:) = coords;
        counter = counter+1;
    else
        if sum(sqrt(sum((c_coords-coords).^2,2)) > radius*2+5)==counter
   -1
            c_coords(counter,:) = coords;
            if mod(counter,5)==0
                fprintf("%4d Circles found\n",counter)
            end
            counter = counter+1;
        else
            f = f+1;
            if f>=50000
                f = 0;
                counter = 1;
                c_coords = [];
            end
        end
    end
end
```

B.2 Elliptical Holes

```
function cs = geometry(porosity,number_ellipsis,r_axis)
b = round(sqrt((porosity*1500*500)/(pi*number_ellipsis*r_axis)),1);
a = b*r_axis;
if a>=245
    cs = [];
    return
end
l_limits = [5 5]+[a b];
u_limits = [495 1495]-[a b];
counter = 1;
c_coords = [];
f = 0;
while counter<=number_ellipsis
    coords = l_limits+rand(1,2).*(u_limits-l_limits);
    bl_coords = coords - [a b] - [1 1];
    tr_coords = coords + [a b] + [1 1];
    if counter==1
        c_coords(counter,:) = coords;
```

```
        bl_ccoords = c_coords - [a b] -[1 1];
        tr_ccoords = c_coords + [a b] + [1 1];
        counter = counter+1;
    else
        c1 = max(bl_ccoords,bl_coords);
        c2 = min(tr_ccoords,tr_coords);
        c = c1 > c2;
        if sum(c(:,1)|c(:,2))==counter-1
            c_coords(counter,:) = coords;
            bl_ccoords = c_coords - [a b] -[1 1];
            tr_ccoords = c_coords + [a b] + [1 1];
            counter = counter+1;
        else
            f = f+1;
            if f>=5e6
                f = 0;
                counter = 1;
                c_coords = [];
            end
        end
    end
end
```

B.3 Circular Hole Geometry Creation

```
# Python Script, API Version = V17
import random
import math
import os
porosity =[0.4]
n = [1000]
variations = ["var1"]
for i in range(len(porosity)):
    for j in range(len(n)):
        for k in range(len(variations)):

            radius = round(math.sqrt(porosity[i]*7.5e5/(math.pi*n[j]))
    ,2)
            c_coords = []
            with open('D:\Administrator\Documents\MATLAB\matrix.txt','r
    ') as file:
                for line in file:
                    currentline = line.split(",")
                    c_coords += [[float(currentline[0]),float(
    currentline[1])]]

            # Sketch Rectangle
            plane = Plane.PlaneXY
            result = ViewHelper.SetSketchPlane(plane)
            point1 = Point2D.Create(MM(0),MM(0))
            point2 = Point2D.Create(MM(500),MM(0))
            point3 = Point2D.Create(MM(500),MM(1500))
            result = SketchRectangle.Create(point1, point2,point3)
            # EndBlock
            for cs in c_coords:
                # Sketch Circle
```

```
                origin = Point2D.Create(MM(cs[0]), MM(cs[1]))
                result = SketchCircle.Create(origin, MM(radius))
                # EndBlock

            # Solidify Sketch
            mode = InteractionMode.Solid
            result = ViewHelper.SetViewMode(mode, Info2)
            # EndBlock

            # Delete Selection
            selection = Selection.Create([GetRootPart().Bodies[0].Faces
    [faces] for faces in range(n[j])])
            result = Delete.Execute(selection)
            # EndBlock

            primarySelection = Selection.Create([GetRootPart().Bodies
    [0].Edges[edges] for edges in range(n[j])])
            secondarySelection = Selection()
            result = NamedSelection.Create(primarySelection,
    secondarySelection)
            NamedSelection.Rename("Group1","circles")
            # Save File
            pathtoFolder = "D:\\LB capacity of Steel\\Simulations\\new
    \\"
            dir1 = os.path.join(pathtoFolder,str(porosity[i]),str(n[j])
    ,"pp",variations[k])
            DocumentSave.Execute(dir1+"\\"+variations[k]+".scdoc")
            # EndBlock
            # Delete Selection
            #selection = Selection.Create(GetRootPart().Bodies[0])
            #result = Delete.Execute(selection)
            # EndBlock
```

B.4 Elliptical Hole Geometry Creation

```
import random
import math
import os
porosity =[0.015,0.06,0.24,0.4]
number_ellipsis = [1,2,10,100,500]
variations = ["var"+str(i) for i in range(1,6)]
r_axis = 10 # can be either 5 or 10
for i in range(len(porosity)):
    for j in range(len(number_ellipsis)):
        for k in range(len(variations)):
            b = round(math.sqrt((porosity[i]*1500*500)/(math.pi*
    number_ellipsis[j]*r_axis)),1)
            a = b*r_axis
            c_coords = []
            pathtoFolder = "D:\\LB capacity of Steel\\Simulations\\
    ellipse_1_"+str(r_axis)+"\\"
            dir1 = os.path.join(pathtoFolder,str(porosity[i]),str(
    number_ellipsis[j]),"pp",variations[k])
            if os.path.exists(os.path.join(dir1,variations[k])+".txt"):
                with open(os.path.join(dir1,variations[k])+".txt",'r')
    as file:
```

```
                    for line in file:
                        currentline = line.split(",")
                        c_coords += [[float(currentline[0]),float(currentline[1])]]

                # Sketch Rectangle
                plane = Plane.PlaneXY
                result = ViewHelper.SetSketchPlane(plane)
                point1 = Point2D.Create(MM(0),MM(0))
                point2 = Point2D.Create(MM(500),MM(0))
                point3 = Point2D.Create(MM(500),MM(1500))
                result = SketchRectangle.Create(point1, point2,point3)
                # EndBlock
                for cs in c_coords:
                    origin = Point2D.Create(MM(cs[0]), MM(cs[1]))
                    majorDir = -DirectionUV.DirU
                    minorDir = -DirectionUV.DirV
                    result = SketchEllipse.Create(origin, majorDir, minorDir, MM(a), MM(b))
                if number_ellipsis[j]>1000:
                    for cs in c_coords:
                        point1 = Point2D.Create(MM(cs[0]-1-a),MM(cs[1]-1-b))
                        point2 = Point2D.Create(MM(cs[0]+1+a),MM(cs[1]-1-b))
                        point3 = Point2D.Create(MM(cs[0]+1+a),MM(cs[1]+1+b))
                        result = SketchRectangle.Create(point1, point2, point3)

                # Solidify Sketch
                mode = InteractionMode.Solid
                result = ViewHelper.SetViewMode(mode, Info2)
                # EndBlock

                # Delete Selection
                selection = Selection.Create([GetRootPart().Bodies[0].Faces[faces] for faces in range(number_ellipsis[j])])
                result = Delete.Execute(selection)
                # EndBlock

                primarySelection = Selection.Create([GetRootPart().Bodies[0].Edges[edges] for edges in range(number_ellipsis[j])])
                secondarySelection = Selection()
                result = NamedSelection.Create(primarySelection, secondarySelection)
                NamedSelection.Rename("Group1","circles")

                if number_ellipsis[j]>1000:
                    primarySelection = Selection.Create([GetRootPart().Bodies[0].Faces[faces] for faces in range(number_ellipsis[j])])
                    secondarySelection = Selection()
                    result = NamedSelection.Create(primarySelection, secondarySelection)
                    NamedSelection.Rename("Group1","b_rectangles")
                    primarySelection = Selection.Create([GetRootPart().Bodies[0].Faces[faces] for faces in range(number_ellipsis[j], number_ellipsis[j]+1)])
```

```
                    secondarySelection = Selection()
                    result = NamedSelection.Create(primarySelection,
secondarySelection)
                    NamedSelection.Rename("Group1","face")
                # Save File
                DocumentSave.Execute(dir1+"\\"+variations[k]+".scdoc")
                # EndBlock
                # Delete Selection
                selection = Selection.Create(GetRootPart().Bodies[0])
                result = Delete.Execute(selection)
                # EndBlock
```